

Nicholas Roberto Drabowski

**MODULATION OF CORTICAL ELECTRICAL ACTIVITY BY DEEP
BRAIN STIMULATION OF THE AMYGDALA IN RATS**

Dissertation presented to the Graduate Program in Automation and Systems Engineering in partial fulfillment of the requirements for the degree of Master in Automation and Systems Engineering.

Advisor: Prof. Alexandre Trofino Neto, Ph.D.

Co-advisor: Prof. Roger Walz, Ph.D.

Florianópolis

2017

Ficha de identificação da obra elaborada pelo autor,
através do Programa de Geração Automática da Biblioteca Universitária da UFSC.

Drabowski, Nicholas

Modulation of Cortical Electrical Activity By
Deep Brain Stimulation of the Amygdala In Rats /
Nicholas Drabowski ; orientador, Alexandre Trofino,
coorientador, Roger Walz, 2018.
138 p.

Dissertação (mestrado) - Universidade Federal de
Santa Catarina, Centro Tecnológico, Programa de Pós
Graduação em Engenharia de Automação e Sistemas,
Florianópolis, 2018.

Inclui referências.

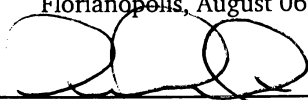
1. Engenharia de Automação e Sistemas. 2. Deep
Brain Stimulation. 3. Brain Computer Interface. 4.
Signal Processing. 5. Brain Amygdala. I. Trofino,
Alexandre. II. Walz, Roger. III. Universidade
Federal de Santa Catarina. Programa de Pós-Graduação
em Engenharia de Automação e Sistemas. IV. Título.

Nicholas Roberto Drabowski

**MODULATION OF CORTICAL ELECTRICAL ACTIVITY BY DEEP
BRAIN STIMULATION OF THE AMYGDALA IN RATS**

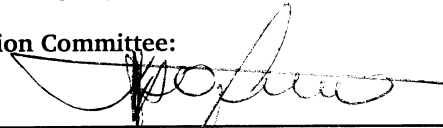
This Dissertation is recommended in partial fulfillment of the requirements for the degree of “Master in Automation and Systems Engineering”, which has been approved in its present form by the Graduate Program in Automation and Systems Engineering.

Florianópolis, August 06th 2018.

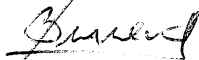


Prof. Werner Kraus Junior, Ph.D
Graduate Program Coordinator
Universidade Federal de Santa Catarina

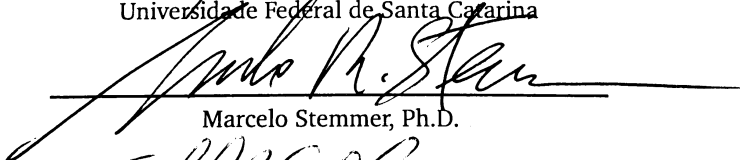
Dissertation Committee:



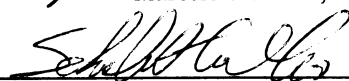
Prof. Alexandre Trofino Neto, (Committee President)
Universidade Federal de Santa Catarina



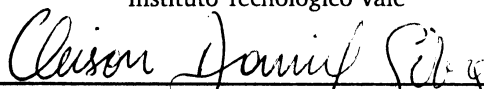
Jefferson Brum Marques, Ph.D.
Universidade Federal de Santa Catarina



Marcelo Stemmer, Ph.D.



Schubert Ribeiro de Carvalho, Ph.D.
Instituto Tecnológico Vale



Cleison Daniel Silva, Ph.D.
Universidade Federal do Pará

ACKNOWLEDGEMENTS

I would like to thank all the support, freedom, respect and resources received by the company InPulse and the Medical Sciences laboratory, in special my fellow advisors Dr. Alexandre Trofino Neto and Dr. Roger Walz. I must also thank my colleagues Lucas Casagrande Neves, Gabriel Veloso Paim and Jonatas Pavei and Douglas Formolo, without which, this dissertation would be impossible.

I must also thank my family for all the support, incentive, patience, lessons and love received: Carlos R. Drabowski, Crystal Couto Bacellar Drabowski, and Bruna Marcela Bacellar Drabowski. With science but without ethics, I would be nothing.

A special thanks to my partner in life Erika Y. Kinoshita for all the support and partnership in both the happy and difficult moments during the last 7 years.

Last but not least, all the Brazilian population, which paid for all my tertiary studies and grants, to whom I expect to return all the investment in form of health systems that improve the quality of life of the population.

I think it matters whether someone has a good heart.
Elon Musk

ABSTRACT

Deep brain stimulation (DBS) is an alternative of treatment for refractory psychiatric disorders that still faces the challenge of correctly configuring the stimulation parameters for each patient individually. The creation of measurable metrics for the clinical effects of DBS, named *biomarkers*, will help improving the DBS programming process. The amygdala (AMY) is a limbic structure that plays a key role in several psychiatric illnesses, therefore being a key structure for DBS. The medial prefrontal cortex (mPFC) is reciprocally connected to AMY and biomarkers built on its neural activity may be useful for the DBS parameter selection in the context of psychiatric diseases. In this dissertation the effect of acute AMY DBS on mPFC modulation and its effects on anxiety reduction were investigated in wistar rats using biomarkers proposed here. The brain signals acquired from rats subjected to DBS were analyzed using the *Power Spectral Density*, *Poincare Map* and *Correlation Dimension* algorithms. The correlation between 112 features acquired from the previous analysis revealed the existence of two biomarkers that were used for anxiety assessment. The results suggest that AMY DBS can be used as a mean to reduce anxiety. Since technological difficulties with the performed experiments reduced the number of subjects that could be taken into account in this study, it is still important to check the generality of the above results for a larger number of subjects. The proposed anxiety biomarkers may allow the development of automated DBS parameter optimization applied to the limbic system in psychiatric diseases, since the anxiety plays a key role in many psychiatric diseases.

Keywords: Deep Brain Stimulation. Brain Computer Interface. Signal Processing. Medial Prefrontal Cortex. Brain Amygdala.

RESUMO ESTENDIDO

A eletroestimulação cerebral profunda (DBS, em inglês) é uma técnica que vem sendo estudada como alternativa aos fármacos para doenças psiquiátricas refratárias, ou seja, as que não respondem à medicação. O DBS vem sendo aplicado com sucesso como tratamento para doenças motoras como Parkinson e distonia a mais de 20 anos. Parte determinante do sucesso da técnica é a configuração dos parâmetros de estimulação, que deve ser feita individualmente para cada paciente.

No caso das doenças motoras, o efeito da estimulação é visível a olho nu (tremor ou rigidez dos membros), o que permite a configuração dos parâmetros pelo profissional de saúde responsável. Para doenças psiquiátricas não há um efeito rapidamente observável que permita a programação dos parâmetros, o que tem impossibilitado a expansão da técnica para essas doenças. O objetivo desta dissertação é descobrir como se pode extrair dos sinais cerebrais tal informação. Nesta dissertação foram realizados experimentos com DBS em ratos wistar ao mesmo tempo que seus sinais cerebrais foram colhidos. Os animais também passaram por testes de labirinto de cruz elevado para medição de seus níveis de ansiedade. A partir dos dados obtidos se construiu um biomarcador de ansiedade para os animais.

A estrutura cerebral alvo do DBS foi a amígdala, devido ao seu papel chave nos circuitos cerebrais relacionados às doenças psiquiátricas, como a depressão, ansiedade e transtorno bipolar. Os sinais cerebrais foram adquiridos no córtex pré-frontal, região cerebral que possui uma conexão neural bidirecional com a amígdala. Os resultados da dissertação mostram que o posicionamento do eletrodo da amígdala é determinante no efeito sobre a ansiedade. Apesar de problemas tecnológicos terem causado uma significativa perda de dados, os resultados sugerem que o DBS aplicado à amígdala sob as condições e parâmetros selecionados nesta dissertação tem efeito redutor de ansiedade. Para a construção do biomarcador de ansiedade foram utilizados dados de 17 animais.

Para a análise dos efeitos do DBS sobre a ansiedade foram utilizados dados de 8 animais, que foram analisados em casos de estudo individuais devido ao posicionamento de eletrodo único de cada um. O animal considerado o padrão ouro, o qual o posicionamento do eletrodo de DBS na amígdala foi perfeito, apresentou redução aguda de ansiedade de acordo com o que se esperava com base na revisão da literatura.

Palavras-chave: Deep Brain Stimulation. Brain Computer Interface. Signal Processing. Medial Prefrontal Cortex. Amygdala.

LEGAL NOTE

All figures from other authors reproduced this dissertation are correctly referenced in accordance to the applicable law of intellectual property: *BRASIL. Lei n° 9.610, de 19 de fevereiro de 1998. Altera, atualiza e consolida a legislação sobre direitos autorais e dá outras providências.*

ACRONYMS

DBS: Deep Brain Stimulation

AMY: Cerebral Amygdala

EPM: Elevated Plus Maze

EEG: Electroencephalography

ECoG: Electrocorticography

LFP: Local Field Potential

PTSD: Post-traumatic stress disorder

PSD: Power Spectral Density

CD: Correlation Dimension

PM: Poincare Map

EEG1200: Electroencephalography device

DBStation5: DBSs stimulation device

GSA: Gold Standard Animal. Only animal with DBS electrode placed perfectly inside the AMY

D0, D1, D2, D3: Refers to the days of the experimental protocol.

LIST OF FIGURES

1.1	X-Ray exam of a patient with implanted DBS electrodes .	20
1.2	DBS Commonly used waveform	21
1.3	Concept map of dissertation	25
2.1	Basic brain anatomy	30
2.2	Amigdalae structures	34
2.3	Internal circuits of the AMY involved with conditioned fear	36
2.4	Amygdala external connections.	38
2.5	Potentiation and depotentiation process	40
2.6	AMY Across species	42
2.7	Elevated Plus Maze	43
2.8	Open Field Test	43
2.9	Stimulation fields of conventional electrodes	46
2.10	Neural activation of axons	47
2.11	Neural activation: Pulse width vs amplitude	48
2.12	Summary of charge density studies	50
2.13	Neural measurement paradigms	52
2.14	Example of two EEG signals	53
2.15	The EEG 10-20 system	54
2.16	EEG1200 input circuit	55
2.17	Square wave being reconstructed using fourier series. . .	58
2.18	Fourier transform of a signal with two frequencies	58
2.19	Correlation dimension integral	61
2.20	Poincaré plot	62
2.21	DBS targets for psychiatric diseases	64
2.22	Development of the CAPS score of a patient implanted with DBS for PTSD	67
3.1	Rat socket	70
3.2	Rat implant schematic	71
3.3	Cages used for the experimental setup	71
3.4	Physical setup of experimentation	72
3.5	DBS electrode implantation	73
3.6	DBStation5 Waveforms	74
3.7	ECoG electrodes implantation	75
3.8	Experimental connections	76
3.9	Experimentation protocol	77
3.10	NRDTool toolbox	78
3.11	ECoG signal imported and marked with stimulations . .	79
3.12	ECoG signal segmented in epochs	80
3.13	PSD graph comparing signal sections	81

3.14	Process used to build the spectral graphs	82
3.15	Alpha rhythm isolated in spectre	83
3.16	Graph example of mean energies contained in each exam section	84
3.17	Mean energies normalized by basal pre-stimulation values	85
3.18	Brain rhythm energies development over time	86
3.19	Poincare Plot	87
3.20	Development of poincare plot parameters over time . . .	88
3.21	Mean values for poincare parameters and their standard error	89
3.22	Correlation dimension values development over time . .	90
3.23	Averaged correlation dimension values	91
3.24	Example of features extracted from the algorithmic anal- ysis	92
4.1	Animal sampling process	95
4.2	Regression lines for the two best fitting features	96
4.3	Indexes used for calculation of BM22 and BM29	98
4.4	SVM classifier for anxiety using two biomarkers	99
4.5	DBS effect on the GSA's anxiety	100
4.6	DBS effect on anxiety in the gold standard animal (Pro- tocol day 2)	101
4.7	The three anxiety measures over time	102
4.8	DBS effect on anxiety in the gold standard animal (Pro- tocol day 1)	103
4.9	Anxiety in an animal not stimulated	104
4.10	Animal stimulated with 50 μA outside amygdala. It seems that the stimulation had an ansiolytic effect	105
4.11	Another animal stimulated with 50 μA outside amyg- dala. It seems that the stimulation had the same ansi- olytic effect	105
4.12	DBS effect in an animal stimulated with 10 μA only . . .	107
4.13	Animal stimulated with 100 μA	108
4.14	Third animal stimulated with 100 μA	109
4.15	D2 result of animal with electrode outside AMY that re- sponded best to the DBS	110
4.16	The same result was observed in the animal during the third day	111
4.17	GSA Spectral analysis	113
4.18	GSA spectrums alpha and gamma	114
4.19	GSA spectrums day 0	115
4.20	GSA spectrum of day 1	116

4.21 Poincare plot of GSA in the day 2	117
4.22 Poincare plot of GSA in the day 1	118
4.23 Correlation dimension of the GSA	119

CONTENTS

1	Introduction	19
1.1	Brain Diseases	19
1.2	Deep Brain Stimulation	19
1.3	Biomarkers	21
1.4	Problem Characterization	23
1.5	Dissertation Goal	23
1.5.1	Specific Goals	23
1.6	Dissertation Structure	24
1.7	How to read this dissertation	24
1.7.1	Map of concepts	25
2	Theoretical Foundation	27
2.1	Mood and Anxiety Disorders	27
2.1.1	Major Depression	28
2.1.2	Bipolar disorder	28
2.1.3	Anxiety	29
2.1.4	Post-traumatic stress disorder	29
2.2	Neural Circuits Involved with anxiety and mood disorders	30
2.2.1	Brain Amygdala	32
2.2.1.1	Amygdala Internal Structure	34
2.2.1.2	Fear Conditioning and Fear Extinction	35
2.2.1.3	Potentiation and depotentiation	39
2.2.2	Kindling	41
2.3	Equivalency between human and rat model in psychiatric diseases	41
2.4	Anxiety behavioral tests	42
2.5	Deep brain stimulation	43
2.5.1	Electrodes	44
2.5.2	Electric fields and DBS neural activation	45
2.5.3	Waveform	48
2.5.3.1	Current vs Voltage stimulation	48
2.5.3.2	Electrolysis	49
2.6	Neural activity measurement	50
2.6.1	Electroencephalography (EEG)/Electrocorticography (ECoG)	51
2.6.1.1	Brain Rhythms as Biomarkers for psychiatric disorders	53
2.6.1.2	Measurement System EEG1200	54
2.7	Analysis tools and algorithms	55

2.7.1	Estimation of power spectral density of a signal (PSD)	57
2.7.2	Correlation Dimension (CD)	59
2.7.3	Poincaré Plot	61
2.8	Review of previous experiments	62
2.8.1	EEG and psychiatric disorders	63
2.8.2	DBS and psychiatric disorders	64
2.8.3	DBS and EEG	67
3	Materials And Methods	69
3.1	Animals	69
3.2	Surgical Procedure	70
3.3	Physical Experimental Setup	71
3.4	Deep Brain Stimulation	72
3.5	ECoG	75
3.6	Experimental protocol	76
3.7	Data preparation and analysis	78
3.7.1	Feature extraction from previous analysis	91
4	Results	93
4.1	Animal sample	94
4.2	Construction of an ECoG biomarker for anxiety assessment	95
4.3	DBS effect on anxiety	100
4.4	DBS Effects on cortical activity	112
5	Discussion	123
6	Conclusion	127
	Bibliography	129

1 INTRODUCTION

The world is moving so fast these days that the man who says it can't be done is generally interrupted by someone doing it.

Elbert Hubbard

1.1 BRAIN DISEASES

The Brain is the body's control centre. The majority of sensory information, cognitive processes, and action responses are processed in the brain, giving rise to it's neural activity. Changes on normal brain activity in different regions give rise to several brain diseases, such as anorexia nervosa, Parkinson's disease, severe treatment-resistant addiction, depression, bipolar disorder, anxiety, post-traumatic stress disorder (PTSD), schizophrenia, Alzheimer's disease, Epilepsy, Tourette's syndrome and Obsessive Compulsive Disorder (OCD) [1][2][3][4]. All these diseases have globally a huge impact on life quality. Nowadays, depression is the disease with biggest impact on life quality, being responsible for 10.3 % of the total years lost to disability. Anxiety appears in sixth place contributing with 3.7 % of the years lost to disability [5]. It is estimated that 4 % to 6 % of the world population suffers from depression [6]. In Europe only, 23% of the years of healthy life is lost and 50% of years of life lived with disability are caused by brain diseases. Also, 35% of all burden of disease is caused by brain diseases. It seems reasonable that one-third of the funding in research in the life sciences field go for advances in neuroscience. [7].

Psychiatric diseases triggered by both acute and repetitive stress are associated with overlapped brain circuits including the amygdala (AMY), cingulate gyrus (CG), and prefrontal cortex (PFC). The similarity on involved brain structures and genetic predisposition of mood disorders may explain the fact that approximately 60% of all patients suffering from depression already have or will develop anxiety disorders [8].

1.2 DEEP BRAIN STIMULATION

Deep brain stimulation (DBS) is a technique consisting of applying focal electrical stimulation pulses through surgically implanted electrodes in the brain (See figure 1.1). The stimulation provides neural-network modulation within a brain circuit or cir-

circuits of interest. Initially, modern DBS systems have been developed to affect dysfunctional circuits in patients diagnosed with treatment-resistant tremor or other movement disorders; recently, DBS's therapeutic role has expanded to several neuropsychiatric disorders [9]. The target for DBS electrode implantation vary significantly based on the disorder being treated. Also, the electrical wave stimulation parameters vary depending on the wanted effect of neuronal inhibition or activation. The stimulation is frequently a squared current signal with parameters of frequency, pulse width, amplitude, and rest between polarity change (See Figure 1.2). DBS was applied to treatment of obsessive-compulsive disorder (OCD), Gilles de la Tourette syndrome [2], severe treatment-resistant addiction, major depression, bipolar disorder [3], and anorexia nervosa [4]. Also, DBS as a new treatment for PTSD was already tested in rat models [10][11] and is currently being tested in humans [12][13].

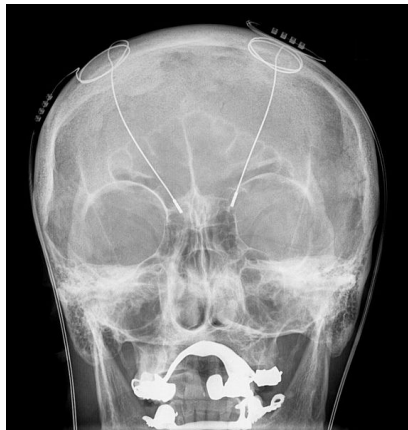


Figure 1.1: Image exam of a patient with implanted DBS electrodes. The white lines at the top of the figure are the electrode wires. At the lower end of the wires are the electrodes, part that has electrical contact with the brain and delivers the stimulation. Source: [14].

For Parkinson's disease and essential tremor, the clinical benefit of DBS is seen instantaneously. The symptoms improvement for psychiatric diseases, however, require a long time (hours, or days in depression) to be perceived, what makes the parameter programming a clinical challenge. The same apply for the treatment of dystonia, in which few months of treatment including several program-

ming sessions are required until the clinical benefit of DBS stimulation is finally observed [15][16].

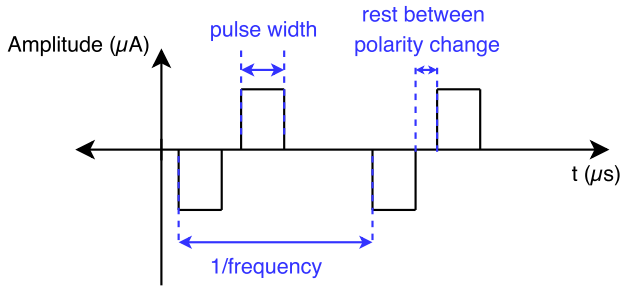


Figure 1.2: Deep brain stimulation commonly used waveform.

Because the DBS technique is relatively recent, it is still performed in open loop¹ and little is known about its effects on the modulation of brain activity. Implanted patients must undergo programming sessions weekly or monthly, where a physician sets the parameters (frequency, amplitude, pulse width) empirically based on questionnaires and visual observations [17]. The problem with this approach is that diseases are dynamic, and the therapeutic effect may become collateral depending on the user's daily life (hours of sleep, stress, use of medications, etc.). The most recent studies investigating closed-loop DBS have obtained promising results [18] [19]. Yet, there are no preferred control system paradigms: which input/output variables to use, how to model the brain interactions, and which sampling frequency to use are still open questions.

1.3 BIOMARKERS

The raw measurable physiological variables used today, such as electroencephalography, electrocardiography, arterial blood pressure, temperature, and blood oxygen saturation, are important for monitoring a patient's instantaneous health state. However, they provide very little or none information of more complex states of

¹Open loop: It means that the stimulation parameters are chosen once, prior to the application of the technique, and are not automatically updated from time to time based in periodic measurements.

a patient, such as responsiveness of a treatment, presence of asymptomatic diseases, and stress levels, amongst others. A solution to this problem is to apply complex algorithms that can extract valuable information from these previously simple measures. The result are, mostly, a huge variety of indexes that provide more clinical valuable information about the patient. These new indexes are known as *Biomarkers*. They may be static or dynamic, and are usually very specific for each disease or state of interest. [20]

The specific brain Biomarkers usually result from linear and non-linear signal analysis performed on brain activity measurements. The signals may be measured using a number of different techniques such as electroencephalogram (EEG), local field potential (LFP), and intracellular measurement (neural spikes). Different choices mean different brain aspects to be monitored. While an intracellular needle acquires the spikes of a single neuron, the EEG records the activity of thousands of strong slow synaptic transfers. For example, several neurons passing to an organized state usually produce a known effect on brain rhythms encountered in EEG signals [21]. The measurement of LFP may record both spikes from several neurons and synaptic dipoles, depending on its mechanical configuration and sampling frequency [22].

Brain activity characteristics that are objectively measured and evaluated as an indicator of normal biological processes, pathogenic processes, or responses to therapeutic intervention are considered *Biomarkers* according to the *National Institutes of Health* (Bethesda, Maryland - United States) definition [23]. Recent studies have discovered several brain biomarkers useful for purpose of diagnostics and treatment response prediction. For example: a) depression in humans is characterized by hypo-activity in the dorsal anterior Cingulate Gyrus while an hyperactivity in Rostral Anterior Cingulate Gyrus means a better treatment response [24]; b) 1 Hz to 10 Hz brain activity in thalamic Centromedian-Parafascicular complex and beta rhythms over brain motor cortex help to detect tics signature in patients with tourette syndrome [25]; c) in rats that underwent fear conditioning (a PTSD model) the local field potential (LFP) presented an increased theta activity in lateral brain amygdala during retrieval of fear memory [26]; d) a study performed in [27] reported greater overall relative and absolute beta wave power in the frontal brain of chronically depressed patients.

1.4 PROBLEM CHARACTERIZATION

One of the factors limiting growth of treatments using DBS is the problem of choosing the stimulation wave parameters. Stimulators are square wave generators of controlled current or voltage. The production of therapeutic or side effects for each patient is highly dependent on the location of the electrodes and the wave parameters used. DBS scientific researches for psychiatric diseases are currently based on selecting fixed parameters and observing the effects over weeks of use. Only then can the parameters be updated to improve the response. The researches are moving toward the development of closed-loop paradigms, to make these processes more efficient. This is the context in which this work fits.

Once it is possible to define stimulation parameters based on specific Biomarkers that are measurable in the short-term, DBS therapies can advance faster, and the parameter programming process may become much simpler, practical, and scalable.

Given the wide range of human brain functions and its related diseases, and the fact that electrode positioning completely influences the results obtained, this work focuses on DBS related to anxiety and depression disorders, which are involved with juxtaposed brain circuits, and are still in the research phase. The DBS applied to these circuits are one of the most challenging programming tasks nowadays, due to the variety of brain functions these structures relate.

The AMY is a key structure in the brain which receives neural pathways from most of the body sensory fibres, crosses the information with its local memory and inhibits or excites several other brain structures. The prefrontal cortex (PFC) is one of these structures, also related with psychiatric diseases. More detailed information on the involved brain circuitry is presented in section 2.2.

1.5 DISSERTATION GOAL

The aim of this dissertation is to investigate the effects of DBS applied in the cerebral AMY on the neuronal activity of the mPFC in rats through the analysis of its electrocorticography signal (ECoG).

1.5.1 Specific Goals

- To perform an integrative literature review and build a map of concepts;

- to choose adequately all experimental parameter ranges and their initial values;
- to build the set-up and perform tests on the experimental arrangement (cables materials and types, build connectors, system electrical configuration for EEG measurement and DBS stimulation of multiple animals simultaneously);
- to acquire pilot experimental data from subjects;
- to develop hypothesis on the relationship between DBS and ECoG, based on the results of the pilot tests;
- to formulate the experiment protocol for testing the hypotheses;
- to acquire experimental data from subjects;
- to adapt Biomarker algorithms to the specific context and build dedicated algorithms for the data analysis.

1.6 DISSERTATION STRUCTURE

The chapter 2 gives all the necessary background on neuroscience (items 2.1-2.3), DBS (item 2.5), ECoG acquisition (item 2.6), tools and algorithms used (item 2.7), and review of previous DBS experiments available in literature (item 2.8); chapter 3 deals with the developments used for the experimentation set-up, the toolbox developed for the signal analysis and its implemented algorithms; chapter 4 presents the results obtained in the experimental tests; chapter 5 presents a detailed discussion on the results; and chapter 6 has the conclusions of the dissertation.

1.7 HOW TO READ THIS DISSERTATION

For the sake of didactics, this dissertation gives all the necessary background to understand the work. It is aimed at engineers, nurses, psychologists and medical practitioners. Due to the interdisciplinary character of this work, the theoretical foundation is extremely long. It is highly recommended that one make use of selective on-demand reading, using the concept map below as a guide. Those familiarized with DBS experimentation may skip the items

3.1 to 3.2 in chapter 3. Those familiarized with linear and non-linear signal processing applied to electroencephalography should skip the item 3.7 of the chapter 3.

1.7.1 Map of concepts

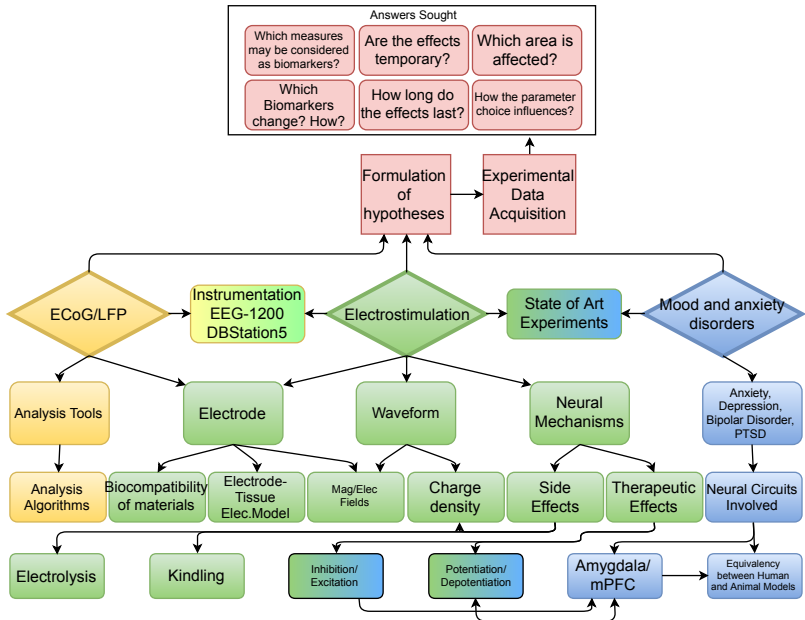


Figure 1.3: Map of concepts. Source: The Author.

The theoretical foundation was built upon the technique called *Integrative Review*, as described in [28]. This technique is adequate for this type of work because the research interdisciplinary character requires too many concepts that are, at the beginning unknown. New sources were added at each round of research, using new keywords related to new concepts, as the knowledge of the researcher expanded, and the research evolved. A map of concepts was built as a result (see figure 1.3). It serves also as a map from this dissertation. The map starts from the three major concepts inside the diamonds. Each new row was added in a different round of investigation. The colors express how the concepts in rectangles

relate to the main concepts in the diamonds. After some hypothesis and key questions were formulated, that served as a guide for the creation of the experimental protocols. The next sections will bring the literature content related to each concept on the map.

2 THEORETICAL FOUNDATION

2.1 MOOD AND ANXIETY DISORDERS

To understand depression and anxiety, and its mechanisms of action in the human brain, it is necessary to start by differentiating two basic concepts: *emotions* and *feelings*. *Emotions* are transient responses to a specific stimulus in the environment (e.g. presence of a threat), in the body (e.g. pain) or, for humans, in the mind (a thought, for example). These stimuli generate instantaneously measurable physiological responses (secretion of hormones, change in heart rate, etc.). The brain structures involved in this processing of information are mainly the thalamus, hypothalamus, AMY, and anterior cingulate cortex. These structures are located in the figure 2.1, and will be dealt with in detail in the item 2.2. *Feelings* are defined as the abstract sensations that can come from emotions (happiness, sadness, etc.), but they involve more abstract cognition in regions of the cerebral cortex. They are more difficult to study due to their effect being observable only in the long run.

When an *emotional state* is extended and becomes dominant over time, it can be called *mood*. Therefore, the mood can be independent of instantaneous personal or environmental circumstances [8]. When an animal's mood is chronically altered, there is a case of mood disorder.

Mood disorders together with *anxiety disorders* are the most common serious mental disorders [29]. *Mood disorders* usually involve depression or euphoria while *anxiety disorders* involve an abnormal regulation of an emotion in specific, fear [8]. In both conditions, the main symptoms have a fundamental emotional component and are accompanied by physiological, cognitive, and behavioral changes [8].

In general, mood and anxiety disorders are treated together, as both involve negative emotional states and appear to encompass overlapping neural circuits, which include the AMY and *anterior cingulate cortex*. The fact that neural circuits and genetic conditions are similar may explain the fact that approximately 60% of patients suffering from depression also suffer from an anxiety disorder. Many times anxiety disorders precede the onset of depression [5].

Performing the study of emotions is considerably simpler than the study of mood due to the existence of more developed animal models and the direct measurement of physiological responses. The mood is a behavioral change that is observed in the medium term, and may not correlate with instantaneous physiological responses,

which makes the experiments in the area more complicated.

In the next subsections (items 2.1.1-2.1.4), the humour and anxiety disorders relevant to the understanding of this dissertation are presented.

2.1.1 Major Depression

Major depression (or unipolar depression) is a type of mood disorder. Symptoms of this disease include: dismay (dysphoria) present most of the day, almost every day, often accompanied by an intense sense of anguish, inability to feel pleasure (anhedonia), and a loss of generalized interest in the world [30]. Sadness is the most common feeling, but anger, irritability, and loss of interest in daily activities may predominate in some patients. Symptoms, if untreated, may extend from 4 to 12 months [8, 31]. Major depression differs from normal sorrow or mourning because of its severity, omnipresence, duration, and association with other physiological symptoms, such as insomnia, loss of appetite, weight loss, lack of energy, slow movement. Cognitive symptoms are evident in the content of thoughts (hopelessness, feeling of worthlessness, guilt, impulses and suicidal ideation) and in cognitive processes (concentration difficulty, slow thinking, and memory impairment). More severe cases may have present psychotic symptoms, hallucinations, and delusions. The most nefarious outcome of depression is suicide. Suicide is the *eighth* leading cause of death in the United States and is the *third* leading cause of death among 15-24-year-olds. More than 90% of suicides are associated with mental disorders, being depression the leading cause.

2.1.2 Bipolar disorder

Bipolar disorder is also classified as a mood disorder. It involves, in addition to the presence of major depression most of the time, episodes of *mania*, which seems to be the opposite of depression. Episodes of mania are characterized by outbreaks that lead the individual to extreme behaviors, for example, [32, 8]:

- hyperactivity;
- insomnia, reduced need for sleep;
- binge eating, drug abuse;
- to have sex with many partners;

- accelerated thoughts that run over;
- excess speaking;
- very high self-esteem (illusion about yourself or your abilities);
- involvement in many activities at the same time;
- great shaking or irritation.

The frequency of symptoms and intensity vary greatly from individual to individual. Some may experience symptoms of depression and mania twice at a time, others may experience symptoms interspersed or simultaneously several times a day. As for intensity, episodes of depression can result in suicide, and episodes of mania in psychosis, a condition in which there is a loss of contact with reality.

2.1.3 Anxiety

Anxiety is characterized by the subjective experience of tension and worry accompanied by physiological changes involving, for example, sweating, dizziness, and increased blood pressure [33]. It may be associated with cognitive and behavioral changes such as concentration difficulty [6].

2.1.4 Post-traumatic stress disorder

Post-traumatic stress disorder (PTSD) is a type of anxiety disorder that occurs in response to a very stressful, threatening or catastrophic event. Are affected by this disorder war veterans, victims of all types of violence, victims of natural catastrophes, among others [34]. Patients have the symptoms of reliving the traumatic event in flashbacks or during sleep when faced with a similar situation. They may be socially isolated, have tachycardia, sweating, dizziness, headache, sleep disturbances, difficulty concentrating, irritability and hypervigilance [34, 35].

By the classification of the World Health Organization (WHO) PTSD cannot be diagnosed in the first month after the traumatic event, in this case, it is an **acute stress reaction**, neither after two years event, when it happens to be classified as **lasting personality modifications** [35].

2.2 NEURAL CIRCUITS INVOLVED WITH ANXIETY AND MOOD DISORDERS

In mood disorders, there are specific brain regions and circuits involved [8]. Before going into detail, it is necessary to understand a little of the physiology of the brain. A simplified schema of the brain structures is presented in the figure 2.1. Those of interest for this dissertation are explained below, according to references [36] and [8].

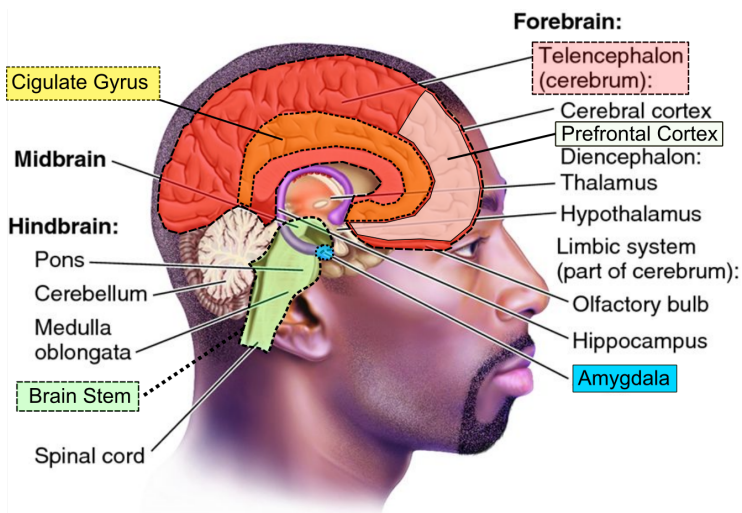


Figure 2.1: Basic brain anatomy. Source: [36].

- **Thalamus:** is at the top of the brain stem and is responsible for the processing of the sensory stimuli that reach the brain. The information of several senses (balance, vision, hearing, etc.) pass through this structure, where they undergo a pre-processing. The output sensing information goes directly to the telencephalon and, in parallel, to the AMY;
- **Amygdala (AMY):** are almond-shaped structures located bilaterally at the tip of each hippocampus that function as a type of alarm. Information from the thalamus is crossed with memories to define whether the stimulus sets received represent a potential threat or reward. Their output pathways trigger physiological responses, which are treated here as *emotions*.

The AMY has an intrinsic memory, which is not usually accessed consciously. The AMY is essential for this dissertation, so it will be treated more deeply in the section 2.2.1;

- **Hippocampus:** a significant part of the work of the hippocampus is the storage of extrinsic long-term memory, i.e. it can be stored in a conscious way.
- **Hypothalamus:** when the AMY, together with the hippocampus detects some potentially dangerous situation, the efferent pathways that will reach the whole body causing physiological responses (perspiration, increased heart rate, etc.) leave the brain through the hypothalamus;
- **Prefrontal Cortex:** in humans, the functions of logical and abstract thinking are assigned to the prefrontal cortex. When the amygdalae are less active (basal state) the activity of their connections with the prefrontal cortex through the cingulate gyrus is bigger. In potentially dangerous situations in which the AMYe are very active, the activity of the nerve pulses in the cingulate gyrus becomes reduced, causing the prefrontal cortex to have a different activity in comparison to the basal one. *In other words, the activity of the AMYe (individual under stress, for example) directly affects the way of thinking (pre-frontal cortex activity)*[36];
- **Anterior Cingulate Gyrus:** little is known about the exact functioning of this structure, but it is investigated that it is involved in abstract functions such as the sensation of reward, detection of errors, control of impulses, and decision making based on emotion. Other functions that relate to this structure are some autonomic functions, such as heart rate and blood pressure regulation [37]. Evidence suggests that depression is characterized by a reduction of neuronal activity in this region [38].

Comparison between patients with and without mood disorders and their neuronal circuit mapping were enabled by the most advanced medical imaging techniques. Some regions may have a basal¹ level of neuronal activity increased or decreased. The etiology of mental illness is multi-factorial and stress plays an important

¹In this context, basal refers to the normal activity presented without any special stimulus.

role in the case of depression and anxiety [30]. In neurophysiological terms, circuits involving the AMY and their connections to the hippocampus and the medial prefrontal cortex (mPFC) occupy a key position in emotional processing and modulation of stress-related behaviors. [39, 40, 8, 37].

Interesting recent findings reveal that the physical size of the AMY is increased in patients with depression. Also, its basal *activity* is increased in depression, bipolar disorder and anxiety disorder [8].

Emotions and feelings, functions in which the AMY take part, are important evolutionary responses since their functions are well preserved among species. This fact makes the conclusions of animal experimentation more translational to the human context [8, 39]. See more on this topic in section 2.3.

2.2.1 Brain Amygdala

Stimuli may have innate *emotional competence*, for example pain or pleasure. When a stimulus without emotional competence (such as a random noise or light) is presented to an animal together with some emotionally competent element, the relation is recorded by the brain AMY and future expositions to the neutral stimulus can trigger the same emotional response [8]. For example, a person who has had an accident and was transported by ambulance to the hospital may associate the pain felt at that time with the sound of the ambulance siren. Thus, after the trauma, when the person hears an ambulance siren can begin to relive the emotion² of the accident: perspiring, tachycardia, etc.

Early studies suggesting the crucial role of the Amygdala in connection with aversive responses were practiced by Lawrence Weiskrantz in 1950 [8]. Monkeys received a *Pavlovian conditioning of fear*: in their cages, in random moments, a whistle would play and, at the end of a few seconds, would cease. When the whistle ceased, the monkeys received an uncomfortable shock. To avoid the shock, the monkeys had to learn to pull a lever before the end of the whistle. The results showed that normal animals learned the task, while animals that had their AMY removed could not learn. For rewarding responses (where pulling the lever brought a reward), the observed result was the same. Some studies that followed this

²Remember that: emotion is characterized by the measurable physiological responses

have done only the Pavlovian conditioning of fear and observed that when the AMY was removed the reactions of learned fear ceased to exist (freezing, increased blood pressure, etc.) [8]. It was later discovered that the AMY is also involved with the innate fear, for example, the instinctive freezing reaction of a rat upon feeling the odor of fox urine, its natural predator.

Now, please consider the figure 2.2. The AMY contains 12 nuclei, but lesions only in the *lateral* (LAd + LAVl + LAVm) or *central* (CEl + CEm) nuclei are enough to extinguish conditioned fear. Nerve pulses from sensory neurons are paired in the AMY when they reach the lateral nucleus. Nervous pulses make several synapses internal to the AMY in an intricate network of neurons, which would be a processing that defines whether the stimulus is potentially dangerous or pleasurable [33]. Information is eventually sent to the central nucleus, the main axon output of the AMY. Signals from the central nucleus can trigger the various emotional responses and also go to the upper cortex, where it is speculated, help to create the abstract sensations of feelings [8].

Amygdala-related findings in animals have been confirmed in humans. Patients with AMY lesions do not develop conditioned fear when exposed to a neutral stimulus that was previously paired with a noxious stimulus. They also fail to recognize facial expressions of fear and express autonomic responses in response.

The AMY has a type of *intrinsic memory* storage, which relates to emotional memory, and cannot be easily accessed consciously, but through a stimulus. The *extrinsic memory*, on the other hand, is the memory that can be accessed consciously. The hippocampus is the fundamental brain structure in the storage of this type of memory. The better understanding of intrinsic and extrinsic memories in humans is product of experiments with victims of lesions in the AMY and hippocampus, for example: a) patients with *bilateral lesions of the AMY* do not demonstrate physiological responses to a stimulus previously conditioned with emotional competence, although they are able to accurately report the conditioning process suffered. Patients with *hippocampal lesions* present physiological responses, but they do not have the conscious memory of the conditioning process experienced [8].

The AMY is also involved in positive emotions in animals and humans. For example, the human AMY is activated when individuals observe photographs of stimuli associated with food, sex, and money, or when people make decisions based on its reward value [8].

2.2.1.1 Amygdala Internal Structure

The AMYe are located bilaterally in the temporal lobes and are composed of multiple nuclei interconnected through *glutamatergic* neurons and/or *GABAergic* neurons. Glutamatergic neurons are neurons that, when excited, release the glutamate transmitter at its output, increasing the excitability of the neurons receiving the synapse. GABAergic neurons, on the other hand, release another transmitter, which decreases the excitability (inhibits) the neurons that receive their synapse.

According to the groups of neurons and axons, the AMY is divided in the following sub-regions [39]:

1. **BLA**: Basolateral complex, contains the following nuclei:
 - LA: lateral
 - BA: basal
 - BM: basomedial
2. **CeA**: Central complex, contains:
 - Cel: centro-lateral;
 - CeM: centro-medial;

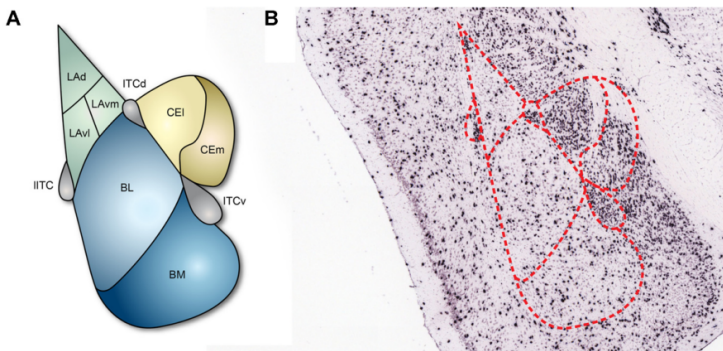


Figure 2.2: A) Nuclei of cerebral AMY. B) Cut of a brain tissue seen under a microscope. The black spots mark the presence of GABAergic neurons. Note that the richest regions in GABAergic neurons are located in the central AMY (CA) and in the ITCs. Source: [41].

Please, consider the figure 2.2. The region of the basolateral (BL) complex is composed of approximately 80% glutamatergic cells (when they receive pulses generate excitatory synapses in their dendrites) and 20% of GABAergic interneurons (generate inhibitory synapses), whereas the central nucleus is composed essentially of neurons GABAergic. Groups of GABAergic cells, called Intercalated Cell Mass (or ITCs), interpose between these two regions and externally to the BL. They are speculated to serve as 'off switch' of the AMY [42].

2.2.1.2 Fear Conditioning and Fear Extinction

One of the main feats of the AMY, widely studied, is the fear conditioning that was previously mentioned. When an unconditioning stimulus (US), an electric uncomfortable shock in the feet, for example, is presented to an animal along with a conditioned stimulus (CS), a beep or light, for example, animals learn to associate one another and respond with fearful behavior not only to the US, but also to CS alone [41]. If the CS is presented several times without the US, the animal extinguishes the aversive behavior, that is, "forgets" the association [41, 39, 40].

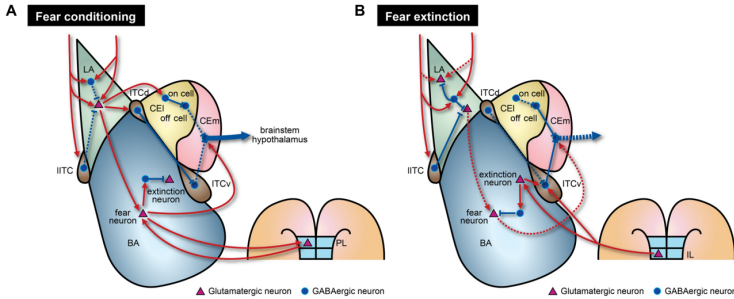


Figure 2.3: Model of the internal circuits of the AMY. The model contains neural connections both *widely known* in the literature and *hypothetical*. Full lines and dashed lines represent more active and less active connections, respectively. Line tips with arrows represent excitatory synapses, whereas dashed tips represent inhibitory synapses. In orange, the brain stem is represented. **A (left)** Shows the connections that become active and inactive during the process of fear conditioning. **B (right)** shows the interactions during the process of fear extinction (only the CS is being presented). Source: [41].

Consider the figure 2.3. Physiologically, the lateral portion (LA) of the basolateral complex is the region where information from the internal and external environment arrives through cortical projections. The convergence of visual, auditory and interoceptive stimuli in this region allows neutral stimuli (e.g., a sound) to be associated with potentially negative outcomes (eg a shock) by the synaptic plasticity mechanism promoting the mnemonic process of *conditioned fear* [39]. The lateral portion (LA) connects with the basal portion (BA) and the lateral portion of the central nucleus (CEI). Both the lateral portion of the central nucleus (CEI) and the basal portion of the basolateral (BA) complex protrude into the medial portion of the central nucleus (CEm). This, in turn, projects the information to sub-cortical structures responsible for triggering the autonomic and behavioral responses associated with the valence of the stimulus (positive or negative).

- **Fear Conditioning:** The figure 2.3-A represents a moment in which the animal is receiving a neutral stimulus together with a noxious stimulus, entering through the upper connections in LA. Nerve impulses excite glutamatergic neurons in LA, which

in turn excite neurons in BA, called fear neurons (this name was due to the realization that these neurons are always active while the animal is afraid [41]). The fear neurons activate GABAergic neurons that inhibit so-called *extinction neurons*. The glutamatergic neurons in LA also activate inhibitory neurons in CE1 and ITCd. All of these actions result in the weakening of the connections that inhibit the GABAergic neurons in CEm and strengthen the excitatory connections, causing the total activity of the CEm neurons (which are GABA type) to increase. **As a result, CEm neurons carry inhibitory nerve pulses to the hypothalamus, brainstem, and prefrontal cortex.** Note also in figure 2.3-A that there is also a feedback of the connections of the neurons of fear with neurons of the PL region of the brainstem, which further strengthen the response of the same.

- **Fear Extinction:** When the neutral stimulus is presented without the noxious stimulus the connections with GABA neurons in LA will lose strength and the connections with glutamatergic neurons will be strengthened. In this way the excitatory connections with the fear neurons decrease, and the connections that inhibit the neurons in CE become stronger. **This whole circuit leads to a decrease in neuron response in CEm which reduce their inhibitory influence to the hypothalamus, brainstem, and prefrontal cortex.**

In addition to what has already been described, the AMY has reciprocal neural projections between the BA region, the *medial prefrontal cortex (mPFC)*, and hippocampal formation; one-way BA projections to the striatum; and projections of CEm to the hypothalamus and brainstem [33, 40].

In summary, the basolateral complex is the main site of information entering the AMY (mainly the LA region), while the central nucleus is the main site of information output of the AMY (mainly the CEm region). The AMY is a very strategically placed brain structure and participates, in addition to fear conditioning, in many other phenomena. Other AMY connections worth mentioning and their functions are shown in the figure 2.4.

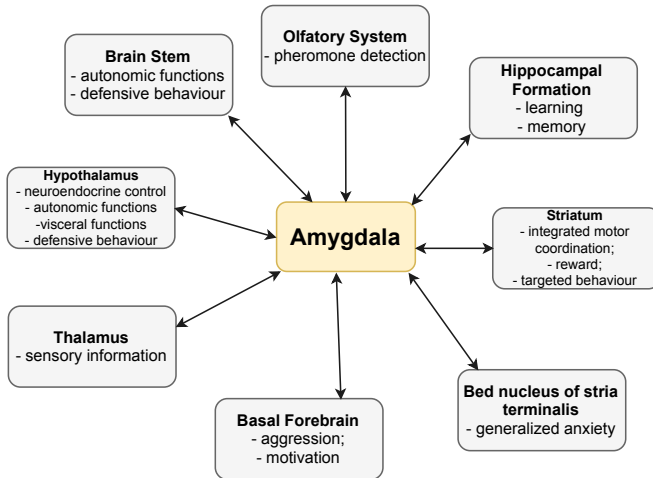


Figure 2.4: Amygdala external connections. Adapted from: [43].

Connecting the functioning of the AMY to the anxiety and mood disorders described in the item 2.1, anxiety modulation involves the coordinated activation of the macro circuit involving the AMY, PFC, hippocampal formation, and the bed nucleus of the stria terminalis (*BNST*). The sequence involves a *bottom-up*³ processing, with the identification of valence of the stimulus in the AMY (positive, neutral or negative), which sends projections to the BNST, ventral hippocampus and prefrontal cortex as well as for subcortical effectors (hypothalamus and brainstem), and triggers the appropriate physiological responses to the confrontation of the situation.

Then a *top-down*⁴ processing occurs, from the medial prefrontal cortex and ventral hippocampus again to the AMY and BNST, which involves executive functions and the weighting of the situation against other stimuli and competing needs in the organism [33]. For example, if a person sees a picture of a snake, the AMY may become active sending pulses to the prefrontal cortex, meaning a potential threat (bottom-up pathway), but it receives an inhibitory feedback from the prefrontal cortex to slow down because

³In this context, the direction bottom-up means from sensory raw information to higher level cognition.

⁴Direction from higher cognition processes to body actuators.

it is only a picture (top-down pathway).

In general, AMY hyperactivity and inadequate top-down processing due to hypoactivity in the ventromedial prefrontal cortex are associated with stress disorders (such as posttraumatic stress disorder) [40, 44], and general emotional regulation deficits [44], including depression [45]. The AMY, therefore, is found as a fundamental structure in the regulation of both anxiogenic and depressive processes.

Despite the high worldwide impact in terms of disability and high economic burden, the pharmacological resources available for the treatment of these diseases appear to be inadequate. **Only 22-40% of patients respond adequately to antidepressants** on the market [45]. Likewise, the relationship between effectiveness at the expense of the side-effects of anxiolytic drugs should also be improved [33, 6]. Regarding anxiolytics, few new drugs, and therapeutic targets have been developed since the 1940s, when compared to other diseases [33].

Given the inefficiency of conventional drugs, the use of new techniques and therapeutic resources for the treatment of psychiatric diseases has been gaining attention from the scientific community and medical industries. In recent years, due to the evolution of technology and the reduction of the size of electronic components, **Deep Brain Stimulation (DBS)** has been emerging as an alternative. In the section 2.5, the uses and advances of DBS are discussed in depth.

2.2.1.3 Potentiation and depotentiation

It was discovered in the mid-1960s that when two neurons are connected, the strength of connection may change based on the frequency of firings (Original article: [46]). Terje Lomo, a Norwegian neuroscientist, and his team observed that when a neuron is triggered electrically with a high-frequency (*trains of 12 Hz during 10 s at intervals of 7 minutes* [47]), the action potentials observed in the next neuron synapses become bigger. This effect became known as **potentiation**. After the potentiation process, a low-frequency stimulation would still produce big synapses in the next neuron. After up to 6 hours using low-frequency stimulation, the neuron returns to its normal state. This is a plastic process that involves a change in morphology of neurons. It was then recognized that the potentiation must have something to do with the way brains retrieve memory, what boosted the investigations [48, 49]. Other

researchers have later discovered that very low-frequency stimulation of a neuron causes an inverse effect, the **depotentialiation**, which makes the next neurons' synapses to become weaker. The potentiation with high-frequency stimulation (HFS) and depotentialiation with low-frequency stimulation (PLFS) is shown in figure 2.5

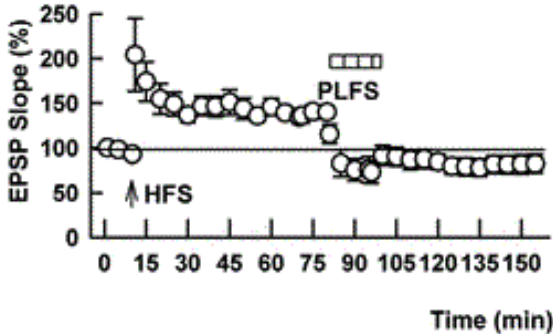


Figure 2.5: EPSP: Excitatory post-synaptic potential. The figure presents the percentual change in a synapse amplitude during the potentiation and depotentialiation process of hippocampal neurons. It shows that the mean amplitude rises to 200% after a high-frequency stimulation (HFS). The low-frequency stimulation was then decreased to 90% using a low-frequency signal (PLFS). Source: [50].

The effects of potentiation and depotentialiation are widely understood in literature as the fundamental part of fear conditioning and extinction processes [51, 52].

For the depotentialiation process three waveforms are frequently used:

- prolonged senoidal single-pulse (1 or 5 Hz);
- square-pulse (1 Hz);
- pp-LFS (paired-pulse low frequency stimulation): 1 Hz for 15 minutes with 50 ms interstimulus interval.

The current or voltage amplitudes used are rarely described because the studies most likely selected empirically a current amplitude until a neuron spike could be observed using their instruments.

The protocols used for this kind of experimentation used as stimulation electrodes glass pipettes with a conductive electrolyte inside. These pipettes have a tip narrow enough to allow the stimulation of a single neuron.

2.2.2 Kindling

A different stimulation pattern and intensity may, instead of only causing potentiation or depotentiation, cause **kindling**. Kindling is a way to produce epilepsy in subjects using electrostimulation for the study of this disease. A standardized process of amygdala kindling is described in [53]. The procedure recommends stimulating the subjects using $500\mu\text{A}$ amplitude, pulse width of 1 msec and pulse interval of 20 msec during 2 seconds. This process should be repeated twice daily with an interval of at least 4 h between the stimulations until they show at least 3 consecutive seizures. From this moment on, the animal is considered fully kindled. The literature fails in describing important details such as:

- is the stimulation monopolar or bipolar? (regarding the number of stimulation electrodes);
- is the stimulation monophasic or biphasic? (regarding the current direction);
- is necessary any protection in the stimulation circuit to avoid tissue damage? (electrolysis effect);

2.3 EQUIVALENCY BETWEEN HUMAN AND RAT MODEL IN PSYQUIATRIC DISEASES

Although humans have a number of cognitive abilities that differentiate them from other animals, many core behaviors are similar. Emotional behaviors, for example, are well preserved between different animal species. The AMY, above all, is responsible for several important instinctive emotions, as seen in figure 2.4. Even non-mammalian species such as reptiles, birds, rodents, and fish have an amygdala-like brain region with similar circuits and functions. By combining fear conditioning tasks originally developed for rodents to humans and functional magnetic resonance imaging (fMRI) it was confirmed that the human AMY has the same role as the rodent AMY [39]. The figure 2.6 extracted from the same article shows the basic AMY structures in different species.

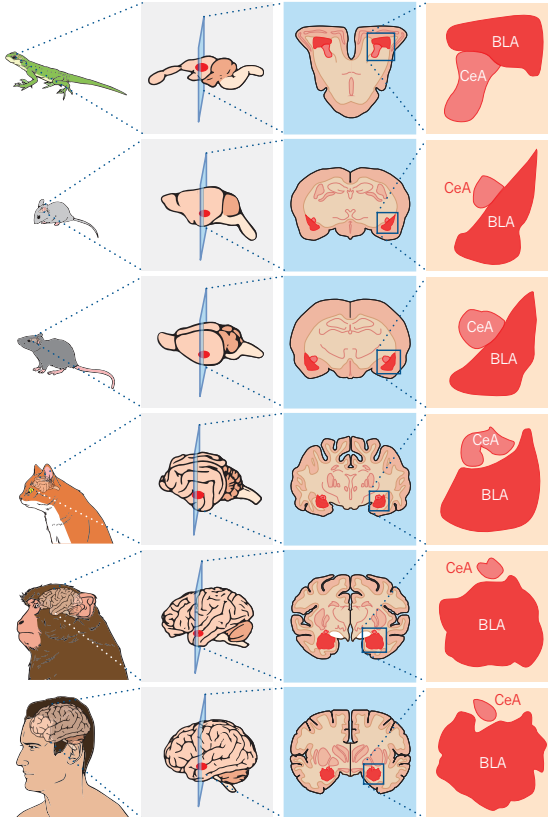


Figure 2.6: AMY Across species. Source: [39].

2.4 ANXIETY BEHAVIORAL TESTS

Experiments with rodents aimed to evaluate the subject's anxiety frequently use two tests:

1. Elevated Plus Maze (EPM): the rodent is left in the center of a maze like in figure 2.7. It has 10 minutes to explore freely the maze. It is expected from normal animals to stay 20% of the time in the open arms of the maze. Animals that spend more time are considered relaxed, and animals that spend less are considered anxious. The test can only be applied one time, since the animals get used to the maze [54].

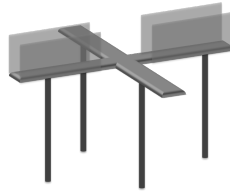


Figure 2.7: Elevated Plus Maze.

2. Open Field (OF): The open field test consists of observing the animal locomotion in an square cage (see figure 2.8) during a period of time. It is used to access general locomotion function of rodents [55].

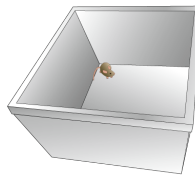


Figure 2.8: Open Field Test.

The OF test is usually applied after the EPM because it is necessary to access if the animal locomotion function is normal, thus eliminating the possibility of motor problems influencing the EPM test evaluation of anxiety.

2.5 DEEP BRAIN STIMULATION

Deep brain stimulation (DBS) is a technique consisting of applying focal electrical stimulation pulses through surgically implanted electrodes in the brain. The stimulation provides neural-network modulation within a brain circuit or circuits of interest. Initially, modern DBS systems have been developed to affect dysfunctional circuits in patients diagnosed with treatment-resistant tremor or other movement disorders; recently, DBS's therapeutic role has expanded to several neuropsychiatric disorders [9]. The target for DBS electrode implantation vary significantly based on the disorder being treated. Also, the electrical wave stimulation

parameters vary depending on the wanted effect of neuronal inhibition or activation. DBS was applied to treatment of obsessive-compulsive disorder (OCD), Gilles de la Tourette syndrome [2], severe treatment-resistant addiction, major depression, bipolar disorder [3], and anorexia nervosa [4]. Also, amygdala DBS as a new treatment for PTSD was already tested in rat models [10, 11] and is currently being tested in humans [12, 13].

The majority of studies that applied DBS to psychiatric diseases imported fixed stimulation parameters derived from classical DBS used for movement disorders. Added to this limitation, most of the psychiatric diseases do not have observable short-term metrics for assessment of DBS' therapeutic or side-effects. To address these problems recent scientific effort is being put on creating tools for closed-loop stimulation. The main advantage of closed-loop techniques is that the stimulation parameters are changed online over time to adapt for each patient, favoring therapeutic effects while avoiding side-effects [56]. The formulation of the closed-loop paradigm is broad and uncertain. So far there is no preferable formulation for this kind of problem in the literature. The closed-loop DBS systems (CLDBS) can use as *process variable* any set of measurable biological parameters, being most popular the use of brain rhythms or neural spikes. The *actuation variables* can be defined ranging from the simplest case: a binary variable used to start/stop the whole stimulation; to the broadest case of using each waveform parameter as an independent actuation variable. The first steps on CLDBS are being taken in the area of Parkinson's disease (PD). A proposed CLDBS for improvement of PD symptoms used neuron spikes recorded in the primary motor cortex (M1) for triggering pulse train stimulation in the globus pallidus internus (GPi) [56].

The next sections will present important parameters that must be chosen in any DBS experimentation.

2.5.1 Electrodes

A crucial part of any deep brain stimulation system is the choice of the electrodes. Their constructive form is crucial to define the affected region and collateral physical damage during surgery. The material choice is important to allow longer periods of stimulation, depending on its biocompatibility. Following, a summary of important characteristics that must be considered when choosing the DBS electrodes:

- **Polarity (number of poles):** The electrode stimulation may be *monopolar*, *bipolar*, or *multipolar*. The *monopolar* stimulation uses a small contact electrode implanted in the target structure while the other pole is much bigger and is placed outside the brain (usually in contact with the skull). *Bipolar stimulation* uses two small electrodes implanted near each other. *Multipolar* is usually a combination of more contacts in the same electrode to address more structures[57]. Monopolar configurations allows the stimulation to spread further with the increase in the stimulation current, activating more cells. Bipolar configurations, however, are known to concentrate more the stimulation area [17, 58].
- **Material:** Good choices are nickel-chromium alloys, gold, silver, stainless steel, titanium, and biopolymers [59];
- **Shape:** The disposition of exposed contacts in the electrodes directly determine the shape of the electromagnetic field applied to the tissue.

2.5.2 Electric fields and DBS neural activation

The mechanical configuration of electrode contact is the determinant factor of the electric field shape. In the figure 2.9 three shapes commonly used are presented. The contact ring total area is 0.06 cm^2 in available commercial implantable pulse generators (IPG).

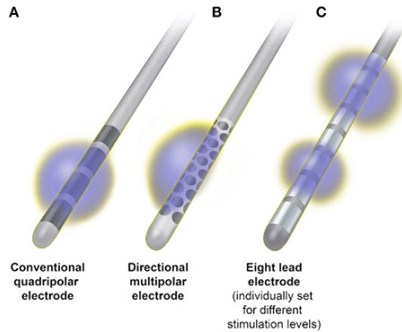


Figure 2.9: A) Conventional quadripolar electrode producing a spherical field that may spread outside the target area, causing side-effects. B) Multipolar 32-contact electrode that allows directional steering of the field, reducing the potential of stimulation side-effects. C) Eight-contact electrode with multiple independent current control, enabling the allocation of completely different stimulation parameters independently to each electrode contact. Source: [60].

It is mentioned in the literature that the electric fields affect mainly neuronal axons within its stimulation range, causing them to depolarise (creating spikes) or hyperpolarize (inhibiting spikes). Still, the mechanism, parameters, and mathematical models underlying the DBS mechanisms are rudimentary. Some qualitative insights on the parameter interaction with tissue activation are presented in [61, 15].

Now, please consider the figure 2.10. It presents the example of DBS in the subthalamic nucleus (STN) used for the treatment of tremor in Parkinson; the circles represent axons of neurons of different calibers passing nearby. The *Internal Capsule* is an adjacent structure that is not intended to be stimulated because its stimulation causes side-effects. A better response is achieved when more axons in the STN are activated. The figure 2.10-a show a monopolar stimulation activating larger axons in green. To activate more neurons, the stimulation amplitude (voltage or current) may be risen (2.10-b). But, the stimulation may activate neurons inside the internal capsule, causing side-effects. Alternatively, the electrode could be moved up (2.10-d), alleviating the load on the Internal capsule. This, frequently, is not possible because the change may affect other undesired areas. Another option is to use a bipolar configuration,

moving the other pole nearer to the stimulation site (2.10-c). It helps shrink and direct the stimulation. Finally, the activation of axons with smaller diameter may be achieved by increasing the pulse width (2.10-e) [62, 63, 64, 65].

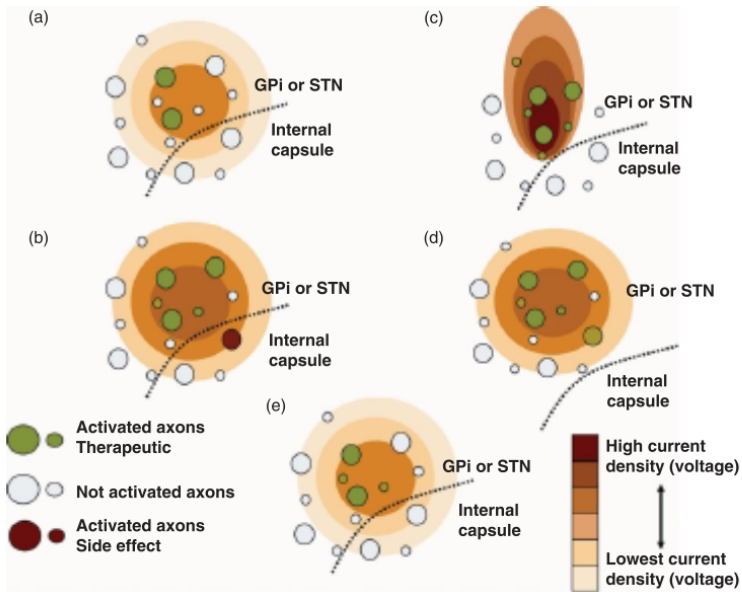


Figure 2.10: Neural activation of axons. See text for explanation. Source: [15].

The amplitude and pulse duration (pulse width) necessary to achieve neural activation have a non-linear relation. Now, consider the figure 2.11. *Rheobase* is the minimum amplitude necessary to activate a neural element with a very long pulse. The chronaxie duration is defined as the pulse width in which the neural element is activated by the double of the Rheobase amplitude. The chronaxie values are typically between **30-200 μs for large myelinated axons, 200-700 μs for small myelinated axons, and 1000-10000 μs for cell bodies and dendrites.** This means that the myelinated axons are the most likely neural elements to be affected by DBS [66, 67, 68, 69].

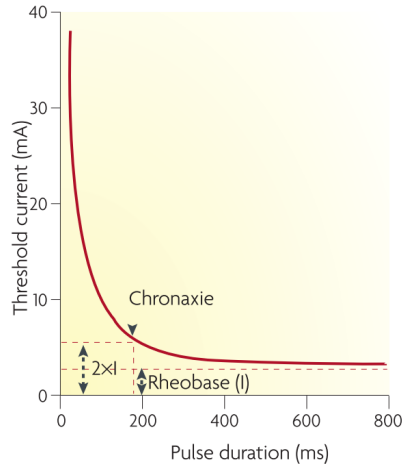


Figure 2.11: Neural activation: Pulse width vs amplitude. Source: [66].

The set of parameters that cause therapeutic effects while avoiding the side-effects is known as **Therapeutic Window**. Are factors that may increase the therapeutic window: better precision in electrode positioning, choice of electrode shape, stimulation direction, and reduction of pulse width [69, 70, 71].

2.5.3 Waveform

Traditionally, the DBS systems used voltage-controlled stimulation because it is easier technically. Recent versions use controlled square current stimulation, because it is much safer. Tissue damage is caused by cumulation of charge, therefore all modern stimulator have charge-balanced waveforms.

Clinically available neurostimulators such as Medtronic's Solettra Model 7426 and Irel II Model 7424 use voltages ranging from 0-10.5 V in 0.115 V increments, pulse widths from 60-450 μs in 30 μs increments, and frequencies from 2-185 Hz (5-100 in increments of 5 Hz, and 2, 33, 130, 135, 145, 160, 170, and 185 Hz) [69].

2.5.3.1 Current vs Voltage stimulation

Voltage stimulators are easier to build, but require an impedance measurement to avoid parameters that may damage the

tissue. If the electrode-tissue impedance becomes bigger over time, the therapeutic effects may fade; if the impedance shrinks, than the stimulation may damage the tissue. The current stimulation, on the other hand, controls the charge delivered by simply applying the same stimulation amplitude positively, and, then, negatively. This makes the process much safer and robust over time [69, 72].

2.5.3.2 Electrolysis

Electrolysis is the name given to the effect of tissue damage caused by electrical stimulation. Several studies during the 50's and 60's extensively studied the parameters and their limits to avoid electrolysis. It was discovered that important parameters in this case are the total *charge applied per stimulation phase*, and the *charge density* (charge per area). Apparently, the total charge applied to the tissue during the positive or negative phase of stimulation changes the charge density limits. But, for the sake of simplicity, it is agreed that charge densities lower than $30 \mu\text{C}/\text{cm}^2$ in charge-balanced systems are safe for chronic use over decades [69, 72]. The figure 2.12 summarizes the results of some studies that investigated electrolysis.

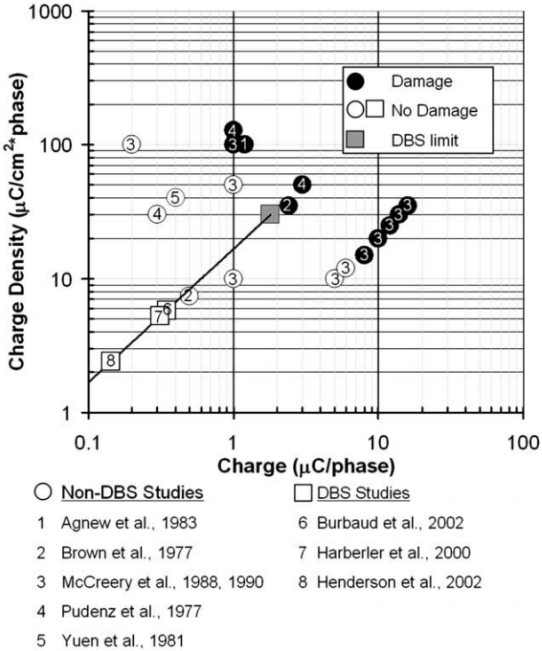


Figure 2.12: Summary of charge density studies. Source: [69].

DC stimulation, in contrast to charge-balanced stimulation, is extremely dangerous. Currents in the order of nano-amperes (one thousand less than charge-balanced levels) are sufficient to cause tissue damage in less than 24h. Therefore, it is frequent to find capacitors in series to the tissue in the implantable pulse generators, known as blocking capacitors, to guarantee no flux of DC current[73].

2.6 NEURAL ACTIVITY MEASUREMENT

This part of dissertation assumes that the reader already has a basic knowledge of the neural structure and spike generation. If it is not the case, please refer to the bibliography in [74]. The brain is an extremely complex network of neurons. Its network arrangement differs from location to location. Also, there are many different types of neurons, according to their morphological structure and function. The prefrontal cortex is of most interest in this dis-

sertation due to its participation in the regulation of stress-related diseases.

The term *Neural Activity* involves any interactions between neurons: the synapses, spikes, metabolism, among others. Different techniques allow monitoring different aspects of the neural activity. Please consider the figure 2.13, that presents a pyramidal neuron in the prefrontal cortex. In the middle, there is a pyramidal cortical cell. An intracellular recording using a micro glass pipette allows one to measure its *action potentials (Spikes)*. Current flowing through the neuronal membrane creates extracellular potentials (**Local Field Potential - LFP**), which can be measured with an extracellular electrode. These potentials can also be measured with electrodes on the scalp (**Electroencephalography - EEG**). Similarly, neural activity produces magnetic fields, measured with magnetoencephalography (**MEG**). Membrane potential can also be seen with a camera after opening the scalp and applying voltage-sensitive dyes onto the surface of the cortex (**optical imaging techniques**). More indirectly, neural activity impacts metabolism, in particular, the blood vessels, which produces signals that can be recorded with intrinsic signal optical imaging and functional magnetic resonance imaging (**fMRI**).

2.6.1 Electroencephalography (EEG)/Electrocorticography (ECoG)

For the measurement of prefrontal cortex activity (cortical activity measurement), EEG, ECoG, and LFP provide analogous measurements of the same signals, therefore they are going to be treated together in this section [22].

EEG and LFP signals display the same characteristics during wake and sleep states [75]. Early studies observed that action potentials have a limited participation in the genesis of EEG or LFPs. Bremer [76, 77] was the first to propose that the EEG is not generated by action potentials, based on the mismatch of the EEG dynamics with action potentials. In 1951 Eccles proposed that LFP and EEG activities are generated by the sum of slow post-synaptic potentials arising from the synchronized excitation of cortical neurons. Intracellular recordings from cortical neurons later demonstrated a close correspondence between EEG/LFP activity and synaptic potentials [78, 79, 80]. Nowadays, it is widely accepted that EEG and LFPs are generated by synchronized synaptic currents arising on cortical neurons, possibly through the formation of dipoles [81]. The little

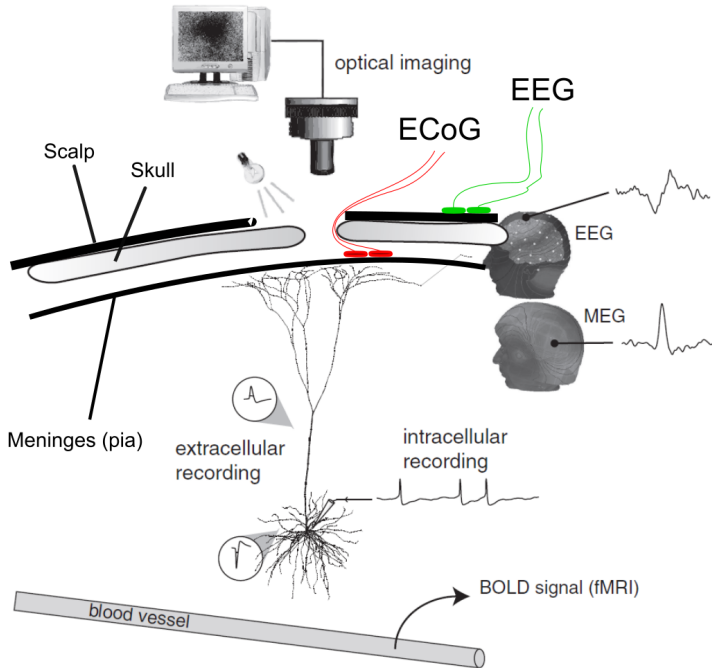


Figure 2.13: Neural measurement paradigms. Adapted from: [22].

presence of neural spikes in EEG signals indicates strong filtering properties of cortical tissue. Frequencies above 100 Hz, such as that produced by action potentials are subject to a severe attenuation, and therefore are visible only for electrodes immediately adjacent to the recorded cell. Synaptic potentials, a relative low-frequency event, is less attenuated with distance. Extracellular electrodes were proven to be much less sensitive to positioning because they record the sum of a large number of neurons from bigger distances. Action potentials are captured only if the electrode is adjacent to the cell, therefore being more selective. In addition, the spectra of EEG signals present a distinct $1/f$ scaling. In other words, its signal spectral energy sharply reduces for increasing frequencies, corroborating with the findings suggesting a low-pass filtering characteristic for the brain tissue. The figure 2.14 presents two typical samples of EEG signals and their spectrums [22].

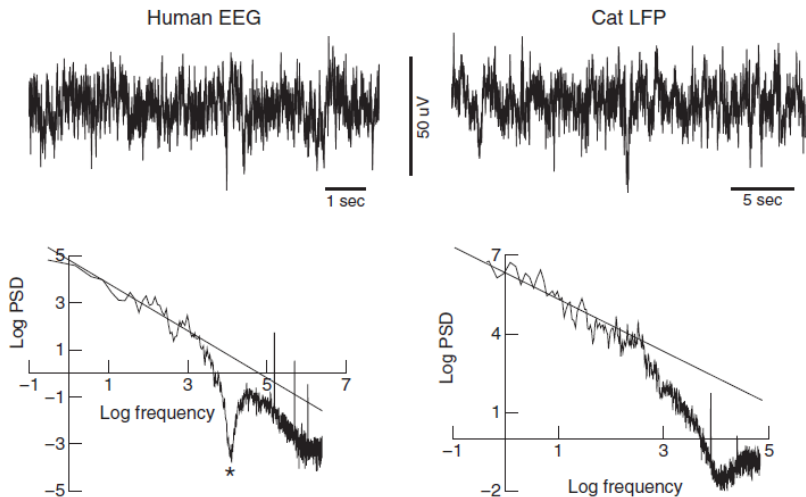


Figure 2.14: Example of two EEG signals. The signals were not filtered, except for a notch filter at 60 Hz (*). Source: [22].

2.6.1.1 Brain Rhythms as Biomarkers for psychiatric disorders

Brain Rhythms are the signals contained in certain EEG/LFP/ECOG frequency bands. Although their ranges may slightly vary amongst authors, they have specific names. The most used frequency limits are:

- 1 - 4 Hz: δ ;
- 4 - 8 Hz: θ ;
- 8 - 13 Hz: α ;
- 13 - 30 Hz: β ;
- 30 - 60 Hz: γ .

Numerous experiments being published try to create new Biomarkers using the brain rhythms [82, 83, 84, 85, 86, 87, 88, 89]. Usually, the EEG signal is divided into epochs with length ranging from 0.5 s to 5 min, depending on the study. The spectral density is calculated and integrated over each energy band. The integrated

energies are then used as input to classification algorithms aimed to distinguish healthy brains from those with psychiatric disorders. The studies vary greatly in measurement location, the number of channels, and signal processing parameters, therefore it is difficult to compare different studies.

Recently, some non-linear signal algorithms started to be used for EEG processing and biomarker development with good improvement on classification accuracies. The most relevant algorithms for this work are explained in the section 2.7.

2.6.1.2 Measurement System EEG1200

The EEG1200 (Nihon Kohden, Japan) is the commercial EEG/ECoG/LFP measurement system used in this thesis. It allows sampling frequencies up to $1kHz$. It is designed to be used in only one patient at a time. It has 36 input leads, allowing the placement of up to 36 electrodes in the scalp of a patient. The electrodes are glued to the scalp according to a placement system, being the most common the 10-20 (see it in figure 2.15). Frequently, the **measurement channels** are obtained by **digitally** subtracting each signal from an electrode used as reference (A2, for example), or subtracting each electrode signal from the average of its neighbours. Other derivation calculation modes may include the use of the average of all electrodes, or subgroups of them.

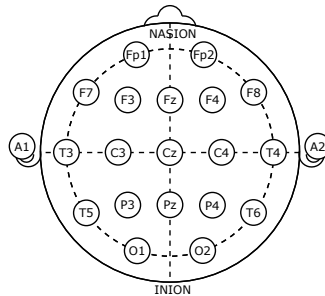


Figure 2.15: The 10-20 system is an internationally recognized method to describe and apply the location of scalp electrodes in the context of an EEG test or experiment. Source: [90].

Now, please consider the input circuit of the EEG1200 system (Figure 2.16). It has an input anti-aliasing filter with -18 dB/oct cen-

tered on 300 Hz, and a high-pass filter. Three of its input electrodes have special functions:

- **C3** and **C4**: The average of these leads is used as reference, and is analogically subtracted from each of other electrodes in the input circuit;
- **Z**: the Z lead is used to insert the common mode noise (average of C3 and C4) back to the patient, thus increasing the input circuit common mode rejection. This lead is usually clipped to the patient's ear.

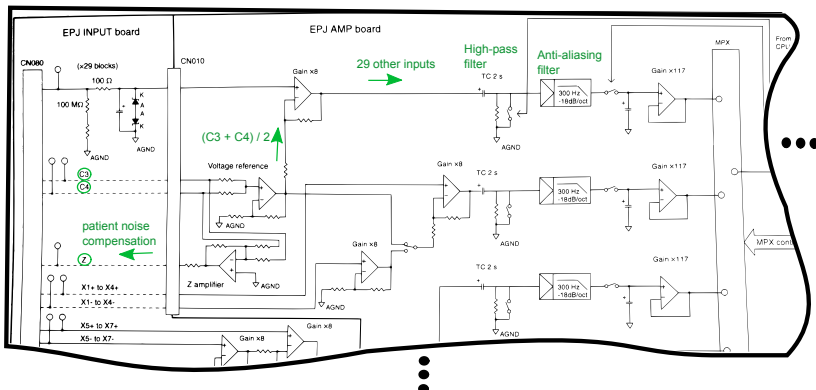


Figure 2.16: The EEG1200 circuit. Adapted from: Device manual.

2.7 ANALYSIS TOOLS AND ALGORITHMS

The survey in [91] provides a beautifully tailored review of the most used algorithms for brain signals analysis and their possible uses as biomarkers so far. The algorithms are briefly summarized below:

Linear analysis:

- **Power Spectral Density (PSD)**: Provides visual evaluation of the frequency content of a signal. It has the *parametric* (based on models) or *non-parametric* methods;

- **Short-time Fourier Transform (STFT):** Same function as the PSD, but provides some evaluation of what happens to the signal over time, and is more susceptible to white noise;
- **Discrete Wavelet Transform (DWT):** Provides spectral content analysis with enhanced time and frequency resolution.
- **Independent component analysis (ICA).** Decomposes the signal in statistically independent components. This approach is very useful for EEG signals with multiple channels, but limited for single-channel measurements.

Nonlinear analysis:

- **Higher Order Spectra (HOS):** Since different signals in time may produce the same spectral power content, the HOS algorithm takes into account the signal phase, thus the shape of signal in the time domain is also considered in the analysis;
- **State Space Reconstruction:** Analysis of a unidimensional signal as a combination of diverse vectors in an euclidian space of order 'm'. In other words, it embeds the signal into a higher dimensional space, trying to reconstruct the signal trajectories into these higher dimensional space;
- **Fractal Dimensions:** Quantifies the signals complexity; it is very useful in biomedical signals and is being used in EEG and ECG analysis for characterization of specific physiological functions.
- **Correlation Dimension (CD):** It is the most used particular case of *Fractal Dimensions*. Estimates the dimension embedded in a signal. A measure of signal 'roughness', or 'chaoticity'. A decreased CD indicates Alzheimer [91].
- **Largest Lyapunov Exponent:** Useful to discriminate between chaotic and periodic dynamics. It analyses the convergence or divergence of neighbor orbits in the state space of a system;
- **Entropy Estimation:** A measurement of the signal "organization";
- **Recurrence Plots:** Plots used for measurement of periodicity and time-variance of a signal. A widely used recurrence plot is the *Poincaré Plot*.

Although several brain signal analysis tools containing these algorithms are currently available (EEGlab toolbox for Matlab, Brain Vision Analyzer, The Neurophysiological Biomarker Toolbox, etc), none was specifically created for EEG analysis synchronized with DBS stimulation. Therefore, a new toolbox for Matlab was created by the author to resolve this problem. The toolbox is named *NRDTool*. The algorithms used in the *NRDTool* are explained in the next subsections.

2.7.1 Estimation of power spectral density of a signal (PSD)

Basic introduction for non-engineers

Any measurements made with a constant frequency, such as EEGs and LFP, are considered *discrete signals*. Jean-Baptiste Joseph Fourier, a French mathematician is known as the first to formulate a mathematical method to decompose periodic signals into sines and cosines of different amplitudes and frequencies, known as Fourier's series. He claimed it would be possible to recreate periodic signals of any shape by using an infinite amount of sines and cosines of frequencies multiple from the original signal (*its harmonics*). See an example in figure 2.17-left. For example, a square wave $f(t)$ that repeats itself 5 times per second has a *fundamental frequency* of 5 Hz. In theory, it is possible to recreate this wave using senoids or cosenoids with frequency 5, 10, 15, 20, and so on. The bigger the number of senoids, the better the approximation is. The sum would look like: $f(t) = a_1 \sin(2\pi \cdot 5 \cdot t) + a_2 \sin(2\pi \cdot 10 \cdot t) + \dots + a_n \sin(2\pi \cdot 5n \cdot t)$, being the a constant coefficients and n tends to infinite. These coefficients can be organized in a graph like in figure 2.17-right.

Later, Fourier described a method to recreate also non-periodic signals, that, this time, uses all intermediary frequencies. It was called the *Fourier Transform*. The organization of all frequencies and their amplitudes in a graph now creates a continuous graph (named *spectrum*). See an example in figure 2.18. Consider the red signal. It has one slow frequency at the beginning. Then, it changes its frequency to a higher frequency at the middle. Taking the spectrum of all the signal shows two lobes (right graph), representing the two frequencies present in the signal. Note that, the blue signal presents exactly the same spectrum, although the same frequencies appear in a different order.

These lobes would be, ideally, extremely narrow because they represent only one frequency, but the Fourier calculation creates a

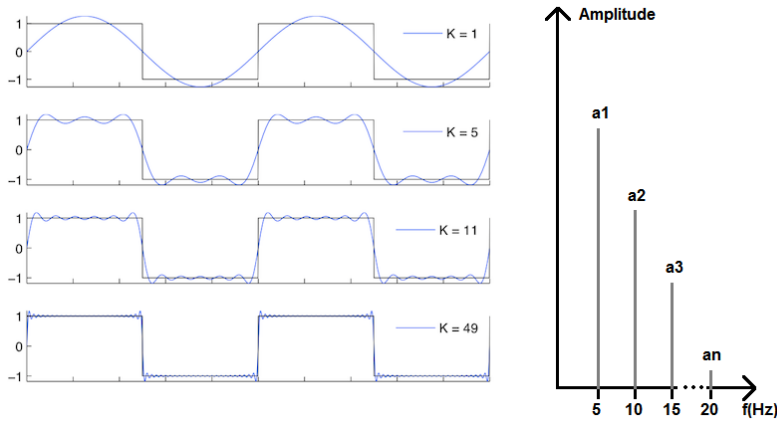


Figure 2.17: Reconstruction of a square wave using Fourier series. 'K' is the number of senoids used. Adapted from: [92].

distortion that widens the lobes. Some mathematical tricks, such as *windowing* help to reduce the lobe widths, ie reducing the spectral interference of one frequency over another.

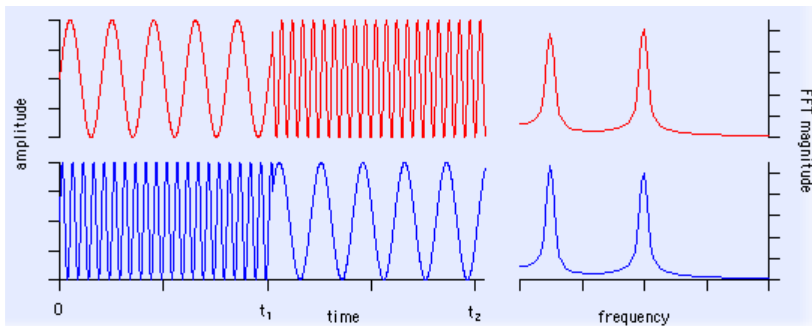


Figure 2.18: Fourier transformation of two signals with a frequency change. Adapted from: [93].

It should now be clear to the reader that, if one divides the signal in two or more parts to calculate more spectrums (windowing process), each spectrum would show the instantaneous frequency,

and allow one to observe how frequencies develop over time. This new method is called *short-term fourier transform* (STFT). If one divides the signal in too many parts, however, each part wouldn't have enough oscillations to provide an accurate spectrum. In other words, the number of divisions should take in account the frequencies present, but one still doesn't know the frequencies present before the spectrum is calculated. This paradox is known as the *time-frequency resolution problem of STFT*.

Finally, the analysis of frequency is not straightforward, there are algorithm parameters such as windowing that may be adequate for the signal context, and may completely influence the final results. More advanced techniques used in this dissertation are explained in the sequel.

Power spectral density

In simple terms, the power spectral density is the squared fourier transform of a signal. It describes how the energy of a signal is distributed over its frequencies. When the signal analysed is stochastic, i.e. random, it is not straight forward to calculate its power spectral density, because the signal may significantly vary over time. Therefore, most advanced methods of PSD estimation such as the *P-Welch* method were described.

P-Welch method

The P-Welch method is a form to estimate spectral power of a signal reducing the noise effect. The signal is divided in overlapping segments. Each segment is multiplied by a window for reduction of spectral leakage and ripples. The spectrums are calculated. The final PSD estimation is an average of all overlapping segments squared [94].

2.7.2 Correlation Dimension (CD)

The *dynamical systems theory* is a branch of the knowledge that studies signals and the systems that originate them. For example, an industrial furnace can be abstracted as a *system*, where the *input variable* is the voltage applied to the resistance that heats it, and the *output variable* is its temperature. Both variables develop over time. The ultimate goal is to create a *control system*, which is a mathematical law that describes how the input variable should be managed to bring the output variable to the desired value. The

brain may be considered as a system and the EEG channels its output variables.

According to the dynamic systems theory, the EEG signals are classified as chaotic, non-linear and time-variant [91]. It means:

- chaotic: very small deviations when comparing the same starting point lead to completely different development over time;
- non-linear: doubling the input stimulus doesn't double the output response;
- time-variant: the same inputs produce different outputs each time.

Thus, the linear analysis, such as the spectral analysis using PSD, have limited capability to capture important features of the system. When the EEG is plotted over time, it never reaches a cycle; it is unstable locally; and stable globally. This characterizes a *Strange Attractor* [95]. The *correlation dimension* is a mathematical concept used to estimate the number of state space variables responsible for generating the output trajectory. Alternatively, it is seen as a **measure for the signal roughness** [91, 96].

Grassberger et al have proposed a practical algorithm for estimating the correlation dimension of a signal [97]:

$$CD = D_2 = \lim_{r \rightarrow 0} \frac{\log C(r)}{\log(r)}, \quad (2.1)$$

where $C(r)$ is the correlation integral given by:

$$C(r) = \frac{1}{N^2} \sum_{x=1}^N \sum_{y=1, x \neq y}^N \Theta(r - |X_x - X_y|), \quad (2.2)$$

where:

X_x, X_y : points of the trajectory in the phase space

N : is the number of data points in phase space

r : radial distance around each reference point X_i

Θ : is the Heaviside function in its discrete form, given by [98]:

$$\begin{cases} 0, & x < 0 \\ \frac{1}{2}, & x = 0 \\ 1, & x > 0 \end{cases}$$

In practice, the correlation integral is calculated numerically using iterations within an empirically defined range of r values. A too small r value causes the algorithm to fail, because it is limited by the acquisition resolution and frequency [99]. Therefore, a log-log graph is plotted (see figure 2.19), and the correlation dimension (CD) is estimated as the slope of the curve. The algorithm used in this dissertation was implemented as described by the references [99, 96].

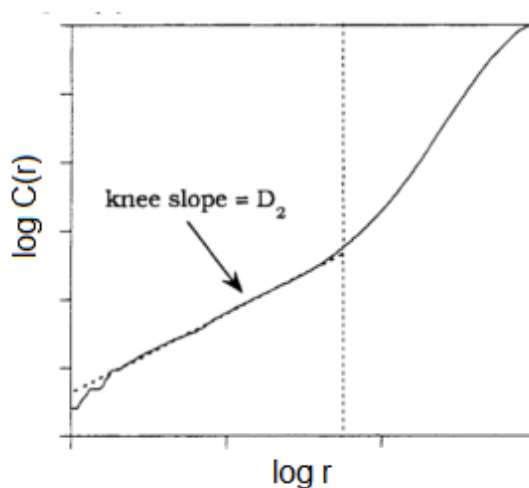


Figure 2.19: Correlation dimension (CD , also known as D_2) calculated from slope. Adapted from: [99].

2.7.3 Poincaré Plot

The *Poincaré Plot* is a recurrence plot used to quantify *self-similarity* in a signal within short and long-term. Similarly to the correlation dimension (item 2.7.2), recurrence plots are used for analysis of chaotic signals. Recurrence plots show, for a given moment in time, the times at which a phase space trajectory visits roughly the same area in the phase space. The plot also helps to distinguish chaos from randomness by embedding a data set into a higher-dimensional state space [100]. The dimension embedding is done by using subsequent points as additional dimensions. For example, the poincare plot is widely used for analysis of the heart rate signal embedded in two dimensions, therefore are plotted points

with the x axis being values $R(t)$, and y axis being values $R(t+1)$. It results in a graph such as in the figure 2.20.

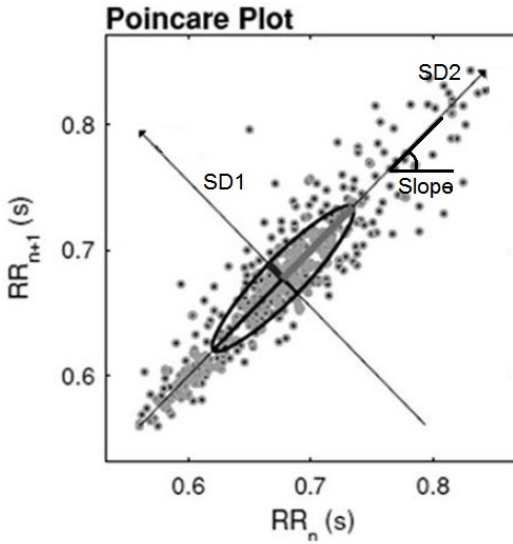


Figure 2.20: Example of poincare plot. Adapted from: [101].

Some interesting measures are calculated from the plot:

- SD1:short-term variability;
- SD2:long-term variability;
- Slope of best fitting line: signal falling and rising ramps slope;
- SD1/SD2: participation of the short-term variability in the long-term variability.

2.8 REVIEW OF PREVIOUS EXPERIMENTS

Because the science underlying the scope of this dissertation is extremely recent, there is no single study to be used for base comparison that follows exactly the same experimentation methods. Therefore, some previous studies presenting findings regarding different aspects of this dissertation are presented in this section.

2.8.1 EEG and psychiatric disorders

Through spectral analysis of EEG signals, it is not visually clear which characteristics in the frequency bands determine each psychiatric condition. Most of the studies being carried in the last decade use classification algorithms trained on real data. Studies using the PSD energies of EEG rhythms as input features achieve accuracies in the range 80% to 98% for detection of some pathologies. For example, the study in [87] achieved 85% accuracy in depression classification using 8 EEG channels. It used the algorithm P-Welch with 50% overlapping hamming windows of 0.5s width. The energy of the rhythms in the spectrums were fed to an artificial neural network with three layers. The input layer had 4 neurons, the hidden layer 4 neurons, and the output layer had three neurons, only.

The gain on classification accuracy achievable using non-linear EEG features was accessed by the study [86]. 45 unmedicated depressed patients and 45 normal subjects participated in this study. EEG signals with 19 channels were acquired. Features used: the energy of four EEG bands (delta, theta, alpha, and beta), detrended fluctuation analysis (DFA), Higuchi fractal (HF), correlation dimension (CD), and Lyapunov exponent (LE). The features were applied to the classifiers: k-nearest neighbour (KNN), linear discriminant analysis (LDA), and logistic regression (LR). The best accuracy using the brain rhythms was achieved with the alpha applied to the LDA or LR (both 73.3%), and the best non-linear feature was the correlation dimension (80.3%). By using all four frequency bands, the accuracy increased to 76.6%. Using all non-linear features together increased the accuracy to 90%. **These findings suggest that depressed brains differ from healthy brains mostly by the content of the alpha band and the correlation dimension.** But, it is not clear which of the 19 channels used are the most important and, if it is really necessary to use 19 channels. According to [91], the correlation dimension was also successfully used to classify Alzheimer's disease in patients.

Emotions such *stress* were also successfully classified using EEG data. Studies tend to agree that: 1) alpha waves reflect a calm, open and balanced psychological state, so Alpha activity decreases in stressful situations; 2) Beta activity reflects cognitive and emotional processes, so it increases with the mental workload and thus with stress. The number of electrodes and location, however, depend on the application [102]. **The cortisol levels and stress tests based on questionnaires presented a positive correlation with**

the high beta activity at the anterior temporal sites when people kept their eyes closed, affirming the aforementioned relationship between the Beta band and stress. In addition, the mean high beta power at the anterior temporal sites of the stress group was found to be significantly higher than of the non-stressed group [102].

2.8.2 DBS and psychiatric disorders

DBS as a treatment for psychiatric disorders is still experimental. The most common DBS targets are shown in figure 2.21.

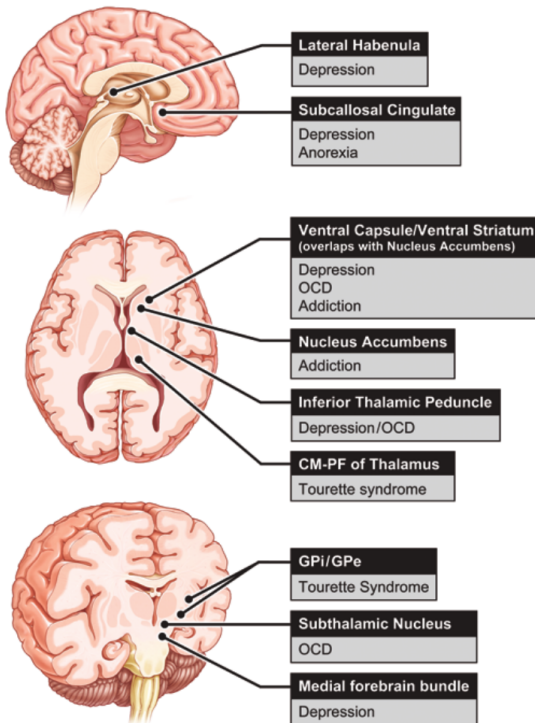


Figure 2.21: DBS targets for psychiatric diseases. Source: [103].

The article in [103] presents a detailed review of experiments and outcomes of DBS applied to Depression, Obsessive-Compulsive Disorder, Anorexia Nervosa, Tourette Syndrome, Addiction and Substance Use Disorder, Aggressive Behavior, and Posttraumatic Stress

Disorder. Only few psychiatric disorders will be treated in the next sections, please refer to [103] for more information.

DBS in Depression

20% of all depression (item 2.1.1) patients do not respond to any medication. They still experience the symptoms during several years of maximal medical and psychiatric therapy, including cognitive-behavioral therapy, pharmacotherapy, and electroconvulsive therapy (ECT). These are the patients eligible for experiments with DBS. Reduction of symptoms is achieved within some weeks of programming sessions. Once the improvements are achieved, they sustain for several years in some patients. Others need to have their implant reprogrammed. Once a response is achieved, it is usually sustained for as long as stimulation continues. Both battery depletion and accidental disconnections have resulted in rapid regression and even suicidal crises [103]. Among the targets being studied, the *Subcallosal Cingulate Cortex* stands out for the frequency it appears in literature. Increased activity in this region correlates with depression, and normalization of activity correlates with clinical response to treatment [104, 105, 106, 107]. Other targets have been used successfully for treatment of depression. They are shown in the table 2.1.

Authors & Year	No. of Pts	Study Type	Target	Results	Outcome Scale	Adverse Events
Mayberg et al., 2005; Lozano et al., 2008; Kennedy et al., 2011	20	Case series	SCC	64% response, 43% remission	HDRS	2 suicides
Puigdemont et al., 2015	5	Randomized, double-blind, sham-controlled	SCC	80% response	HDRS	
Puigdemont et al., 2012	8	Case series	SCC	62% response, 50% remission	HDRS	1 suicide attempt
Merkel et al., 2013	6	Randomized, double-blind	SCC	33% response	HDRS	
Holtzheimer et al., 2012	17	Open label, single-blind	SCC	65% response, 41% remission	HDRS	9 relapses w/ battery depletion
Lozano et al., 2012	21	Multisite case series	SCC	29% response	HDRS	1 suicide
Malone et al., 2009	15	Multisite case series	VC/VS	53% response, 40% remission	HDRS	
Dougherty et al., 2014	30	Randomized, double-blind, sham-controlled, multi-site	VC/VS	23% response; no significant difference btwn sham & control arms	MADRS	
Bewernick et al., 2010, 2012	11	Case series	NACC	45% response, 9% remission	HDRS	1 suicide
Schlaepfer & Bewernick, 2013	7	Case series	MFB	86% response by MADRS; 29% response by HDRS	MADRS, HDRS	
Kiening & Sartorius, 2013	1	Case report	LHb	Remission	None	
Jiménez et al., 2005	1	Case report	ITP	Remission	HDRS	

Pts = patients.

Table 2.1: DBS studies on depression. Source: [103].

DBS in PTSD

PTSD (item 2.1.4) affects 6.8% of the US population and is most common among military personnel and victims of disasters. Even with the most advanced pharmacotherapy and psychotherapy treatments, **30% of the patients remain debilitated by the condition [108]**. The brain Amygdala is the most important brain structure related to PTSD. Imaging studies have found an increased activity of the amygdala in patients with PTSD. **The increased activity is correlated with the degree of symptoms, and similarly, a decrease in amygdala activity corresponds to improvement and response to treatment.** The amygdala size is also known to be correlated with PTSD. Patients with PTSD tend to have their amygdala reduced in size [103].

During the year 2014, Jean-Philippe Langevin and Scott E. Krahl, in Los Angeles, conducted the first DBS experiment on a human to reduce PTSD symptoms (previously described in the item 2.1.4). The results were published in 2015 in the journal *Biological Psychiatry* (impact factor 10.255) [109]. Although the number of individuals is 1, therefore statistically insignificant, the results were impressive and are in perfect agreement with what is known about electrostimulation of the amygdala.

The patient is a 48-year-old United States veteran. He developed PTSD due to exposure to the bodies of allies and enemies. Even after 20 years of conventional antidepressant treatment, he could not be touched, slept on average 2 hours a night, had daily absence crises, *flashbacks* and terrible nightmares. His CAPS score (a test that evaluates the intensity of PTSD symptoms) was 119, which placed him among the most severely affected patients.

The patient was implanted with two bipolar electrodes in the basolateral nuclei of the amygdala, one pair of electrodes in each hemisphere. The parameters used were pulse width equal to 60 μ s, the frequency of 160 Hz, the amplitude of 1.4 V in the right amygdala and 0.7 V in the left amygdala. After the surgery, an imaging test was performed to confirm the location of the electrodes.

In the fifth month tensions were increased to 2 V and 1.1 V but again reduced to the original values in month number 6, after a worsening occurred. The increase in tension applied to the fifth month, in addition to the worsening CAPS score, led the patient to report different symptoms, such as being compelled to finish poorly finished projects and hobbies, and exaggerated self-esteem (see figure 2.22).

After eight months of treatment with DBS, his daily crisis of absence was reduced to monthly, his average sleep hours passed to 5h and his symptom score fell 37.8%.

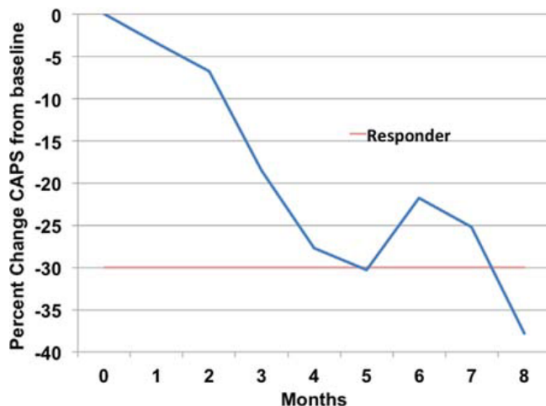


Figure 2.22: Development of the CAPS score of a patient implanted with DBS for PTSD. The red line represents the minimum CAPS score to be eligible for the study, according to the researchers definition. Source: [109].

The above-mentioned study presented two interesting facts: 1) the stimulation produced strong clinical effects, both therapeutic and side-effects; 2) the over-stimulation caused symptoms similar to the symptoms encountered in patients with bipolar disorders during the *mania* episodes.

2.8.3 DBS and EEG

Studies comprising the use of EEG measurement together with DBS stimulation are extremely rare due to its technological difficulties. The only mentioning-worth study found by the author describes the use of EEG to trigger DBS stimulation when brain beta oscillations exceed some thresholds, in the context of Parkinson Disorder: [58]. The system was implanted in a real patient and the study concluded that this closed-loop switch scheme led to better therapeutic results while strongly reducing the duration of the stimulations applied. Even though the control system was incredibly simple, the study proved the stimulation in closed-loop superiority.

3 MATERIALS AND METHODS

All animal handling and surgical procedures were carried by authorized personnel in the *Medical Sciences Laboratory - UFSC* in accordance to the local Committee for Ethics in Animal Research (CEUA-UFSC, project number 893), under the responsibility of Prof. Dr. Med. Roger Walz, co-advisor of this work.

The next paragraph presents the methodology in a simplified form. Deeper details will be presented in the next sections.

Subjects underwent a surgical procedure for implantation of DBS and ECoG electrodes. After some days of rest, they were subjected to three days of experimental sessions of 3 to 6 hours each. During the sessions, they received 10 minutes to 1 hour of stimulation while their ECoGs were recorded, and, in the sequel, were tested using the Elevated Plus Maze and Open Field (section 2.4). After the experiment, the animals were anesthetized and euthanized. Afterward, the brain tissue surrounding the amygdala electrode was electro-cauterized by applying a DC current to the electrode. The animals were then dissected and had their brains removed and sliced. The slices, marked by the electro-cauterization, were compared to a rat brain atlas to access the electrode position. The ECoG data were analyzed using the NRDTool, a toolbox for Matlab specially created for the purpose of this dissertation. The signals were analyzed using the algorithms of *Power Spectral Density*, *Correlation Dimension* and *Poincaré Plot*. The measurements obtained in the signal analysis were then compared to the behavioral tests measurements to investigate any relationship between the proposed ECoG metrics and the anxiety tests. In the next sections, each step of the previously described methodology will be presented in detail.

3.1 ANIMALS

The subjects were adult male wistar rats, (2 - 3) months old and weighing (200 - 300) g. While not under experimentation they were grouped in 4-5 per home cage and housed under controlled temperature ($22 \pm 2^{\circ}C$) in a 12-12 light-dark cycle for at least 7 days before initiating the experiments, with free access to food and water.

3.2 SURGICAL PROCEDURE

8-pin female *sockets* containing the insulated electrodes were implanted in the rats (figure 3.1). After deeply anesthetized the animal's skull surface was exposed and a dental screw was used to make one hole on the skull right above the right medial prefrontal cortex (coordinates: 4.5 mm anterior to bregma, 0.5 mm lateral to midline), where the two ECoG electrodes were kindly placed (see details in figure 3.2). Another hole was made for implantation of the monopolar DBS electrode inside the right amygdala (coordinates: 2.8 mm posterior to bregma, 5 mm lateral to midline and 8.5 mm below the skull surface). The socket was then attached to the skull using dental cement. Additionally, two screws were also implanted to be used as second DBS pole and ECoG reference. Animals were allowed 7 days of recovery after the surgery before any experiment. The implantation coordinates were obtained from [110].

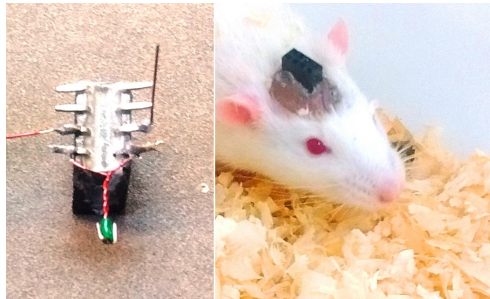


Figure 3.1: Rat socket. Left: Bottom view; Right: Socket after implantation.

All electrodes were composed of biocompatible materials. The two screws used for ECoG reference and DBS return electrode were 4 mm long with a diameter of 2 mm made of stainless steel. The wires connecting the screws to the socket, the DBS amygdala electrode, and the two ECoG wires were made with insulated nickel-chromium filaments of 0.3 mm diameter (red lines in the figure 3.2-right). The DBS electrode is completely insulated, except for its lower tip, allowing a circular electrical contact area of 0.070 mm^2 .

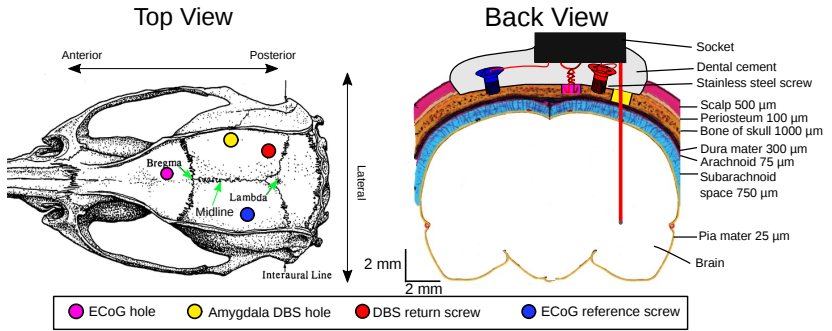


Figure 3.2: Rat implant schematic. Left: Top view; Right: posterior view. Adapted from: [111, 112].

3.3 PHYSICAL EXPERIMENTAL SETUP

During the experimental procedures, the animals were removed from their home cages and brought to an experimental cage (Plexiglas cage 30 cm x 25 cm) in which they stayed alone during the DBS stimulation in groups of up to three (see figure 3.3). The Plexiglas cages had a swivel coupled to its top, allowing free rotational movement of the subjects.

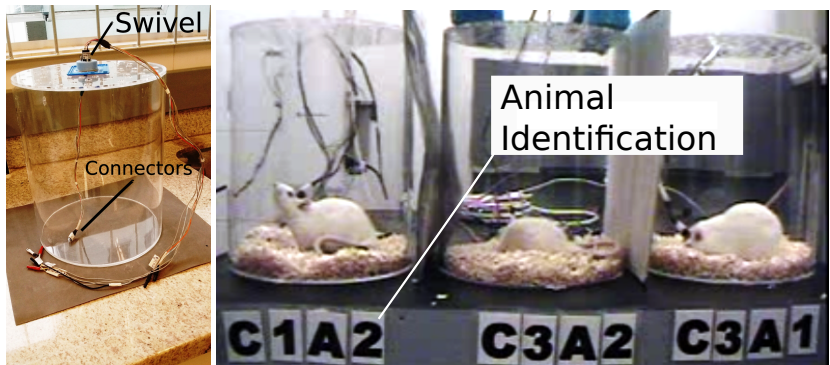


Figure 3.3: Cages used for the experimental setup. Left: photo of a plexiglas cage. Right: Image obtained from the monitoring cameras during experimentation.

The experimenter monitored the rats from a separated room through cameras and was instructed to turn off the stimulation at any sign of pain or suffering. The EEG system used to acquire the ECoG signal was the *EEG1200* (*Nihon Kohden, Japan*). The electrostimulation system used to apply the DBS signals was the *DBStation5* (*InPulse, Brazil*). All experiments were performed between 8 AM and 19 PM. The experimentation room has no window, what provides a better isolation from outside sounds. See the detailed physical configuration in figure 3.4.

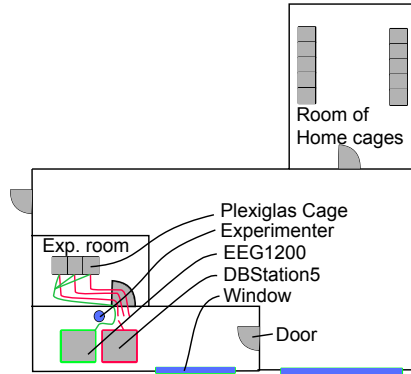


Figure 3.4: Physical setup of experimentation.

3.4 DEEP BRAIN STIMULATION

The DBS setup used was *monopolar*, *biphasic*, and *charge-balanced*. Monopolar in this context refers to the number of electrodes intended to affect the local brain activity (only one). The pole intended to deliver therapeutic current was implanted in the basolateral amygdala (BLA) (implant location in figure 3.5) and the other pole, intended to serve only as the return for current was a screw implanted in the skull external surface. The larger contact area of the screw in comparison to the area of amygdala (AMY) electrode is necessary to avoid the return pole to concentrate current and deliver unwanted DBS therapy. The monopolar configuration was chosen because it spreads more with increments in the current (as explained in the item 2.5.1), thus increasing the affected area within amygdala.

The stimulator *DBStation5* allows the configuration of 10 parameters. The stimulation *waveform* is defined only by the param-

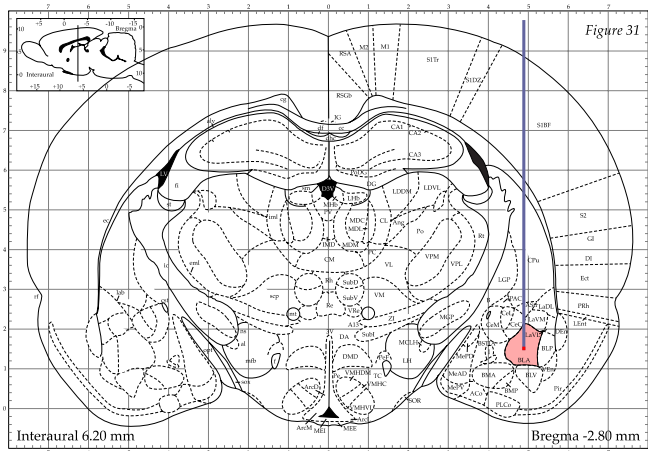


Figure 3.5: DBS electrode implantation (purple). The red tip represents the area with electrical contact with tissue. Adapted from: [110].

eters of *stimulation frequency*, *stimulation width*, and *neutral time width*. The device also allows the choice of extra parameters that influence how long the stimulation is applied and automatic increments/decrements in current. Therefore, the DBStation5 has also the following adjustable parameters: *delay to start*, *number of stimulation sections*, *initial amplitude*, *amplitude variation between sections*, *section duration*, *duration of rest between sections*, *number of sections*, *number of full process repetitions*. The figure 3.6 shows the adjustable parameters in a comprehensive way.

The stimulation parameters chosen for the experiments performed for this dissertation were based in the studies presented in the section 2.8.2. They are:

- pulse width: $90 \mu s$;
- neutral width: $90 \mu s$;
- frequency: $130 Hz$;
- start delay: $5 s$;
- delta amplitude: $0 \mu A$;
- num repetitions: 1.

The stimulation currents applied were $10 \mu A$, $50 \mu A$, or $100 \mu A$. Animals were stimulated either 1 time during 10 minutes (*section width = 10 min, num sections = 1, num repetitions = 1*) or 15 times of 1 minute stimulation intercalated with 1 minute rest (*section width = 1 min, rest width = 1 min, num sections = 30*). The experimentation protocols are better explained in section 3.6. Each animal received the same current amplitude during all experimentation days.

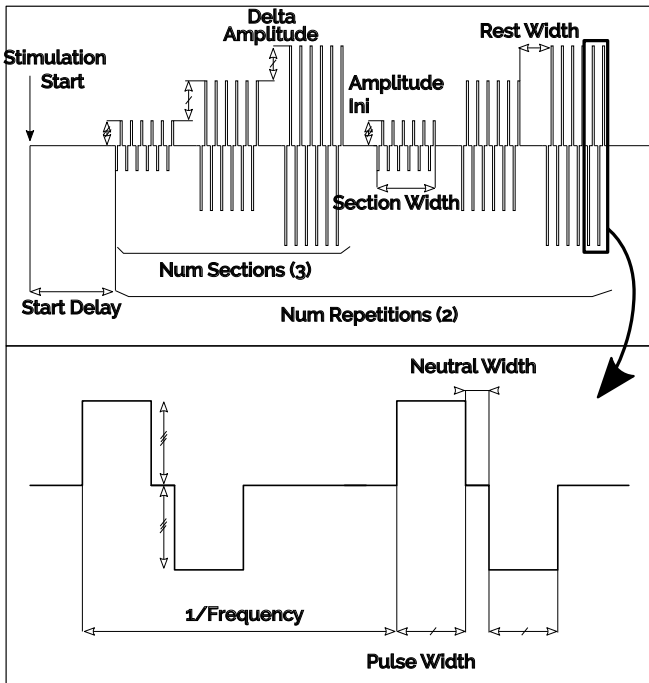


Figure 3.6: DBStation5 waveform and configurable parameters. Source: device datasheet.

Current Limits

Please note that the DBS electrode used has a contact area of 0.070 mm^2 , thus allowing a maximum current of $235.67 \mu A$, considering the charge density limit of 30 C/cm^2 explained in the item 2.5.3.2. The equation used to test the current max limit was de-

duced in this dissertation:

$$I_{max} = \frac{3 \cdot 10^5 \cdot A_{elec}}{P_w} \mu A, \quad (3.1)$$

where: P_w is the pulse width in microseconds, A_{elec} is the electrode contact area in squared millimeters.

3.5 ECoG

The rat brain neural activity was measured using ECoG. The ECoG was chosen because it is adequate to measure the *brain rhythms* and is fixed inside the body, making the measurement more robust to movement artifacts while having more sensitivity than the EEG and less invasive than the LFP. The measurement electrodes were implanted inside the bone of the skull, over the medial pre-frontal cortex (figure 3.7). The coordinates were presented in item 3.2.

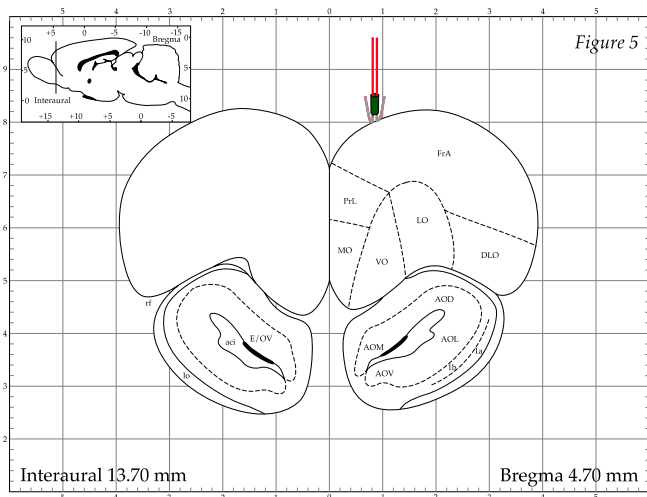


Figure 3.7: ECoG electrodes implantation. Adapted from: [110].

The device used for the ECoG measurement is the EEG1200 (presented in item 2.6.1.2). An adaptation in the connections was made to allow the measurement of multiple subjects simultaneously, because the device was not designed for this purpose (see figure 3.8).

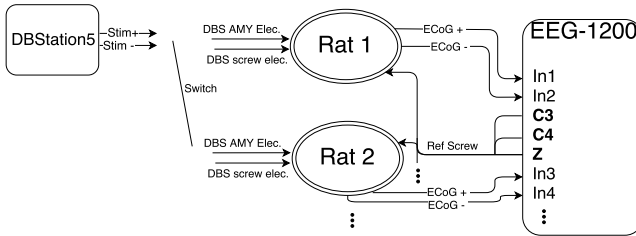


Figure 3.8: EEG1200 connections for simultaneous measurement of multiple subjects.

3.6 EXPERIMENTAL PROTOCOL

The experimental protocol was designed to acquire information of the animals normal brain activity before any DBS intervention, under continuous DBS stimulation (10 minutes), under intermittent DBS stimulation (1 minute on, 1 minute off repeated 30 times) and after all DBS procedures.

The animals were tested in the Elevated Plus Maze (EPM) right after DBS stimulation. Please remember that the EPM test can only be performed once in each animal, therefore it is present only in one day of the experiment.

The figure 3.9 presents a full schematic of the experimental sessions, which were divided into four days, explained below:

- **Day 0:** animals had their ECoG recorded for 3h under normal circumstances. The data acquired is used to access the brain state prior to the tests, and the normal values for each animal. It is also important to let the animals get used to the experimentation cage;
- **Day 1:** Animals receive 10 minutes of DBS stimulation. The stimulation current depends on the group of each animal ($10\mu A$, $50\mu A$, or $100\mu A$). The other stimulation parameters were the default parameters mentioned in the section 3.4. Animals stimulated received the process **DBS A**, while animals of the control group received no stimulation (process **DBS C**). Immediately after the stimulation, the animals were subjected to the anxiety test (Elevated Plus Maze - EPM). After, they were transferred to the motor test (Open Field - OF). Finally, their ECoGs were recorded during 3 hours;

- **Day 2:** The same stimulation applied in *Day 1* was applied in the *Day 2*. But, this time, the ECoGs were recorded uninterruptedly after the stimulation process. The objective is to access the brain activity dynamic right after the stimulation;
- **Day 3:** Animals received the process *DBS B*. This new process repeats the stimulation and rests thirty times, but during only one minute. The purpose of this is to evaluate what happens in the brain as the DBS stimulation starts or stops, and how repeatable these changes are. The stimulation current was the same amplitude they received the previous days, except for the control group, that received the stimulation for the first time.

In the following days after experimentation, the animals were deeply anesthetized and euthanized. Afterward their brains were electro-cauterized by applying a DC current of 7.5 mA for 30 s in the same socket pins used for the DBS application. The laboratory team sliced the brain in 100 μm thick slices and accessed the electrode positioning visually using 10 fold amplification and comparing with the rat brain atlas ([110]).

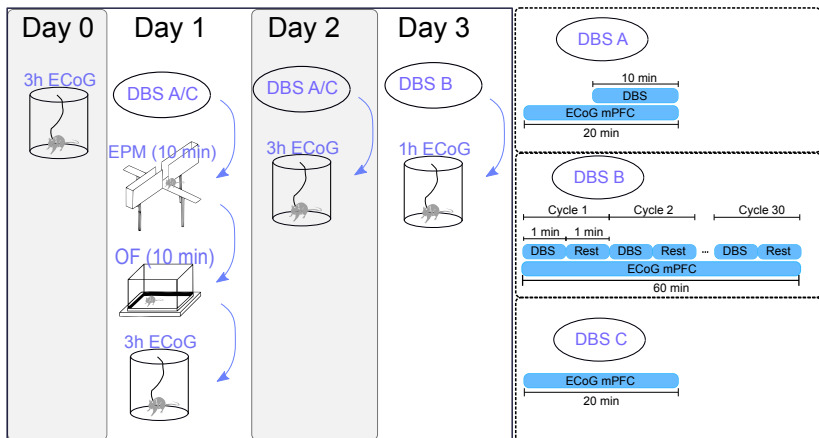


Figure 3.9: Experimentation protocol.

3.7 DATA PREPARATION AND ANALYSIS

The data analysis was performed using the NRDTTool, a Matlab toolbox created in this dissertation (see figure 3.10). It is not yet publicly available, but people interest in contributing may contact the author at nicholas.drabowski@gmail.com. The algorithms used as the basis were explained in the section 2.7: PSD, Correlation Dimension, and Poincaré Plot.

The *spectral analysis* using PSD was chosen because of its simplicity, and because it is the most used tool for analysis of ECoG signals in literature. Although not fully understood, the rhythms also provide some insights on what level of mental functions are being processed in the brain. The *correlation dimension* was chosen because of its efficacy when used as a feature for classification in the context of psychiatric diseases. The *poincaré plot* was chosen because it is widely used for analysis of chaotic systems, but was not yet widely explored for brain signals analysis.

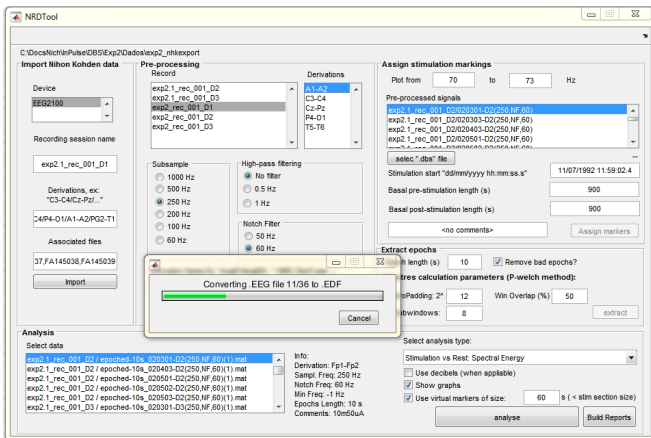


Figure 3.10: NRDTool toolbox.

The signals exported from the EEG1200 system, sampled at 1 kHz, were imported in the NRDTTool. The EEG1200 files are saved in one file per hour, which were concatenated in Matlab. Signals were then sub-sampled to 250 Hz after being phase-compensated-filtered by an eighth order low-pass Butterworth with the cut-off frequency in 100 Hz. The sub-sampling process was necessary for the enhancement of computational performance. The signals were

then notch-filtered at 60 Hz. For each ECoG file, the periods of stimulation (*stimulation markers*) were assigned accordingly (figure 3.11). The markers received four possible tags:

- *Basal Pre-Stimulation*: 10 minutes before stimulation. Contains the animal ECoG prior to the stimulation;
- *Stimulations*: Moments in which the animal received DBS stimulation;
- *Rests*: It is always the first minute after the stimulation stops;
- *Basal Post-Stimulation*: 10 minutes immediately after stimulation.

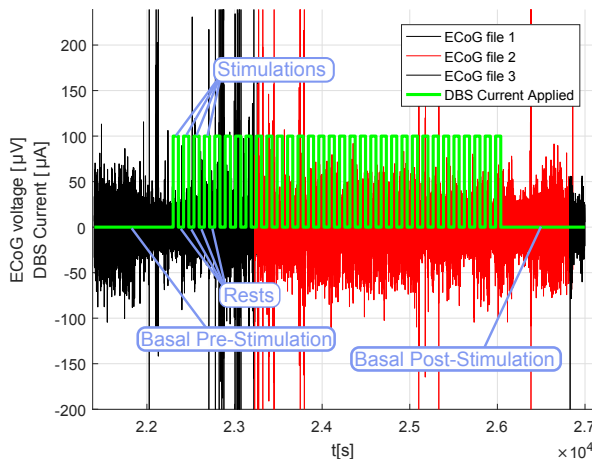


Figure 3.11: ECoG signal imported and its stimulation times marked (green line). This sample is the protocol DBS B, acquired in the third day of a subject experimentation.

The signals were then divided into 10 s long epochs. The epoch segmentation was designed to avoid creating epochs containing signal from different markers, and each epoch received the tag of its marker. The algorithm *FASTER* (*Fully Automated Statistical Thresholding for EEG artifact Rejection* [113]) is an automated method for detecting outlier epochs from statistical analysis

of a long EEG signal. The algorithm was simplified for the single-channel measurement used in this dissertation and applied to the signals. A result example of this pre-processing phase is shown in figure 3.12.

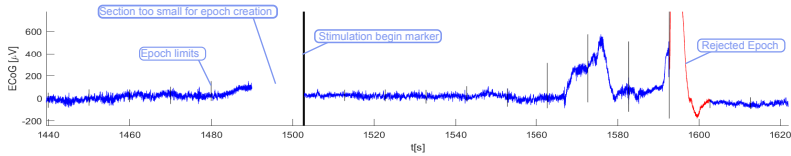


Figure 3.12: ECoG signal segmented in epochs and marked.

After importing the data, preprocessing, segmenting in epochs and removing epochs contaminated with artifacts, the signals passed through 5 different types of analysis. The graphs generated were automatically saved as a report document (40 pages in total). One report per animal per experimentation day was generated (21 reports in total).

In the sequel, the graphs generated in the reports will be presented and explained.

PSD Analysis

The figure 3.13 compares the averaged spectral content of the four sections of a DBS session (basal pre, basal post, stimulation, and rests). Each epoch of 10 s not removed by the FASTER algorithm had their spectrum calculated using the P-welch method with 8 hamming windows 50% overlapped and zero padding with 2^{12} points. The average and standard error were calculated using these specters. The frequency bands of the brain rhythms are drawn in the background. The graph is in the log-log format. The dotted lines show the standard error over frequency. The hole process used to build this graph is illustrated in the figure 3.14.

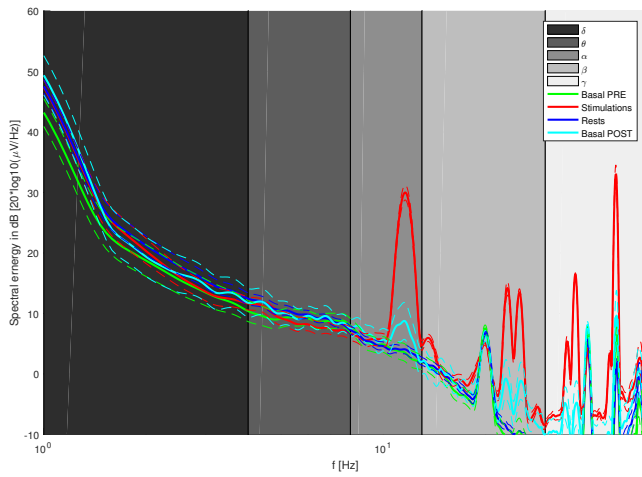


Figure 3.13: PSD graph comparing signal sections.

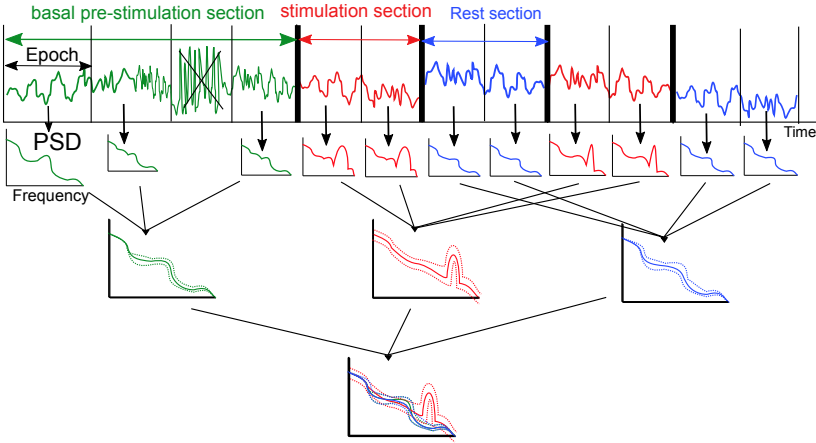


Figure 3.14: Process used to build the spectral graphs. The epoch marked with a black 'X' represent the epochs discarded by the adapted algorithm FASTER. The *Basal Post-stimulation* section was omitted for simplicity.

Additional graphs were created for exploring each brain rhythm isolated. The difference is that it is filtered in the rhythm band before the PSD calculation, what produces a purer visualization from the independent rhythms. See, for example, the graph created for the rhythm α in the figure 3.15.

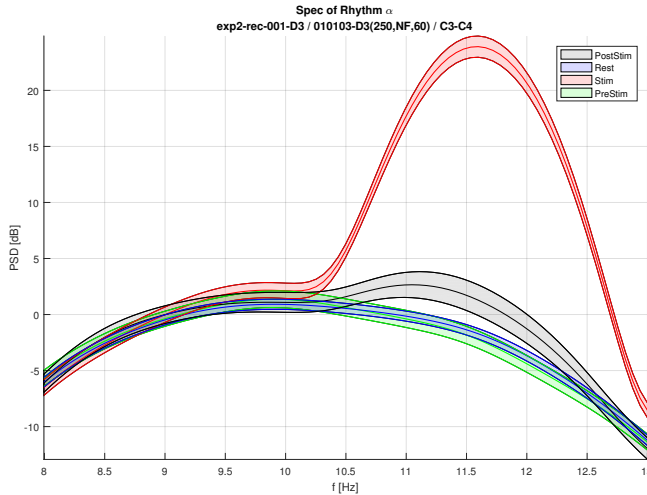


Figure 3.15: Alpha rhythm isolated in spectre. Note that this visualization is less contaminated with spectral leakage and ripples of other frequencies outside the rhythm band.

The graph 3.16 summarizes all spectral graphs in one. It shows the comparison between spectral rhythms integrated, i.e. the average energy of each rhythm and standard error. The next graph (3.17) is an adaptation containing the same information, but it was normalized by the basal pre-stimulation energies. In other words, values of Stimulation, Rest, and Basal-Post are percentages of the energies measured in the Basal Pre-stimulation. The error bars are calculated using the standard error:

$$StandardError = \pm \frac{\sigma}{\sqrt{E - 1}} \quad (3.2)$$

where: σ : it's the estimated standard deviation; E : is the number of epochs used to calculate σ . Bad epochs that are removed alter the value of E .

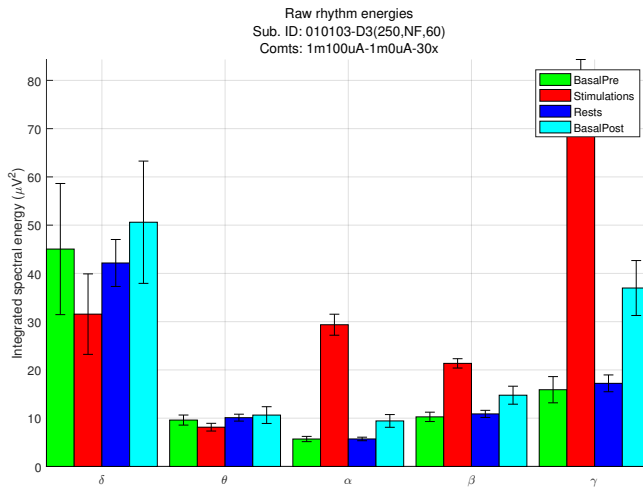


Figure 3.16: Graph example of mean energies contained in each exam section.

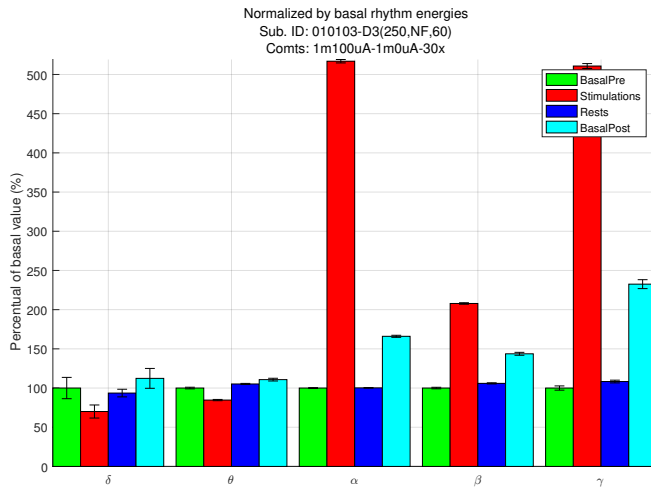


Figure 3.17: Mean energies normalized by basal pre-stimulation values.

One last graph (3.18) type was built for each rhythm, showing the rhythms energy development over time, instead averaging it.

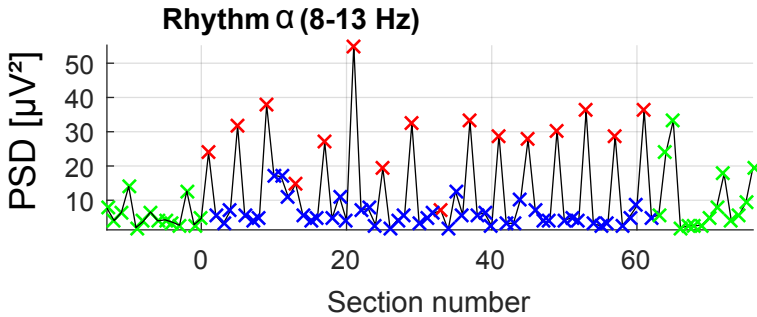


Figure 3.18: Brain rhythm energies development over time. Each 'x' represents 1 minute of signal averaged. The green crosses represent the sections *basal pre* and *basal post*, the red represent the stimulation, and the blue the rests.

Poincaré Analysis

An example of the Poincaré plots built for the ECoG data is in figure 3.19. One graph per epoch was plotted, and the values of SD1, SD2, Slope, and SD1/SD2 were extracted. Each pair of neighbor points in the ECoG signal is plotted as one single green dot in this graph; this process embeds one additional dimension to the signal. The development over time (from each epoch) of the values extracted from this graph were plotted in graphs like 3.20. Finally, the averaged values and their standard error were plotted in the graph 3.21.

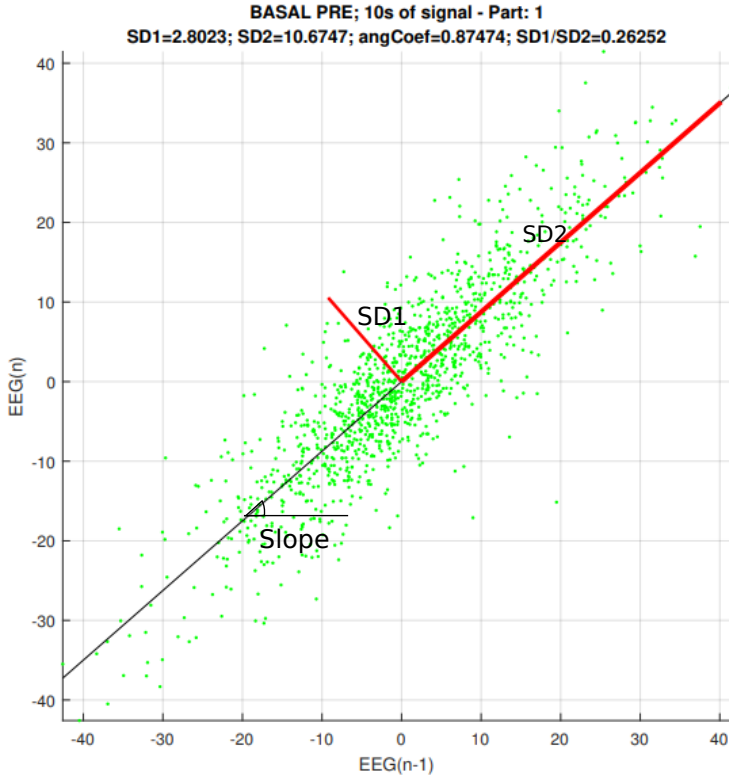


Figure 3.19: Poincaré Plot.

From each epoch of 10 seconds an independent Poincaré plot was constructed, and the four parameters give rise to the graph in the Figure 3.20. The colors of the graph represent the different stimulation sections.

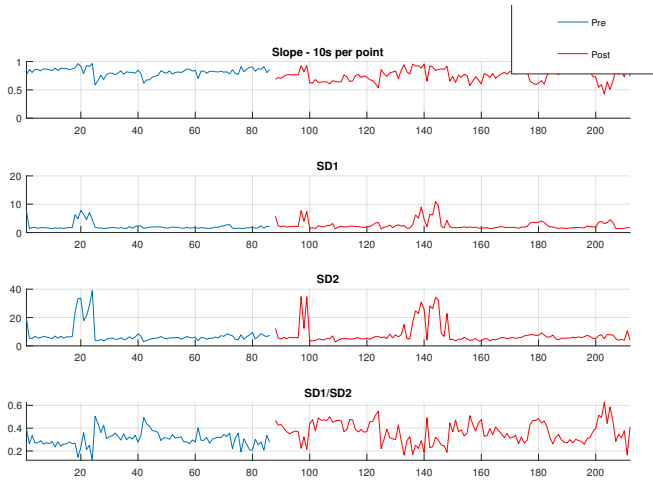


Figure 3.20: Development of poincare plot parameters over time.

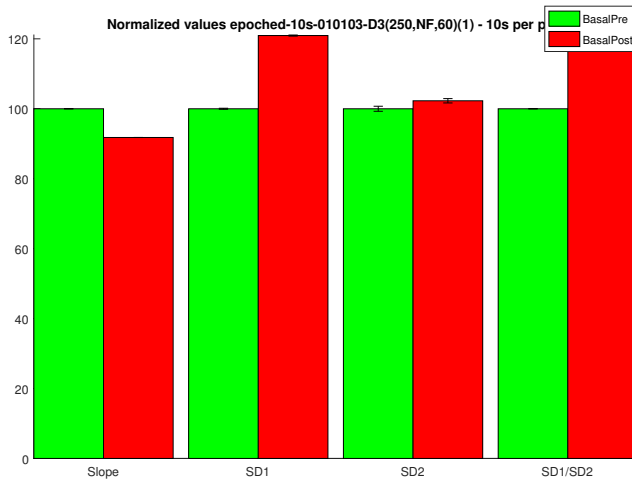


Figure 3.21: Mean values for Poincaré parameters and their standard error.

Correlation Dimension Analysis

The correlation dimension values were also calculated over time for each animal exam 3.22. The averaged values were plotted in graphs similar to 3.23.

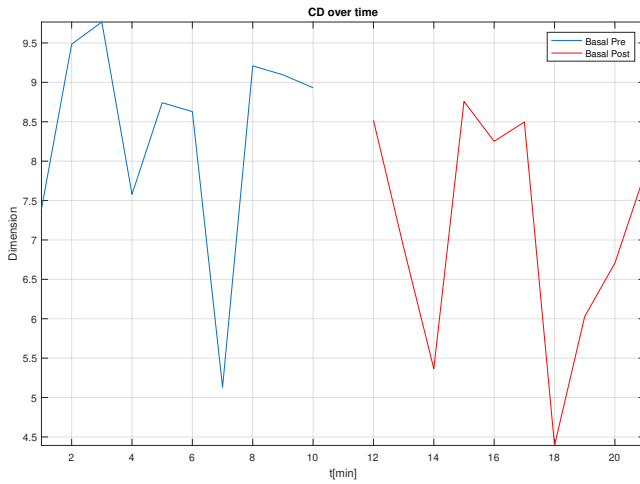


Figure 3.22: Correlation dimension values development over time for a rat ECoG.

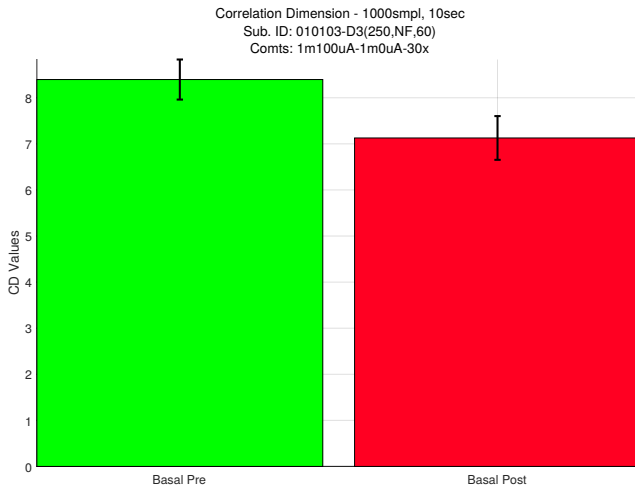


Figure 3.23: Averaged correlation dimension values and the standard error.

3.7.1 Feature extraction from previous analysis

All the graphical analysis presented before served as a basis for extraction of features. These features were, for example, areas under rhythms in PSD, relations between these areas and the areas of other rhythms, mean correlation dimension, etcetera. In total, **112** features have been extracted from all three analysis (PSD, Correlation Dimension, and Poincare map). The figure 3.24 presents some of the features extracted from the PSD specter.

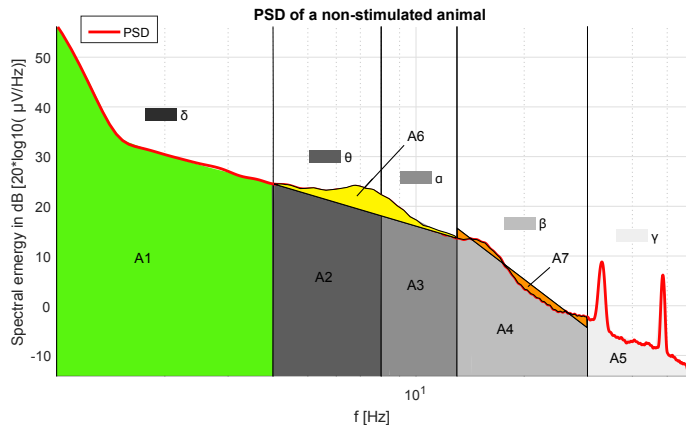


Figure 3.24: Example of features extracted from the algorithmic analysis. Observation: some features are calculated on the PSD graph in *decibels* (A6 and A7, for example) while others are calculated from the PSD in *magnitude* (A1-A5, for example).

For example, amongst the 112 features extracted there are some types such:

- raw areas under the rhythms (A1 to A5);
- proportions of areas of rhythms such as $A3/A2$, $(A2 + A3)/A1$;
- ripples measured in relation to the $1/f$ curve (A6, calculated over two rhythms together);
- ripples measured in relation to the best fitting curve (A7 for the beta rhythm);
- other relations such $A7/A6$, $A7/A4$, $A6/(A2 + A3 + A6)$

The coefficients of determination (r^2) between every single feature and the values resulting from the anxiety tests (item 2.4) were calculated. The features with higher determination coefficients were used to assess anxiety levels in the animals.

4 RESULTS

SUMMARY OF RESULTS

The results presented in this chapter consist of three parts:

1. creation of an anxiety biomarker;
2. analysis of the DBS effects on the anxiety biomarker;
3. analysis of the DBS on brain activity

In total, 26 animals were used in the experiments. Due to technical difficulties, only 17 of them were eligible to be used for investigation of ECoG anxiety biomarkers.

The anxiety tests of these animals were compared against 112 features calculated from their ECoG signals using the Pearson's correlation. Three of these features were found to be statistically correlated with anxiety. Two of these features were combined to build a two-dimensional graph of anxiety, which is used in this dissertation as the anxiety biomarker. The process used to build this biomarker is presented in the section 4.2.

The post mortem tissue analysis of the electrode placements revealed that this process is not perfect, i.e. there is a random error in position in each placement. Therefore, the animal with the DBS electrode placed in the AMY more precisely is treated separately in this chapter, because its results are inferred to be the most trustworthy to the DBS inside AMY itself. From now on, this animal is referred to as the *Gold Standard Animal (GSA)*. In the other subjects, the AMY electrodes were placed in the areas surrounding the AMY, what brings some uncertainty aspects to the analysis, since the DBS electrical field may also be affecting other neighbor brain structures known to influence the anxiety.

The previously discovered anxiety biomarker was used to investigate the **DBS effects on anxiety** in the 17 subjects plus the GSA. Therefore, the GSA's data was purposely not used in the biomarker creation. It was clearly observed that the application of DBS reduced the GSA's anxiety instantaneously. After the stimulation ceased, the anxiety level slowly increased and returned back to its original value after approximately 30 seconds. These same findings could be observed in some of the other subjects (specially those stimulated with 100 μA). The complete results are presented in the section 4.3.

The final section of this chapter (4.4) presents other general effects observed in the brain activity of subjects due to the DBS stimulation only (section 4.4).

The selection of the data samples for each above-mentioned study and the technical problems involved in the process are explained in the section 4.1.

4.1 ANIMAL SAMPLE

The study started with 26 animals. One of them had to be excluded from the study because it got sick after surgery and other had a bad healing process. From the 24 remaining animals four had to be excluded from study due to problems with the ECoG measurement. One of them had their head socket gnawed, other learned how to pull-off the cable from its socket during the experiment. In the other two of them the measurements were in extremely bad quality, probably due to a bad contact between tissue and ECoG electrode. It resulted in remaining 20 animals with good ECoG measurements.

From the 20 animals 80 ECoGs were recorded, one record per animal experimentation day (D0, D1, D2, D3), according to the experimental protocol (figure 3.9), with 60 of them with DBS sessions (D1-D3). The day with anxiety measurement after ECoG recording were the D1. Amongst these records 2 were in bad quality and had to be excluded. The resulting 18 exams, excluding one that was from the GSA, were used to produce the results found in the section 4.2), which is: to build anxiety biomarkers.

In the group of 20 animals, 9 were part of the control group (received no DBS stimulation). The remaining 11 animals were used to study the effects of DBS in their ECoG measurements (results presented in section 4.4).

One of the remaining 11 animals had the DBS electrode perfectly positioned inside the amygdala. It was used to access the effect of amygdala DBS stimulation on anxiety. This animal is treated in this chapter as the gold standard animal (GSA). The remaining 10 animals had the electrode positioned outside the AMY (5), partially outside AMY (3), or the electrode position couldn't be accessed due to unknown problems in the electro-cauterization process (2).

For better understanding, the animal sampling process is represented graphically in the figure 4.1.

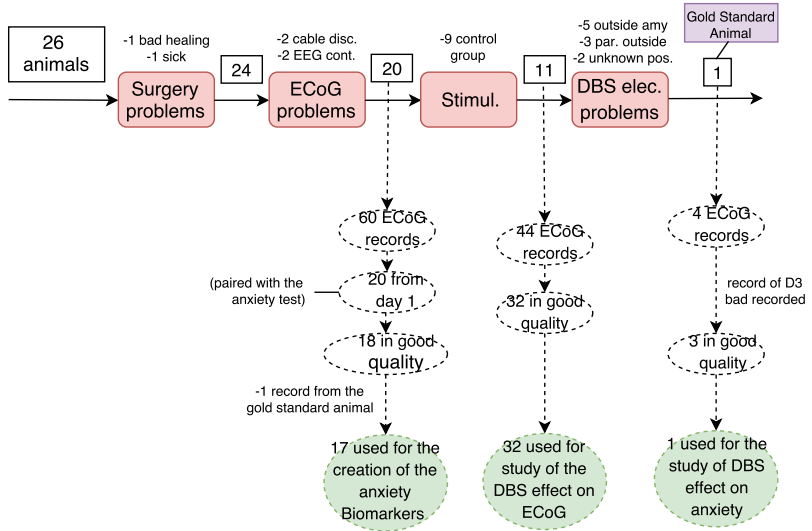


Figure 4.1: Animal sampling process. This figure presents technological difficulties that led part of the data to be discarded..

4.2 CONSTRUCTION OF AN ECOG BIOMARKER FOR ANXIETY ASSESSMENT

Three of the 112 features extracted from the algorithmic analysis (algorithms presented in 3.7) were found to have statistical significance to anxiety. The names given to them were BM22, BM29 and BM57. See in the table 4.1 the Pearson's coefficient and p-values found. The calculation of each of these three features from the ECoG signal is presented later in this section.

Table 4.1: Anxiety Biomarkers.

	Pearson's correlation (r)	p-value	number of samples
BM22	0.5569	0.020	17
BM29	0.5423	0.024	17
BM57	0.5233	0.031	17

The graphs from which the correlation coefficients were calculated are presented in the figure 4.2. Note that all the three

biomarkers rise with increasing anxiety (i.e. positive slope). Since the anxiety values were obtained from the Elevated Plus Maze test, it is expected that the valid values must be in the range between 0 to 100%. Also, the threshold between stressed and relaxed is 20%. Below that value animals are considered anxious while values above mean the absence of stress (relaxation).

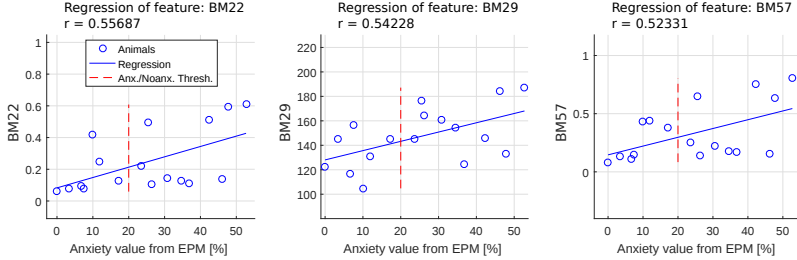


Figure 4.2: Regression lines for the three best fitting features. Note that all three biomarkers rise with anxiety.

It follows from the regression lines presented in the graph above that the anxiety can be estimated using three independent equations:

$$A_{22} = 153.23 \cdot BM_{22} - 12.68 \quad (4.1)$$

$$A_{29} = 1.327 \cdot BM_{29} - 168.69 \quad (4.2)$$

$$A_{57} = 132.44 \cdot BM_{57} - 19.33 \quad (4.3)$$

where: A_{22} , A_{29} and A_{57} are anxiety measures, and BM_{22} , BM_{29} and BM_{57} are the features (or biomarker candidates) calculated from the ECoG PSD in dB. These three features happened to be simply the ratio between the PSD variation and the mean PSD in the bands of interest. The features were calculated using the following equations:

- BM_{22} is the integrated absolute error between spectrum and the best fitting line in the alpha rhythm divided by the mean al-

pha rhythm (band between 8 and 13 Hz), or, mathematically:

$$BM22 = \frac{\int_{f=8}^{13} |PSD_{dB}(f) - L_{8,13}(f)| df}{L_{8,13}(10.5)} \quad (4.4)$$

where: $L_{8,13}$ is the best fitting line calculated between 8 Hz and 13 Hz, $L_{8,13}(10.5)$ is estimated power of the center of the alpha rhythm band.

- BM29 is the integrated absolute error between spectrum and the best fitting line in the gamma rhythm, or, mathematically:

$$BM29 = \int_{f=30}^{60} |PSD_{dB}(f) - L_{30,60}(f)| df \quad (4.5)$$

where: $L_{30,60}$ is the best fitting line calculated between 30 Hz and 60 Hz.

- BM57 is the integrated absolute error between spectrum and the line connecting the beginning and the end of alpha band, or, mathematically:

$$BM57 = \frac{\int_{f=8}^{13} |PSD_{dB}(f) - L_{8,13}(f)| df}{L_{8,13}(10.5)} \quad (4.6)$$

where: $L_{8,13}$ is the line connecting PSD(8 Hz) and PSD(13 Hz).

Note that the BM57 is calculated in the same band as BM22 (alpha), therefore they are dependent. The only difference between them is how the line is calculated. Given this fact, the BM57 will be ignored for now on, and assumed to be redundant to the BM22.

The figure 4.3 shows the parameters used for calculation of the biomarkers.

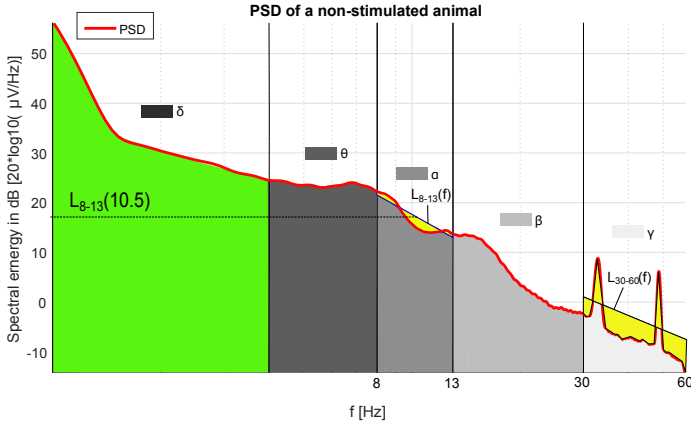


Figure 4.3: Indexes used for calculation of BM22 and BM29.

Using the BM22 and BM29 as classification features and the anxiety as class, a simple support vector machine (SVM) classifier with a Radial Basis Function kernel was trained using the Matlab's toolbox *Statistics and Machine Learning Toolbox* (see the figure 4.4). All the 17 brain measurements were standardized by their mean and standard deviation and then used as training set. Since the dataset is too small, there was no test and validation sets. The SVM classifier is used as a mean to create a simple threshold that separates the two groups. The dots represent measurements of the biomarkers calculated on the 10 minutes of brain activity recorded immediately before the EPM test, in 17 animals, thus it is a 'photography' of the brain state in these ten minutes. Animals with EPM tests result bigger than 20%, thus non-anxious, are the blue dots, while animals with EPM results below 20%, thus anxious, are the red dots. The background color shows the classification map of SVM.

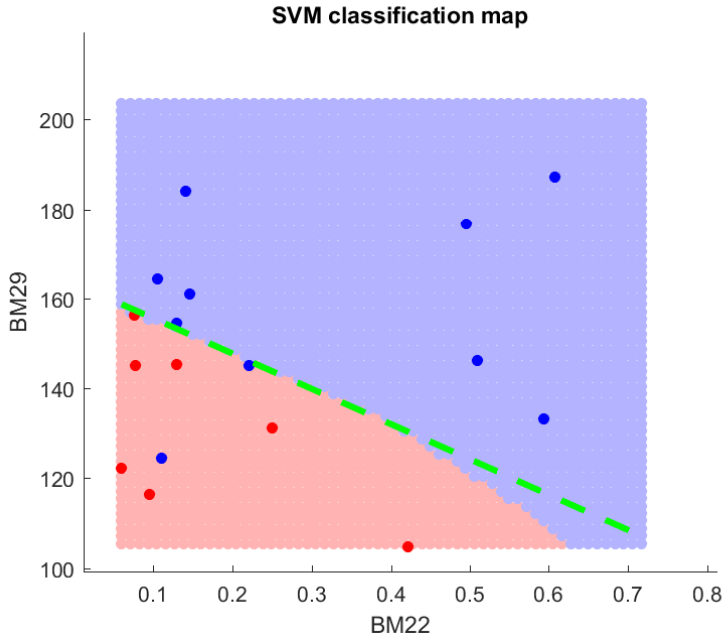


Figure 4.4: SVM classifier for anxiety using two biomarkers. The pale red area define the region in which the points are classified as anxious by the SVM, while the blue pale area mean non-anxious points.

As the figure shows, the classification surface can be simplified down to a line, which separates the two classes:

$$0 = -BM_{29} - 78.3747 \cdot BM_{22} + 163.4025 \quad (4.7)$$

Also, a pair of biomarker values resulting in a point above the line represent an anxious state, while points below the line mean absence of anxiety. This map and the biomarkers are used in the next section for assessment of anxiety under DBS stimulation.

4.3 DBS EFFECT ON ANXIETY

In the gold standard animal

The data from the GSA was applied to the anxiety classification map built in the item 4.2. In case you don't know what the GSA is, please read carefully the item 4.1.

The biomarkers BM22 and BM29 were calculated for each minute of the experiment of the day 2 of the experimental protocol. Points outside the SVM map were considered outliers and removed because they are probably result of a movement artifact. The remaining points were then averaged in the 10 minutes to provide only one point for each of the sections: 1)pre-stimulation, 2)under stimulation and 3)post stimulation. The result is shown in figure 4.5.

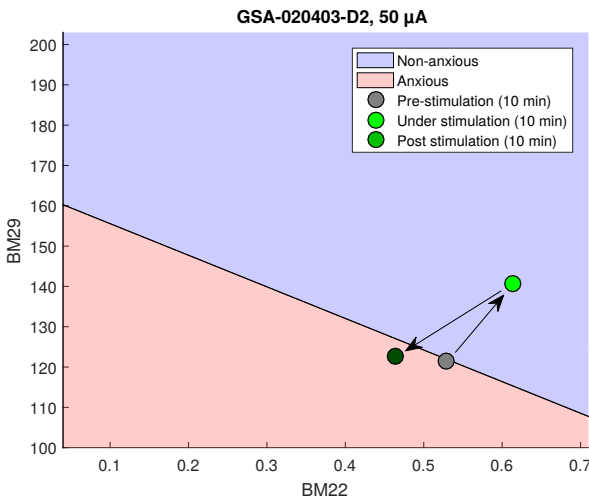


Figure 4.5: DBS effect on the GSA's anxiety. Each point represents 10 minutes of brain signal.

As observed in the Figure 4.5, the DBS stimulation in this animal ($50 \mu A$) caused its brain activity to move from the anxiety sector of the graph to the non-anxious sector, therefore instantaneously reducing the animal's anxiety. After the stimulation ceased, the brain activity returned to the anxious area. In other words:

the average brain activity during 10 minutes of stimulation

presented reduced anxiety in comparison to the 10 minutes before and after, therefore revealing the existence of an acute anxiolytic effect of DBS.

For a better understanding of the anxiety *dynamic* under DBS, the previous figure were exploded in its 10-second epoch points. The points were then moving-averaged on 1 minute (6-sample sliding window). The exploded graph is shown in figure 4.6. Although there is a considerable variation of the brain activity inside 10 minutes of experiment, it becomes clear that the average brain activity is shifted to a less anxious state during the 10 minutes of DBS stimulation, as the arrows presents. 1.0

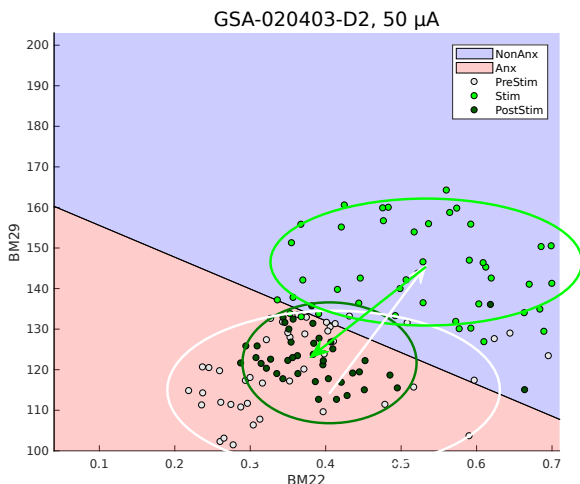


Figure 4.6: DBS effect on anxiety in the gold standard animal (day 2 of the experimental protocol). Each point represents 10 seconds of brain signal. The ECoG were acquired during 10 minutes prior to the stimulation, then 10 minutes of DBS was applied, then 10 minutes after stimulation were recorded.

Additionally to the SVM map, the anxiety values calculated using the equations found in the previous section are also presented here, in the figure 4.7. Sadly, the graphs are inconclusive because they do not present a clearly visible pattern that differs between stimulation and non-stimulation parts. The reason is probably because the correlations between each biomarker alone and

the anxiety are low and there is a lack of robustness against other brain changes not related to the anxiety. Considering the before-mentioned facts, from now on, the SVM map will be used as the only measurement of anxiety, and the A_{22} , A_{29} and A_{57} will be ignored.

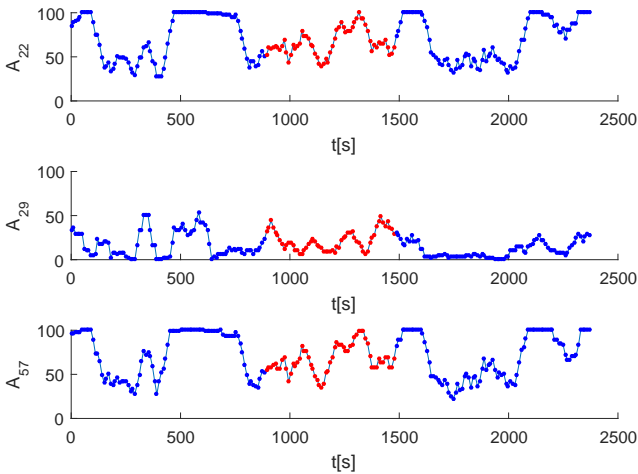


Figure 4.7: The three anxiety measures over time. Each graph alone does not show any clear distinction between the stimulation and no stimulation parts. Note that the measures A_{22} and A_{57} are well correlated, therefore one of them could be ignored.

In the day before, D1, the animal was already in a relaxed state, and the DBS seemed to have no effect in its anxiety (figure 4.8).

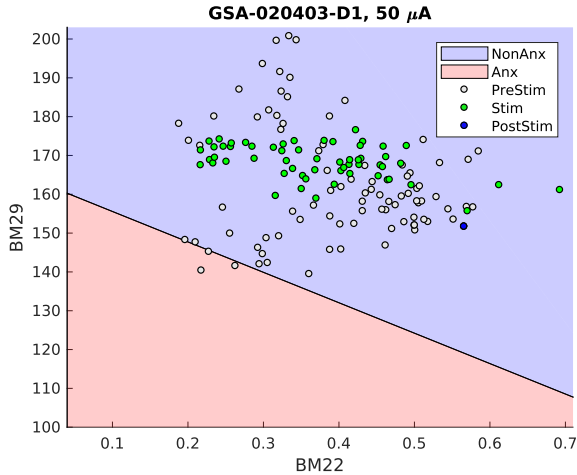


Figure 4.8: DBS effect on anxiety in the gold standard animal (Protocol day 1). There are not many points corresponding to the 'Post-Stim' because in the D1 the animals were rapidly moved from the ECoG measurement to the anxiety test.

Sadly, the signal quality of the ECoG data from the GSA animal in the third day degraded and could not be used. Probably, the electrodes lost contact with the brain tissue, therefore it was not possible to access the data of the same animal in the third day.

In the other animals

First, the analysis of the animals that **were not stimulated** revealed the baseline dynamics of the animals anxiety. There is no clear separation among two consecutive periods of ten minutes. An example is shown in the figure 4.9.

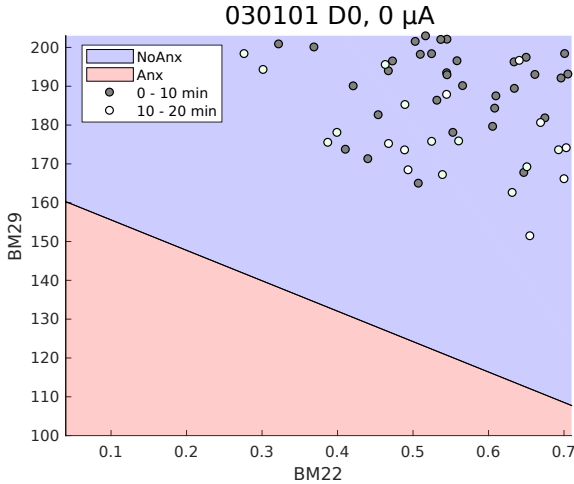


Figure 4.9: Anxiety dynamics observed in an animal of the control group (not stimulated). The other animals of the control group presented a similar distribution of brain measurements, but with different mean values.

The results observed in animals that received stimulation but the electrode wasn't perfectly inside the AMY will be presented in the sequel.

The other two animals that were stimulated with 50 μA (the same current as the GSA) also seemed to present an instantaneous acute reduction of anxiety, as observed in the figures 4.10 and 4.11. Sadly, the post-stimulation parts of these animals have few points because in the day 1 of experimentation, they were removed from the ECoG measurement immediately after the stimulation and sent to the elevated plus maze test. Surprisingly, the direction of the shift in the brain activity is different in each one of the three animals, although they all seem to become less anxious.

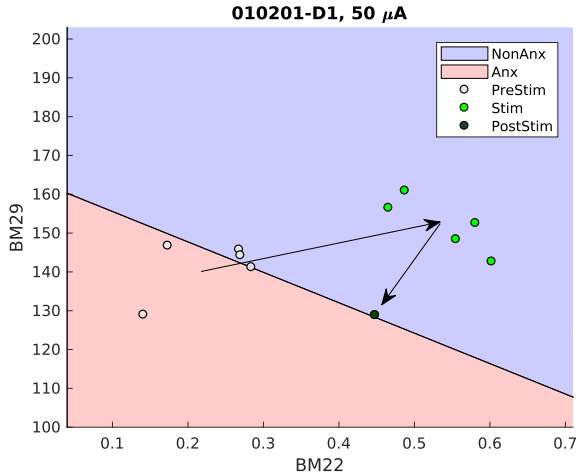


Figure 4.10: Animal stimulated with 50 μ A outside amygdala. The figure reveals that the stimulation had the same ansiolytic effect previously observed in the GSA.

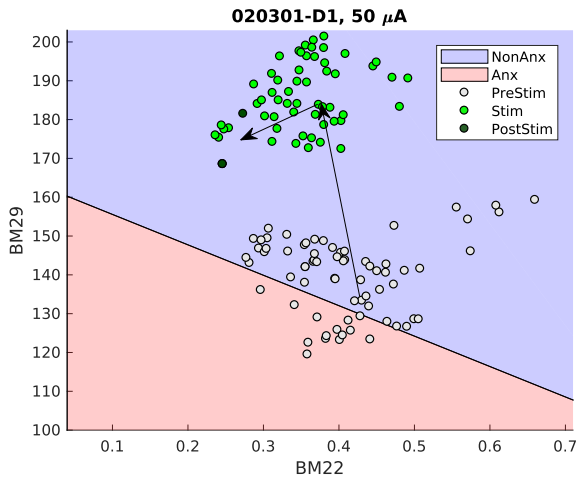


Figure 4.11: Another animal stimulated with 50 μ A outside amygdala. The figure reveals that the stimulation had the same ansiolytic effect observed in the GSA and the subject 010201 (4.10).

In the case of animals stimulated with $10 \mu A$, the DBS didn't have any visible effect on anxiety (see two examples in the figure 4.12). This may have three possible causes: 1) the amplitude of $10 \mu A$ is too low to cause any effect on anxiety from outside AMY; 2) these animals have the electrode implanted too far from the AMY; 3) they didn't present anxiolytic effect because they were already relaxed.

In the special case of the animal 020503 one can even argue that an increase in anxiety took place, although there is a big intersection between stimulated and no stimulated points.

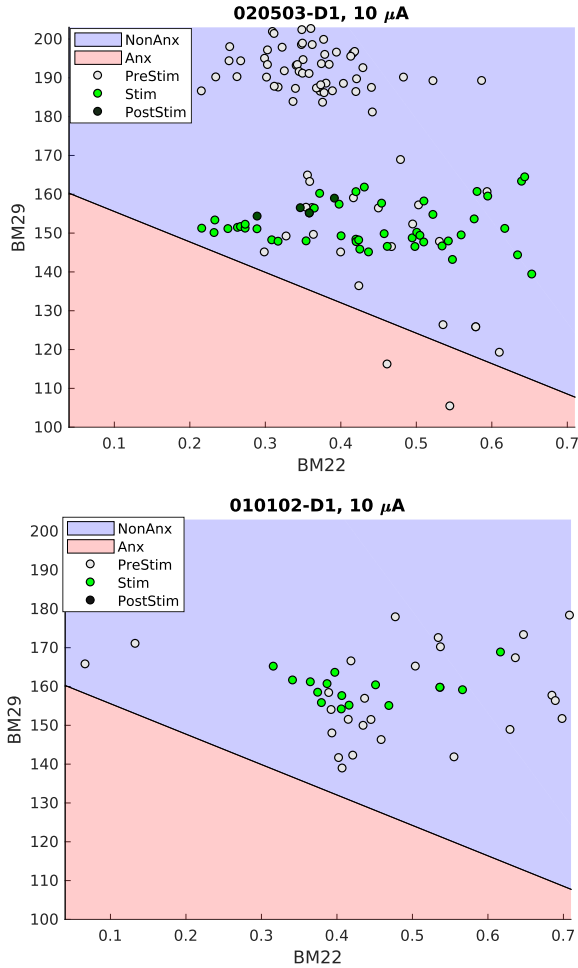


Figure 4.12: DBS effect in an animal stimulated with 10 μ A only.

Animals stimulated with 100 μ A outside AMY also did not present clear DBS effect on anxiety, although some very small shift in the points may be present. See two examples in the figure 4.13.

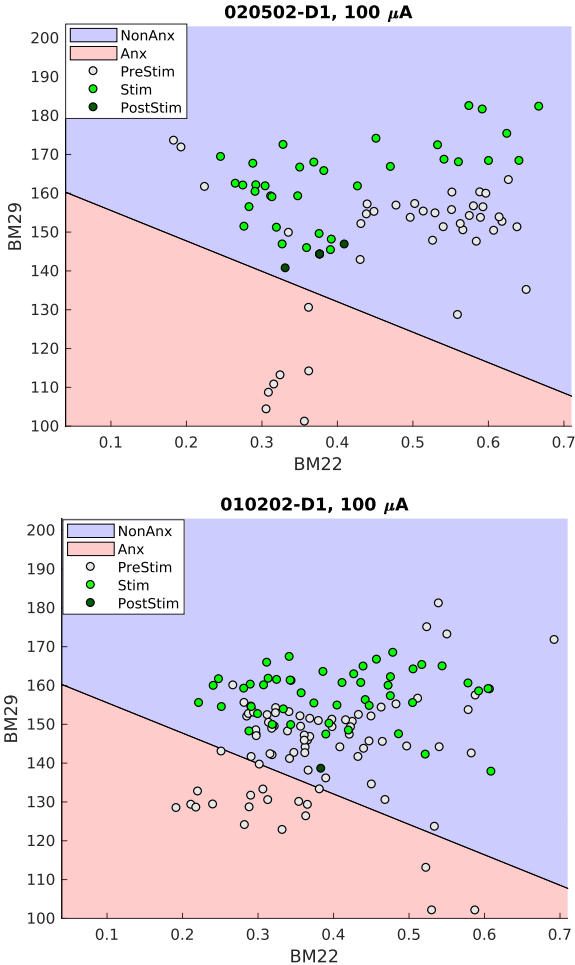


Figure 4.13: Animal stimulated with 100 μ A. It seems that there is a very small overall reduction on anxiety during stimulation, although the DBS electrodes were outside AMY.

A third animal stimulated with the same current (100 μ A) do not show any visual difference in its anxiety under stimulation. Probably, in this animal, the electrode positioning was further, or in a place outside AMY with less effect on anxiety. What is special in this subject in comparison to the two previously presented is that the green points seem to be shifted towards a slightly more anxious

state. See the figure 4.14

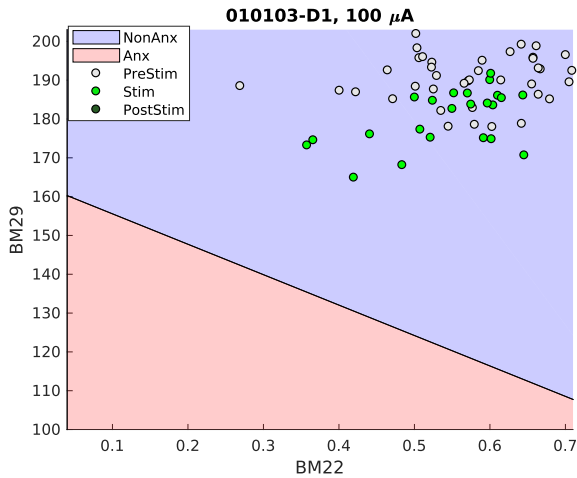


Figure 4.14: The third animal stimulated with 100 μ A did not present effects on anxiety under its stimulation.

The animal 020301, stimulated with 50 μ A, was the animal with DBS electrode outside the AMY that had the biggest anxiolytic response to the stimulation (fig 4.11). The results of the same animal in the next day (D2) are presented in the figure 4.15. It presented the same anxiolytic response in the day before.

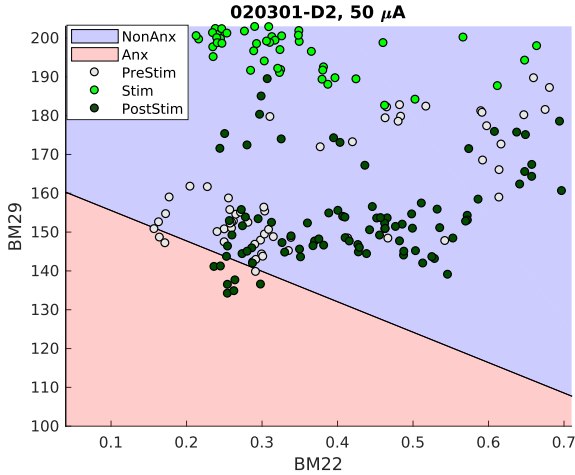


Figure 4.15: D2 result of animal with electrode outside AMY that responded best to the DBS.

The result was also reproduced in the same animal in the third day. In the third day, however, the stimulations were in sections of one minute intercalated with 1 minute of rest. The graph presented in the figure below shows that the effect is indeed acute.

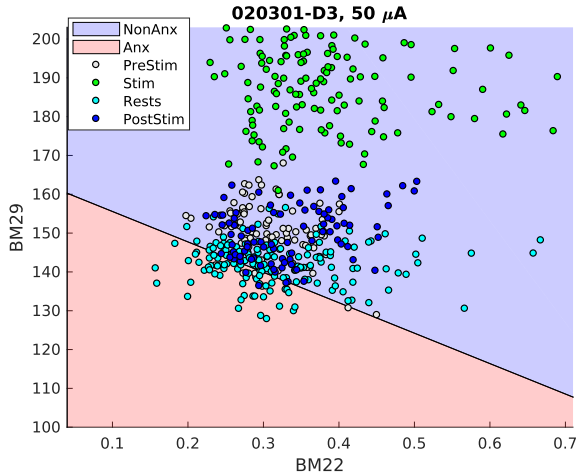


Figure 4.16: The same anxiety reduction effect was observed in the animal during the third day.

The summary of the results on anxiety is shown in the table 4.2. According to the table, the effect of DBS on anxiety seems not to change too much from day to day in the same animal. Each animal presented different effects, probably due to the difference in the electrode implantation position. The animals in more anxious states presented more reduction in anxiety. The animals stimulated with 50 μ A had stronger responses, but this cannot be viewed as consequence of the current, because each animal had the electrode implanted in different places. It may have been a coincidence.

Table 4.2: Summary of results.

	DBS Electrode Position	Current μA	Initial state			Anxiety under DBS stimulation		
			D1	D2	D3	D1	D2	D3
020403 (GSA)	IN	50	rlx	anx	?	-	↓↓	?
010201	OUT	50	anx	?	rlx	↓↓	?	-
020301	OUT	50	bor	rlx	bor	↓↓↓	↓↓↓	↓↓↓
020503	OUT	10	rlx	rlx	?	↑	↑	?
010102	OUT	10	rlx	rlx	rlx	-	↑	-
020502	OUT	100	rlx	rlx	rlx	-	↓	↓
010202	OUT	100	bor	rlx	rlx	↓	↓	↓
010103	OUT	100	rlx	rlx	rlx	-	-	-

rlx: relaxed state; **anx**: anxious state; **bor**: bordering state (on threshold); **IN**: electrode inside the AMY; **OUT**: electrode outside the AMY; ↓: Small decrease on anxiety; ↓↓: Distinctive decrease on anxiety; ↓↓↓: Strong decrease on anxiety; ↑: Small increase on anxiety; ?: Lost data because of problem in the ECoG measurement.

4.4 DBS EFFECTS ON CORTICAL ACTIVITY

This section is dedicated to the analysis of the effects of DBS stimulation on the brain neural activity only, without the anxiety analysis. The order of presentation follows the same order used in the section 4.3. First, all different aspects observed in the brain activity of the GSA are presented, then, these aspects are compared with the subjects with electrodes implanted outside the AMY.

In the gold standard animal

- **Brain Rhythms**: The spectrum of the GSA (subject 020403) in the second day (D2) showed two pronounced peaks in the alpha and gamma bands, the same bands in which the anxiety biomarkers were calculated. The second graph show the integrated areas under each brain rhythm and the error bar. There is significant increase in all frequency bands under stimulation, including the two bands that presented distinctive peaks (α and γ):

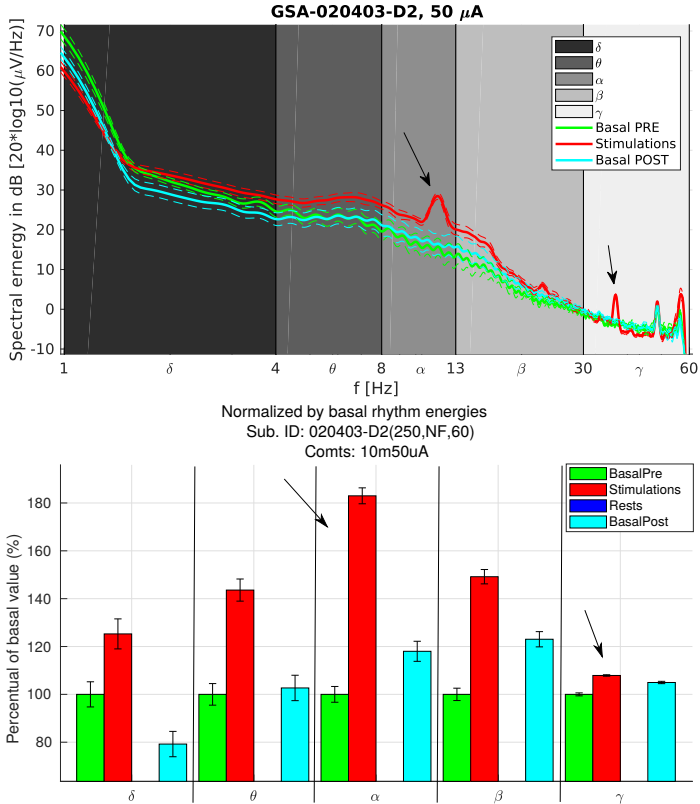


Figure 4.17: GSA Spectral analysis.

Below, the spectrums calculated after the band filtering shows in detail the distinctive peaks. While under stimulation, all alpha band energies increased, specially between 10.5 and 12.5 Hz. The gamma band, while under stimulation, presented a distinctive peak between 36 and 38 Hz. Please remember that this subject had a reduction in its anxiety under stimulation.

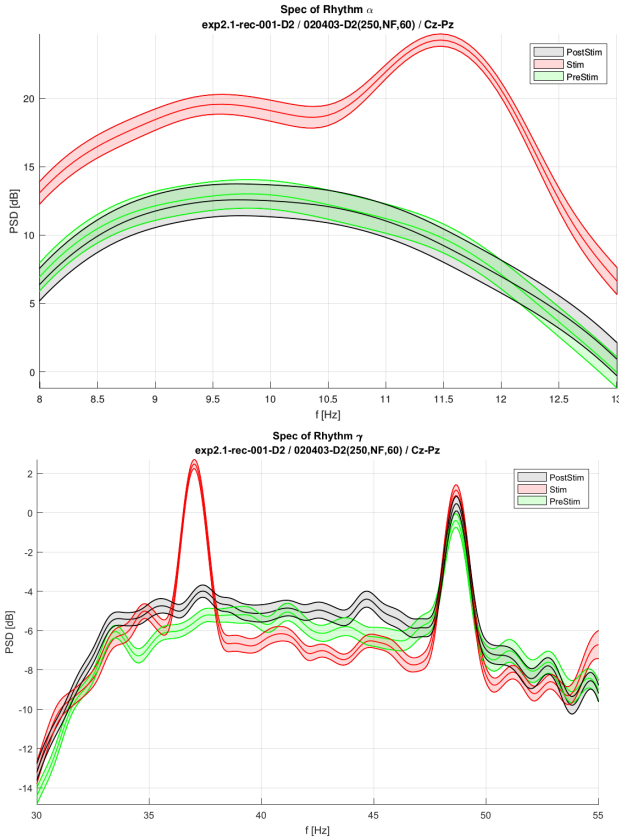


Figure 4.18: GSA spectrums of rhythms α and γ .

The peak in the spectrum of the animal in alpha did not appear in the analysis of the day 0, in which the subject never received DBS. The peak in the gamma frequency was present all the time, while some two new peaks in the beta band were present after 10 minutes in the basal state of the animal. The PSD of the day 0 is shown in the figure 4.20.

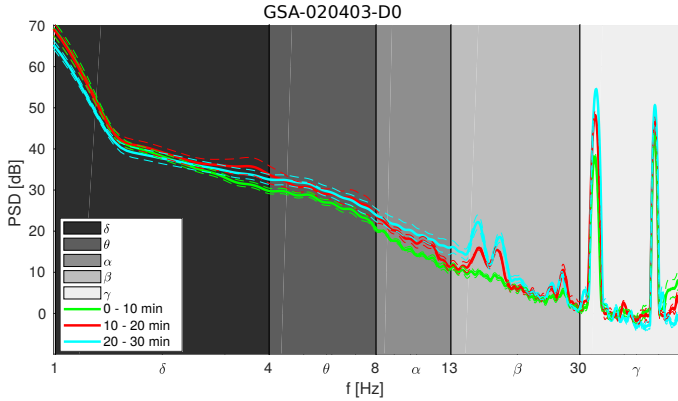


Figure 4.19: GSA spectrum of day 0. The graph contains three spectrums calculated from three different periods in time.

The PSD of the animal in the day 1 presented many different behaviors not previously seen in the days 0 and 2. Although in the D1 the DBS stimulation did not caused differences in the animal's anxiety, the spectrum seems to change greatly in many different bands. A strong component in the beta frequency was present all the time that day. Both the alpha and the gamma peaks seem to have appeared under stimulation, but the gamma peak was shifted some Hz toward a higher frequency.

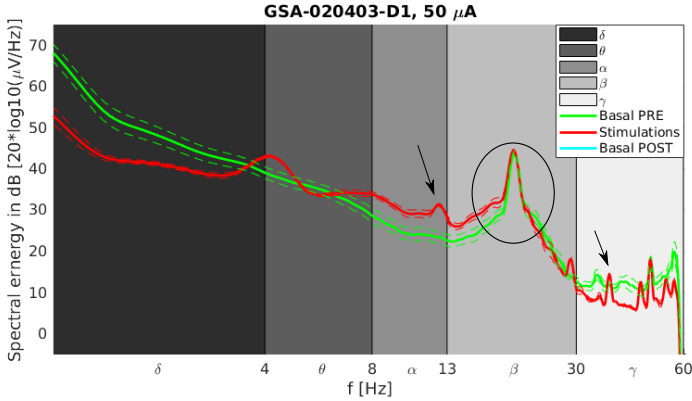


Figure 4.20: GSA spectrum of day 1. The stimulation caused many distortions.

- **Poincaré Plot:**

Poincaré plots were built for each epoch of 10 seconds and the four features main features calculated, as described in the section 3.7. The development of the parameters in the poincare plot over time revealed that the SD1 and SD2 shifted during stimulation. The slope and the relation SD1/SD2 are increased at the beginning of the stimulation, but returned slowly to the original values only after 15 seconds. The change in these variables, contrarily to the anxiety behavior, last a few moments after the stimulation stops.

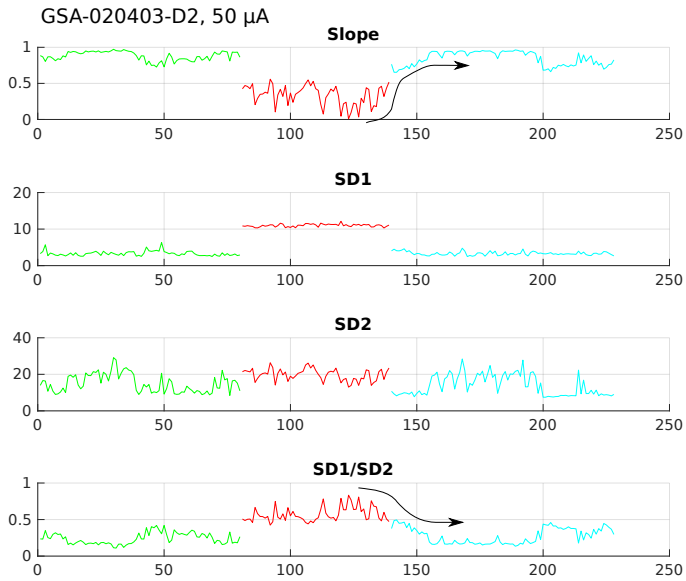


Figure 4.21: GSA's Poincaré plot parameters development over time in day 2. The green and blue lines are the moments in which the subject wasn't receiving stimulation, and the red line is the moment in which the DBS stimulation was applied.

In the day 1, in which there was no anxiety response, the patterns observed in the figure 4.21 are not present (see figure 4.22). The result observed in the day 0, without stimulation, is similar to the result of the day 1.

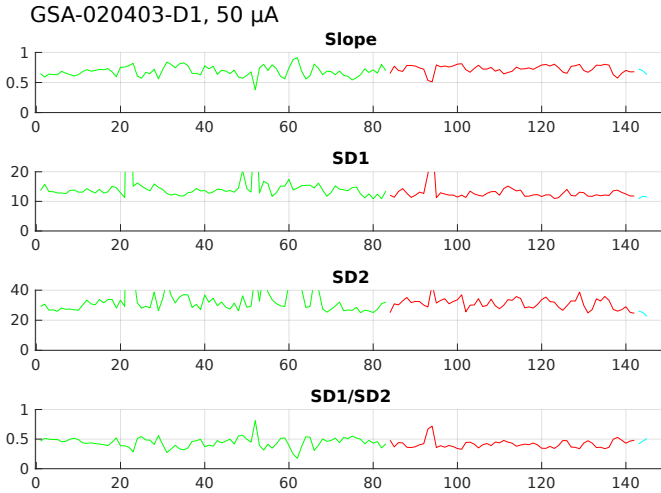


Figure 4.22: GSA's Poincaré plot parameters development over time in day 1. The green and blue lines are the moments in which the subject wasn't receiving stimulation, and the red line is the moment in which the DBS stimulation was applied.

- Correlation Dimension:** The CD values were calculated in the 32 seconds immediately before stimulation, and the 32 seconds immediately after the stimulation, because it demands an incredible amount of computational power to be calculated, and the process cannot be parallelized. The CD of the animal in the basal state of day 0 and day were around 12, but in the day 2 was 10. The value 'Basal Post' of the animal in the day 0 changed to around 9.5, but the animal was not stimulated that day. It seems that the correlation dimension naturally varies significantly from a moment to another. In the day 2, the CD after stimulation is 13, bigger than the value before. But, since the CD could not be accessed over time, it is not clear whether the change was due to the stimulation or not.

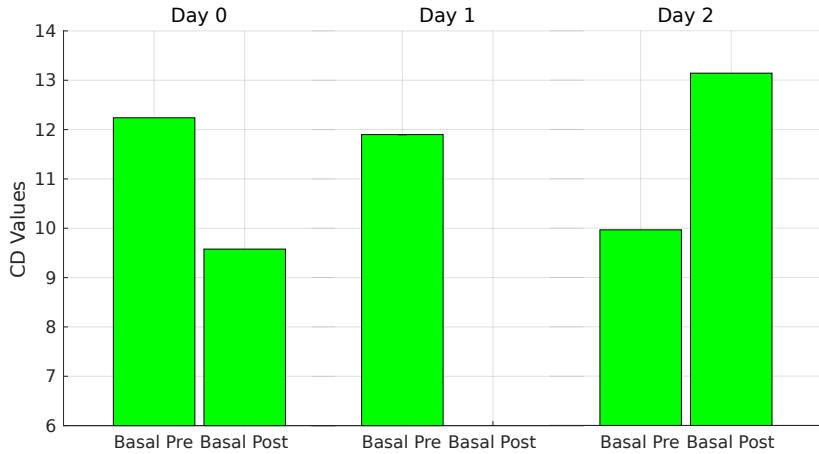


Figure 4.23: Correlation dimension of the GSA.

In the other animals

The same analysis performed for the GSA in the previous subsection was performed in the other subjects with DBS electrode outside the AMY. The presence of the findings observed in the GSA was accessed in the other subjects. The result is summarized in the next three tables, one for each day of experimentation.

The analysis of the tables could not build any rule regarding the presence of the findings and the DBS effect on anxiety. After the tables, some observations are mentioned.

Table 4.3: Comparison between DBS effect on anxiety and brain activity findings in day 1.

	DBS Elec. Pos.	Curr. μ A	Anx	D1							
				Peak α	Peak γ	PC slp	PC SD1	PC SD2	PC SD1/SD2	CD pre	CD post
020403 (GSA)	IN	50	-	Y	Y	N	N	N	N	11.9	?
010201	OUT	50	↓↓	N	N	Y	Y	Y	Y	12.0	?
020301	OUT	50	↓↓↓	N	Y	Y	Y	Y	Y	11.6	?
020503	OUT	10	↑	N	N	N	N	N	N	10.1	?
010102	OUT	10	-	N	N	N	N	N	N	10.4	?
020502	OUT	100	-	N	N	N	N	N	N	12.7	?
010202	OUT	100	↓	N	Y	N	N	N	N	9.5	?
010103	OUT	100	-	N	N	N	N	N	N	11.4	?

Table 4.4: Comparison between DBS effect on anxiety and brain activity findings in day 2.

	DBS Elec. Pos.	Curr. μ A	Anx	D2							
				Peak Alph.	Peak Gamm.	PC slp	PC SD1	PC SD2	PC SD1/SD2	CD pre	CD post
020403 (GSA)	IN	50	↓↓	Y	Y	Y	Y	Y	Y	10.0	13.0
010201	OUT	50	?	Y	Y	Y	N	N	Y	11.2	11.9
020301	OUT	50	↓↓↓	Y	Y	Y	Y	N	Y	11.9	12.5
020503	OUT	10	↑	Y	Y	Y	N	N	Y	10	13.1
010102	OUT	10	↑	N	N	N	N	N	N	7.1	8.5
020502	OUT	100	↓	Y	Y	Y	N	N	Y	10.4	11.8
010202	OUT	100	↓	N	Y	N	N	N	Y	7.3	12.5
010103	OUT	100	-	Y	Y	Y	N	N	Y	10.8	11.7

Table 4.5: Comparison between DBS effect on anxiety and brain activity findings in day 3.

	DBS Elec. Pos.	Curr. μA	Anx	D3							
				Peak Alph.	Peak Gamm.	PC slp	PC SD1	PC SD2	PC SD1/SD2	CD pre	CD post
020403 (GSA)	IN	50	?	?	?	?	?	?	?	?	?
010201	OUT	50	-	N	N	N	N	N	Y	12.3	11.1
020301	OUT	50	↓↓↓	Y	Y	Y	Y	N	Y	11.3	12.8
020503	OUT	10	?	?	?	?	?	?	?	?	?
010102	OUT	10	-	N	N	N	N	N	N	11.1	9.7
020502	OUT	100	↓	N	N	N	N	N	N	12.4	10.5
010202	OUT	100	↓	N	N	N	N	N	N	11.1	9.7
010103	OUT	100	-	Y	Y	N	N	N	N	10.5	7.9

OBSERVATIONS:

- The peak in α and γ seem to appear preferably in animals that had a reduction on anxiety, or were already relaxed (no change in anxiety).
- The Poincare findings (specially *PC slp* and *PC SD1/SD2*) seem to be present only in animals with big reductions in anxiety during the DBS stimulation, but there are exceptions.
- The correlation dimension seems not to have any relation to the anxiety. The stimulation randomly increased or decreased the correlation dimension of the subjects, independently to the changes observed in anxiety.

5 DISCUSSION

Due to the multidisciplinary and innovative character of this dissertation it is hard to find adequate literature to compare the results obtained. This chapter will focus on comparing the dissertation results to the answers sought at the beginning of the theoretical foundation (figure 1.3).

Anxiety classification

The results showed that it is possible to create a classification map of anxiety for rats using one-channel ECoG of the medial prefrontal cortex and static anxiety measures obtained in the elevated plus maze test. The process used to create the classification map can easily be applied to non-invasive human EEG, since the origin of the EEG and ECoG signals are the same, as explained in the theoretical foundation. There are also substitute tests to access anxiety of humans that may apply. The choice of the prefrontal ECoG signal is result of an extensive literature review of the amygdala connections. Since these connections are well preserved amongst mammalian species, it is a good choice to use brain activity of the same region when translating this study to humans. There are also public EEG datasets with stress measurements that may be used.

The proposed biomarkers were adjusted for the group of subjects of this dissertation and cannot be adjusted for each specific animal, since the anxiety test can only be performed once. That processes makes the biomarkers more generic, but with less accuracy for each specific animal.

Statistical significance of the features

One factor that is worth mentioning is that a high number of features were tested to find their correlation with anxiety (112), and the p-value considered statistically significant was $p < 0.05$. One must argue that a correction factor should have been applied, such as the *Bonferroni correction*, which further reduces the acceptable p-value for multiple comparisons. This correction was not applied in this dissertation because all the hypothesis came from meticulously chosen paradigms and parameters. For example: instead of using several ECoG channels, only the ECoG channel placed in the prefrontal cortex was used, since the prefrontal cortex activity is strongly connected to the AMY; many important details such as the physical process that give rise to the ECoG signal, and the relation

of this phenomena to the neural activity intended to be correlated to the AMY modulation of the mPFC were not neglected; all the algorithms used in the analysis were carefully chosen to access the specific brain activity aspects of interest for the mPFC modulation; even simply details, such as the sub-window width used to calculate the PSDs in the P-welch method were carefully chosen to reflect physical brain aspects of interest.

DBS effect on anxiety

The DBS effect on anxiety, according to the results, varies greatly from subject to subject. In some subjects the effect is anxiolytic, in others it is anxiogenic. Although some animals had their anxiety increased by the DBS stimulation, no animal had its state changed from non-anxious to anxious stimulation. The gold standard animal (GSA) and others, however, do crossed the threshold from anxious to non anxious. It suggests that the DBS use in the AMY and its nearby regions using the chosen parameters are much more prone to relax the animals than to stress them.

The differences in anxiety response under DBS stimulation observed from animal to animal are probably due to the unique electrode positioning in each one of them. The technological difficulties encountered in the process of electrode implantation made it impossible to group the animals by the stimulation current applied. Each subject was unique, and had to be analyzed individually.

The fact that the effects on anxiety in each animal were preserved in subsequent experimentation days (table 4.2) corroborates to the hypothesis that the electrode positioning is determinant in this type of experiment, and each subject was unique.

The GSA

Although there was only one gold standard animal, the analysis of it lead to strong conclusions, because all parameters were perfectly controlled: 1) the ECoG was clean; 2) the DBS electrode was inside the AMY; 3) there was no contamination or healing problems following the surgery; 4) stimulation parameters well constrained to avoid tissue damage and, luckily 5) it was in the anxious zone at the beginning of the experiment.

The GSA experimented a strong reduction in anxiety, presented in the figure 4.6. This reduction in anxiety was acute, i.e. its effect ceased immediately after the stimulation stopped. While un-

der stimulation, the ECoG presented distinctive peaks in the α and γ brain rhythms (4.18) that may or may not be related to a relaxed brain state. In the day 1 the same peaks were present while the animal received stimulation, but its anxiety wasn't reduced, probably because it was already relaxed.

The Poincare Map of the GSA animal revealed two parameters that have a decaying curve of 15 seconds after the stimulation ceases, suggesting that some effect lasts a few moments after stimulation, but these are probably not correlated with anxiety changes.

DBS effect on ECoG

The many different analysis on the ECoG revealed that it is not worth studying the ECoG effects under stimulation without a biological behavior (such as using the anxiety measures). Too many differences are observed in the brain activity under stimulation, for almost all animals, but these findings are not useful if not correlated with a biological behavior/emotion.

Both the parameters extracted from the Poincare Map and the peaks observed in the ECoG's PSD seem to have something to do with anxiety, but there are too many exceptions that prevents any conclusion to be drawn.

Interestingly, one of the features that happened to be correlated to anxiety in rats was calculated on the gamma rhythm (30 Hz to 60 Hz). Although this frequency band is frequently mentioned in the literature, it is not frequently used. The vast majority of the EEG experiments presented in the literature, however, are performed in humans, what makes the comparison with this dissertation difficult.

Answers previously sought

- **Which measures may be considered as biomarkers?** The biomarkers found (BM29 and BM22) alone are weak anxiety biomarkers, but a SVM map built using them both was proven to be useful for anxiety assessment.
- **Are the effects temporary?** The classification maps showed that the DBS effect on anxiety is acute and ceases immediately after the stimulation stops. The Poincare Map, however, showed a 15 s transient after the stimulation ceases, suggesting that some other brain state not correlated with anxiety had also changed, and the effect is lasts few moments after the stimulation stopped.

- **Which area is affected?** It is still unknown, but electrodes outside AMY seem to have some of the effects observed with the electrode inside AMY, such as anxiety reduction. To answer this question, a post-Morten tissue physiological analysis is needed.
- **Which biomarkers change? How?** An increase both in BM29 and BM22 suggest less anxiety. These biomarkers are a measure of the PSD ripples in the alpha and gamma ECoG bands. In other words, more ripples (or spikes) in these bands suggest less anxiety.
- **How long do the effects last?** The measures showed that the brain activity returns to normal just a few moments after the stimulation stops. That is an interesting result because it opens the possibility of testing different DBS parameters after the last DBS effects cease.
- **How the parameter choice influences?** The DBS stimulation frequency was chosen to cause inhibition of the neural activity, any conclusions of this experiment must take this into consideration. A change in frequency of stimulation polarity may, probably, alter all results. The effects of the different stimulation currents could not be accessed because the electrode positioning was unique in each animal. The strongest responses were observed in the animals stimulated with 50 μA . Few anxiety changes were also observed in animals stimulated with 10 or 100 μA . Since the electrode positioning was not perfectly accessed for each animal, it is impossible to draw any conclusions regarding the currents applied.

6 CONCLUSION

This dissertation shined some light upon very complex questions regarding the DBS experimentation focused on closed-loop systems. The process and biomarkers discovered in this dissertation can help create smarter DBS systems and boost the experimentation for psychiatric diseases.

Some important lessons that this dissertation provides for future researchers are: 1) several initial parameters from which the experimentation can start were fixed based on physiological phenomena, previous studies and translational studies, such as the stimulation parameters, the choice of electrodes polarity, shape and material, and many others; 2) the surgery and electrodes positioning (both DBS and ECoG) are extremely important, and more resources must be allocated for these issues; 3) some important conclusions regarding the effects of DBS on anxiety were drawn; 4) the analysis of brain activity alone are useless. It is very important to focus on the behavioral response that is being studied; 5) in such an emergent science it is very important to use the medical and neuroscience literature as basis as well as have strong interaction between the medical doctors and the engineers to help direct the experimentations.

Future experiments may use the anxiety biomarker created in this dissertation as basis, and focus on studying the effect of chronic DBS (more than 1 hour of stimulation). Improvements in the anxiety biomarker found here may lead to the creation of a dynamic variable useful for closed-loop experimentation and system modeling. Researchers focused in human experimentation may use the same process described here to find specific brain biomarkers for other psychiatric diseases.

Last but not least, the roots of technological problems regarding the DBS experimentation are very subtle and lead to significant losses in data. Future scientists must first study all possible roots of problems before experimenting using a formal technique, such as fishbone diagrams.

BIBLIOGRAPHY

- 1 OLESEN, J. et al. The economic cost of brain disorders in europe. *European journal of neurology*, Wiley Online Library, v. 19, n. 1, p. 155–162, 2012.
- 2 ROSSI, P. J. et al. Scheduled, intermittent stimulation of the thalamus reduces tics in tourette syndrome. *Parkinsonism & related disorders*, Elsevier, v. 29, p. 35–41, 2016.
- 3 DELALOYE, S.; HOLTZHEIMER, P. E. Deep brain stimulation in the treatment of depression. *Dialogues in clinical neuroscience*, Les Laboratoires Servier, v. 16, n. 1, p. 83, 2014.
- 4 NESTLER, E. J. Treating the brain deep down: brain surgery for anorexia nervosa? *Nature medicine*, Nature Research, v. 19, n. 6, p. 678–679, 2013.
- 5 SMITH, K. Mental health: a world of depression. *Nature*, v. 515, n. 7526, p. 181, 2014.
- 6 FAJEMIROYE, J. O. et al. Treatment of anxiety and depression: medicinal plants in retrospect. *Fundamental & clinical pharmacology*, Wiley Online Library, 2016.
- 7 OLESEN, J.; LEONARDI, M. The burden of brain diseases in europe. *European Journal of Neurology*, Wiley Online Library, v. 10, n. 5, p. 471–477, 2003.
- 8 KANDEL, E. et al. *Princípios de Neurociências-5*. [S.l.]: AMGH Editora, 2014.
- 9 WILLIAMS, N. R.; OKUN, M. S. Deep brain stimulation (dbs) at the interface of neurology and psychiatry. *The Journal of clinical investigation*, Am Soc Clin Investig, v. 123, n. 11, p. 4546–4556, 2013.
- 10 STIDD, D. A. et al. Amygdala deep brain stimulation is superior to paroxetine treatment in a rat model of posttraumatic stress disorder. *Brain stimulation*, Elsevier, v. 6, n. 6, p. 837–844, 2013.
- 11 LANGEVIN, J.-P. et al. Deep brain stimulation of the amygdala alleviates post-traumatic stress disorder symptoms in a rat model. *Journal of psychiatric research*, Elsevier, v. 44, n. 16, p. 1241–1245, 2010.
- 12 PAGE. Deep brain stimulation of the basolateral amygdala for treatment-refractory posttraumatic stress disorder. 2015.

- 13 KOEK, R. J. et al. Deep brain stimulation of the basolateral amygdala for treatment-refractory combat post-traumatic stress disorder (ptsd): study protocol for a pilot randomized controlled trial with blinded, staggered onset of stimulation. *Trials*, BioMed Central, v. 15, n. 1, p. 356, 2014.
- 14 HYDE, D. *Swedish Hospital Patient Walks Again With Deep Brain Stimulation*. 2014. 1 p. Disponível em: <http://kuow.org/post/swedish-hospital-patient-walks-again-deep-brain-stimulation>.
- 15 JR, W. J. M. *Deep brain stimulation management*. [S.l.]: Cambridge University Press, 2015.
- 16 SHUKLA, A. W.; BONA, A. R.; WALZ, R. Troubleshooting in dbs. In: MEHANNA, R. (Ed.). *Deep brain stimulation*. 1. ed. [S.l.]: Nova Science Publishers, 2015. cap. 10, p. 213–261.
- 17 JR, M.; WILLIAM, J. *Deep brain stimulation management*. [S.l.]: Cambridge University Press, 2015. ISBN 9780511763281.
- 18 ZHANG, H.; WANG, Q.; CHEN, G. Control effects of stimulus paradigms on characteristic firings of parkinsonism. *Chaos*, set. 2014.
- 19 ROSIN, B. et al. Closed-loop deep brain stimulation is superior in ameliorating parkinsonism. *Neuron*, out. 2011.
- 20 YENER, G. G.; BAŞAR, E. Brain oscillations as biomarkers in neuropsychiatric disorders: following an interactive panel discussion and synopsis. *Supplements to Clinical neurophysiology*, v. 62, p. 343–363, 2013.
- 21 ZHANG, Q.; LEE, M. Emotion development system by interacting with human eeg and natural scene understanding. *Cognitive Systems Research*, Elsevier, v. 14, n. 1, p. 37–49, 2012.
- 22 BRETTE, R.; DESTEXHE, A. *Handbook of neural activity measurement*. [S.l.]: Cambridge University Press, 2012.
- 23 STRIMBU, K.; TAVEL, J. A. What are biomarkers? *Current Opinion in HIV and AIDS*, NIH Public Access, v. 5, n. 6, p. 463, 2010.
- 24 PIZZAGALLI, D. et al. Anterior cingulate activity as a predictor of degree of treatment response in major depression: evidence from brain electrical tomography analysis. *American Journal of Psychiatry*, Am Psychiatric Assoc, v. 158, n. 3, p. 405–415, 2001.

- 25 SHUTE, J. B. et al. Thalamocortical network activity enables chronic tic detection in humans with tourette syndrome. *NeuroImage: Clinical*, Elsevier, v. 12, p. 165–172, 2016.
- 26 JANG HYERAN, C. S.; HAN MOOKYOUNG, B. K. C. D. J. J. Analysis of fear memory signals in the rat amygdala and thalamus. *Neural Engineering*, 2007.
- 27 KNOTT, V. et al. Eeg power, frequency, asymmetry and coherence in male depression. *Psychiatry Research: Neuroimaging*, Elsevier, v. 106, n. 2, p. 123–140, 2001.
- 28 SOUZA, M. T. de; SILVA, M. D. da; CARVALHO, R. de. Revisão integrativa: o que é e como fazer. *Einstein*, SciELO Brasil, v. 8, n. 1 Pt 1, p. 102–6, 2010.
- 29 GROUP, N. P. The burden of depression. *Nature*, n. 515, p. 163–163, 2014.
- 30 BLAS, E.; KURUP, A. S. *Equity, social determinants and public health programmes*. [S.l.]: World Health Organization, 2010.
- 31 Associação de Apoio aos Doentes Depressivos e Bipolares. *Doença Unipolar*. 2016. 1 p. Disponível em: <http://www.adeb.pt/pages/doenca-unipolar>.
- 32 VIDA, R. minha. *Transtorno bipolar*. 2016. 1 p. Disponível em: <http://www.minhavidacom.br/saude/temas/transtorno-bipolar>.
- 33 CALHOON, G. G.; TYE, K. M. Resolving the neural circuits of anxiety. *Nature Neuroscience*, Nature Publishing Group, v. 18, n. 10, p. 1394–1404, 2015.
- 34 Site Drauzio Varella. *Transtorno do estresse pós-traumático*. 2014. 1 p. Disponível em: <http://drauziovarella.com.br/letras/e/transtorno-do-estresse-pos-traumatico/>.
- 35 MACHADO, R.; GAUER, J. C. Transtorno de estresse pós-traumático e transtorno de humor bipolar (Posttraumatic stress disorder and bipolar mood disorder). *Revista Brasileira de Psiquiatria*, v. 25, n. Supl I, p. 55–61, 2003.
- 36 Center for Adolescent Studies. *Trauma and the Brain: An Introduction for professionals working with teens*. 2016. 1 p. Disponível em: <http://centerforadolescentstudies.com/trauma-and-brain/>.

- 37 ALLMAN, J. M. et al. The Anterior Cingulate Cortex. *Annals of the New York Academy of Sciences*, Blackwell Publishing Ltd, v. 935, n. 1, p. 107–117, jan 2006. ISSN 00778923. Disponível em: <http://doi.wiley.com/10.1111/j.1749-6632.2001.tb03476.x>).
- 38 PIZZAGALLI, D. A. et al. Anterior cingulate activity as a predictor of degree of treatment response in major depression: evidence from brain electrical tomography analysis. *American Journal of Psychiatry*, v. 158, n. 3, p. 405–415, 2001. ISSN 0002-953X. Disponível em: <http://ajp.psychiatryonline.org.myaccess.library.utoronto.ca/doi/abs/10.1176/appi.ajp.158.3.405> (delimitador "026E30F\$files/523/Pizzagallietal.-2001-AnteriorCingulateActivityasaPredictorofDegr.pdf).
- 39 JANAK, P. H.; TYE, K. M. From circuits to behaviour in the amygdala. *Nature*, Nature Publishing Group, v. 517, n. 7534, p. 284–292, 2015.
- 40 BENARROCH, E. E. The amygdala functional organization and involvement in neurologic disorders. *Neurology*, AAN Enterprises, v. 84, n. 3, p. 313–324, 2015.
- 41 LEE, S. et al. Inhibitory networks of the amygdala for emotional memory. *Frontiers in Neural Circuits*, Frontiers, v. 7, p. 129, 2013. ISSN 1662-5110. Disponível em: <http://journal.frontiersin.org/article/10.3389/fncir.2013.00129/abstract>).
- 42 DUVARCI, S.; PARE, D. Amygdala microcircuits controlling learned fear. *Neuron*, Elsevier, v. 82, n. 5, p. 966–980, 2014.
- 43 WHALEN, P. J.; PHELPS, E. A. *The human amygdala*. [S.l.]: Guilford Press, 2009.
- 44 HANEY, M.; EVINS, A. E. Does cannabis cause, exacerbate or ameliorate psychiatric disorders? an oversimplified debate discussed. *Neuropsychopharmacology*, Nature Publishing Group, v. 41, n. 2, p. 393–401, 2016.
- 45 ANTHES, E. Depression: a change of mind. *Nature*, v. 515, p. 185–187, 2014.
- 46 ANDERSEN, P.; LØMO, T. Control of hippocampal output by afferent volley frequency. *Progress in brain research*, Elsevier, v. 27, p. 400–412, 1967.

- 47 LØMO, T. The discovery of long-term potentiation. *Philosophical Transactions of the Royal Society of London B: Biological Sciences*, The Royal Society, v. 358, n. 1432, p. 617–620, 2003.
- 48
- 49 ALGER, B.; TEYLER, T. Long-term and short-term plasticity in the ca1, ca3, and dentate regions of the rat hippocampal slice. *Brain research*, Elsevier, v. 110, n. 3, p. 463–480, 1976.
- 50 IZUMI, Y.; ZORUMSKI, C. F. Neuregulin and dopamine d4 receptors contribute independently to depotentiation of schaffer collateral ltp by temperoammonic path stimulation. *eNeuro*, Society for Neuroscience, v. 4, n. 4, p. ENEURO-0176, 2017.
- 51 KIM, J. et al. Amygdala depotentiation and fear extinction. *Proceedings of the National Academy of Sciences*, National Acad Sciences, v. 104, n. 52, p. 20955–20960, 2007.
- 52 SIGURDSSON, T. et al. Long-term potentiation in the amygdala: a cellular mechanism of fear learning and memory. *Neuropharmacology*, Elsevier, v. 52, n. 1, p. 215–227, 2007.
- 53 DÜRMEÜLLER, N.; PORSOLT, R. Electrical amygdala kindling. *Current protocols in pharmacology*, Wiley Online Library, p. 5–33, 2003.
- 54 ELEVATED plus maze - Wikipedia. Disponível em: (https://en.wikipedia.org/wiki/Elevated_plus_maze).
- 55 OPEN field (animal test) - Wikipedia. Disponível em: ([https://en.wikipedia.org/wiki/Open_field_\(animal_test\)](https://en.wikipedia.org/wiki/Open_field_(animal_test))).
- 56 SANTOS, F. J.; COSTA, R. M.; TECUAPETLA, F. Stimulation on demand: closing the loop on deep brain stimulation. *Neuron*, Elsevier, v. 72, n. 2, p. 197–198, 2011.
- 57 ALMEIDA, L. et al. Deep brain stimulation battery longevity: comparison of monopolar versus bipolar stimulation modes. *Movement disorders clinical practice*, Wiley Online Library, v. 3, n. 4, p. 359–366, 2016.
- 58 KÜHN, A. A.; VOLKMANN, J. Innovations in deep brain stimulation methodology. *Movement Disorders*, Wiley Online Library, v. 32, n. 1, p. 11–19, 2017.

- 59 DAVIS, J. Overview of biomaterials and their use in medical devices. *Handbook of materials for medical devices. Illustrated edition*, Ohio: ASM International, p. 1–11, 2003.
- 60 HICKEY, P.; STACY, M. Deep brain stimulation: a paradigm shifting approach to treat parkinson's disease. *Frontiers in neuroscience*, Frontiers Media SA, v. 10, 2016.
- 61 JR, E. B. M. *Deep brain stimulation programming: principles and practice*. [S.l.]: Oxford University Press, 2010.
- 62 MCINTYRE, C. C. et al. Electric field and stimulating influence generated by deep brain stimulation of the subthalamic nucleus. *Clinical neurophysiology*, Elsevier, v. 115, n. 3, p. 589–595, 2004.
- 63 KRINGELBACH, M. L. et al. Translational principles of deep brain stimulation. *Nature reviews. Neuroscience*, v. 8, n. 8, p. 623–635, 2007. ISSN 1471-003X (Print); 1471-003X (Linking).
- 64 KÜHN, A. A.; VOLKMANN, J. Innovations in deep brain stimulation methodology. *Movement Disorders*, Wiley Online Library, 2016.
- 65 HARIZ, M. Deep brain stimulation: new techniques. *Parkinsonism & related disorders*, Elsevier, v. 20, p. S192–S196, 2014.
- 66 KRINGELBACH, M. L. et al. Translational principles of deep brain stimulation. *Nature reviews. Neuroscience*, Nature Publishing Group, v. 8, n. 8, p. 623, 2007.
- 67 RANCK, J. B. Which elements are excited in electrical stimulation of mammalian central nervous system: a review. *Brain research*, Elsevier, v. 98, n. 3, p. 417–440, 1975.
- 68 NOWAK, L.; BULLIER, J. Axons, but not cell bodies, are activated by electrical stimulation in cortical gray matter i. evidence from chronaxie measurements. *Experimental brain research*, Springer, v. 118, n. 4, p. 477–488, 1998.
- 69 KUNCEL, A. M.; GRILL, W. M. Selection of stimulus parameters for deep brain stimulation. *Clinical neurophysiology*, Elsevier, v. 115, n. 11, p. 2431–2441, 2004.
- 70 REICH, M. M. et al. Short pulse width widens the therapeutic window of subthalamic neurostimulation. *Annals of clinical and translational neurology*, Wiley Online Library, v. 2, n. 4, p. 427–432, 2015.

- 71 DEMBEK, T. A. et al. Directional dbs increases side-effect thresholds—a prospective, double-blind trial. *Movement Disorders*, Wiley Online Library, 2017.
- 72 COFFEY, R. J. Deep brain stimulation devices: a brief technical history and review. *Artificial organs*, Wiley Online Library, v. 33, n. 3, p. 208–220, 2009.
- 73 ORTMANNS, M. Charge balancing in functional electrical stimulators: A comparative study. In: IEEE. *Circuits and Systems, 2007. ISCAS 2007. IEEE International Symposium on*. [S.l.], 2007. p. 573–576.
- 74 NEURON - Wikipedia. Disponível em: (<https://en.wikipedia.org/wiki/Neuron>).
- 75 STERIADE, M. *Neuronal substrates of sleep and epilepsy*. [S.l.]: Cambridge University Press, 2003.
- 76 BREMER, F. *Lactivit électrique de lecorce cerebrale*. [S.l.]: Hermann, 1938.
- 77 BREMER, F. Considerations sur lorigine et la nature des ondes cerebrales. *Electroencephalography and clinical neurophysiology*, Elsevier, v. 1, n. 1, p. 177–193, 1949.
- 78 KLEE, M. R.; OFFENLOCH, K.; TIGGES, J. Cross-correlation analysis of electroencephalographic potentials and slow membrane transients. *Science*, American Association for the Advancement of Science, v. 147, n. 3657, p. 519–521, 1965.
- 79 CREUTZFELDT, O. D.; WATANABE, S.; LUX, H. D. Relations between eeg phenomena and potentials of single cortical cells. i. evoked responses after thalamic and epicortical stimulation. *Electroencephalography and clinical neurophysiology*, Elsevier, v. 20, n. 1, p. 1–18, 1966.
- 80 CREUTZFELDT, O. D.; WATANABE, S.; LUX, H. D. Relations between eeg phenomena and potentials of single cortical cells. i. evoked responses after thalamic and epicortical stimulation. *Electroencephalography and clinical neurophysiology*, Elsevier, v. 20, n. 1, p. 1–18, 1966.
- 81 NIEDERMEYER, E.; SILVA, F. L. da. *Electroencephalography: basic principles, clinical applications, and related fields*. [S.l.]: Lippincott Williams & Wilkins, 2005.

82 AKAR, S. A. et al. Nonlinear analysis of eeg in major depression with fractal dimensions. In: IEEE. *Engineering in Medicine and Biology Society (EMBC), 2015 37th Annual International Conference of the IEEE*. [S.l.], 2015. p. 7410–7413.

83 HOU, X. et al. Eeg based stress monitoring. In: IEEE. *Systems, Man, and Cybernetics (SMC), 2015 IEEE International Conference on*. [S.l.], 2015. p. 3110–3115.

84 TOMITA, Y.; ITO, S.-i.; MITSUKURA, Y. The eeg analysis method for obtaining the feeling. In: IEEE. *Control, Automation and Systems, 2008. ICCAS 2008. International Conference on*. [S.l.], 2008. p. 2555–2558.

85 SAEED, S. M. U. et al. Psychological stress measurement using low cost single channel eeg headset. In: IEEE. *Signal Processing and Information Technology (ISSPIT), 2015 IEEE International Symposium on*. [S.l.], 2015. p. 581–585.

86 HOSSEINIFARD, B.; MORADI, M. H.; ROSTAMI, R. Classifying depression patients and normal subjects using machine learning techniques and nonlinear features from eeg signal. *Computer methods and programs in biomedicine*, Elsevier, v. 109, n. 3, p. 339–345, 2013.

87 MANTRI, S. et al. Non invasive eeg signal processing framework for real time depression analysis. In: IEEE. *SAI Intelligent Systems Conference (IntelliSys), 2015*. [S.l.], 2015. p. 518–521.

88 QURAAAN, M. A. et al. Eeg power asymmetry and functional connectivity as a marker of treatment effectiveness in dbs surgery for depression. *Neuropsychopharmacology*, Nature Publishing Group, v. 39, n. 5, p. 1270, 2014.

89 MENDELSON, W. B. et al. Frequency analysis of the sleep eeg in depression. *Psychiatry research*, Elsevier, v. 21, n. 2, p. 89–94, 1987.

90 10–20 system (EEG) - Wikipedia. Disponível em: [https://en.wikipedia.org/wiki/10%E2%80%9320_system_\(EEG\)](https://en.wikipedia.org/wiki/10%E2%80%9320_system_(EEG)).

91 SUBHA, D. P. et al. Eeg signal analysis: A survey. *Journal of medical systems*, Springer, v. 34, n. 2, p. 195–212, 2010.

92 COMMON Fourier Series. Disponível em: <http://pilot.cnxproject.org/content/collection/col10064/latest/module/m34770/latest>.

- 93 SIGNAL Processing. Disponible em: (<https://www.wavemetrics.com/products/igorpro/dataanalysis/signalprocessing.htm>).
- 94 WELCH'S method - Wikipedia. Disponible em: (https://en.wikipedia.org/wiki/Welch%27s_method).
- 95 ATTRACTOR - Wikipedia. Disponible em: (https://en.wikipedia.org/wiki/Attractor#Strange_attractor).
- 96 KOSTELICH, E. J.; SWINNEY, H. L. Practical considerations in estimating dimension from time series data. *Physica Scripta*, IOP Publishing, v. 40, n. 3, p. 436, 1989.
- 97 GRASSBERGER, P.; PROCACCIA, I. Measuring the strangeness of strange attractors. In: *The Theory of Chaotic Attractors*. [S.l.]: Springer, 2004. p. 170–189.
- 98 HEAVISIDE step function - Wikipedia. Disponible em: (https://en.wikipedia.org/wiki/Heaviside_step_function).
- 99 LAI, Y.-C.; LERNER, D. Effective scaling regime for computing the correlation dimension from chaotic time series. *Physica D: Nonlinear Phenomena*, Elsevier, v. 115, n. 1, p. 1–18, 1998.
- 100 RECURRENCE plot - Wikipedia. Disponible em: (https://en.wikipedia.org/wiki/Recurrence_plot).
- 101 CASTRO, B. C. de et al. Auditory stimulation with music influences the geometric indices of heart rate variability in response to the postural change maneuver. *Noise and Health*, Medknow Publications, v. 16, n. 68, p. 57, 2014.
- 102 ALBERDI, A.; AZTIRIA, A.; BASARAB, A. Towards an automatic early stress recognition system for office environments based on multimodal measurements: A review. *Journal of biomedical informatics*, Elsevier, v. 59, p. 49–75, 2016.
- 103 CLEARY, D. R. et al. Deep brain stimulation for psychiatric disorders: where we are now. *Neurosurgical focus*, American Association of Neurological Surgeons, v. 38, n. 6, p. E2, 2015.
- 104 GOLDAPPLE, K. et al. Modulation of cortical-limbic pathways in major depression: treatment-specific effects of cognitive behavior therapy. *Archives of general psychiatry*, American Medical Association, v. 61, n. 1, p. 34–41, 2004.

- 105 MAYBERG, H. S. et al. Regional metabolic effects of fluoxetine in major depression: serial changes and relationship to clinical response. *Biological psychiatry*, Elsevier, v. 48, n. 8, p. 830–843, 2000.
- 106 MOTTAGHY, F. M. et al. Correlation of cerebral blood flow and treatment effects of repetitive transcranial magnetic stimulation in depressed patients. *Psychiatry Research: Neuroimaging*, Elsevier, v. 115, n. 1, p. 1–14, 2002.
- 107 NOBLER, M. S. et al. Decreased regional brain metabolism after ect. *American Journal of Psychiatry*, Am Psychiatric Assoc, v. 158, n. 2, p. 305–308, 2001.
- 108 BRESLAU, N. Outcomes of posttraumatic stress disorder. *The Journal of clinical psychiatry*, Physicians Postgraduate Press, 2001.
- 109 KOEK, R. J. et al. Deep brain stimulation of the basolateral amygdala for treatment-refractory combat post-traumatic stress disorder (PTSD): study protocol for a pilot randomized controlled trial with blinded, staggered onset of stimulation. *Trials*, v. 15, n. 1, p. 356, dec 2014. ISSN 1745-6215. Disponível em: <http://www.scopus.com/inward/record.url?eid=2-s2.0-84907394986&partnerID=tZ0tx3y1http://trialsjournal.biomedcentral.com/articles/10.1186/1745-6215-15->.
- 110 PAXINOS, G.; WATSON, C. *The rat brain atlas in stereotaxic coordinates, compact*. [S.l.]: Academic Press, New York, 1997.
- 111 ELECTRODE placement in a brain slice of a rat at bregma:... Disponível em: https://www.researchgate.net/figure/51156762_fig2_Electrode-placement-in-a-brain-slice-of-a-rat-at-bregma-360mminteraural-540mm.
- 112 NAVIGATOR through the Brain - Stereotaxic Atlases for Neuroscience Research: Leica Biosystems. Disponível em: <http://www.leicabiosystems.com/pathologyleaders/navigator-through-the-brain-stereotaxic-atlases-for-neuroscience-research/>.
- 113 NOLAN, H.; WHELAN, R.; REILLY, R. Faster: fully automated statistical thresholding for eeg artifact rejection. *Journal of neuroscience methods*, Elsevier, v. 192, n. 1, p. 152–162, 2010.
- 114 COEFFICIENT of determination - Wikipedia. Disponível em: https://en.wikipedia.org/wiki/Coefficient_of_determination.